A COMPARISON OF TWO *IN VITRO* ASSAYS
TO ASSESS RADIOSENSITIVITY IN PATIENTS
RECEIVING RADIOTHERAPY

SHARON JAYNE MITCHELL

A thesis submitted in partial fulfilment of the
requirements of the University of Glamorgan/Prifysgol Morgannwg
for the degree of Master of Philosophy

This research programme was carried out
in collaboration with Velindre Hospital, Cardiff.

April 1994

I think over again my small adventures;

My fears, those small ones and those that seemed so big,

For all the vital things I had to get and reach.

And there is only one great thing, the only Thing;

To live, to see the great day that dawns

And the Light Who fills the world.
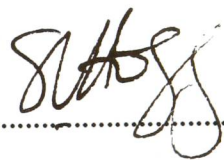
(Ancient Inuit Song)

Declaration

I hereby certify that the work presented in this thesis has not been accepted for any other degree and is not currently being submitted in candidature for any other degree. The work presented in this thesis is the result of my own investigations except where reference has been made to published literature.
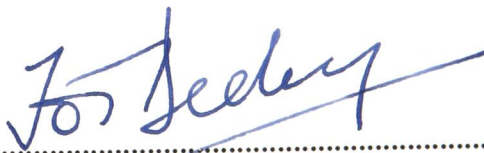
Signed (Candidate)

Signed (Director of Studies)

Signed (Supervisor)

Acknowledgements

I am indebted to Dr. J.O.T. Deeley (DNA/Tissue Repair Group, Velindre Hospital, Cardiff) for his supervision, advice and encouragement during my period of study.

I am especially grateful to my Director of Studies Dr. S. I. Hogg (School of Applied Sciences, University of Glamorgan) for his constant guidance, support and help during the preparation of this thesis.

I would like to thank Professor J. L. Moore (Head of Radiation Science Laboratories, Velindre Hospital) for his encouragement and advice and for enabling me to perform the necessary practical work in his department.

A special thanks to Dr. I. Kerby for providing blood samples from patients attending the out-patients clinic at Velindre Hospital.

Many thanks to all the staff of the Radiation Science laboratories, Velindre Hospital for their friendliness and help during the course of this study. In particular I would like to thank Mrs. A. Sanders, Mrs. A. Reece, Miss. G. Davies and Dr. J. Court.

Finally, I want to thank my husband, Simon and my parents for their support and encouragement during this study.

Abstract

This thesis addresses the occurrence of normal tissue damage as a limiting factor in curative radiotherapy and the need for predictive radiosensitivity testing. Patients who display unusual sensitivity to radiation may also exhibit a poor DNA repair capacity. Consequently, *in vitro* assays which assess radiation-induced DNA damage and its subsequent repair may have potential in predicting a patient's response to radiotherapy.

Nuclear Lysate Sedimentation (NLS) and Microgel Electrophoresis (MGE) were examined as rapid means to assess DNA damage and repair in human lymphocytes. NLS involves the centrifugation of histone-free DNA (HF-DNA) through a neutral 0-20% sucrose gradient - where DNA damage in a population of lymphocytes is detected as an upward shift in HF-DNA sedimentation distance. MGE involves the electrophoresis (in alkaline buffer) of cells embedded in agarose and lysed *in situ* - where DNA damage in single cells is detected as an increased migration of DNA material from the cell cavity site towards the anode, giving the appearance of a "comet" when stained and visualised using fluorescence microscopy.

NLS and MGE were suitable for detecting DNA damage and repair after a clinically relevant dose and each exhibited similar dose response curves over 0.5 - 10 Gy (with MGE proving the more sensitive at doses > 2 Gy). However, the techniques showed: (i) no correlation between basal DNA damage, radiation-induced damage and repair proficiency and (ii) no significant differences in HF-DNA sedimentation and electrophoretic behaviour between donor and patient groups. Both assays detected individuals who displayed a poor DNA repair proficiency. The relationship of DNA damage and repair to radiosensitivity (determined from cell survival) was also investigated. The potential of MGE to study the molecular processes of DNA repair and predict *in vivo* tumour and normal tissue radiation response was discussed. The future of MGE as a simple, rapid screening test for unusual radiosensitivity was highlighted.

Publications

(i) Deeley, J.O.T., Moore, J.L., and Mitchell, S.J., (1989). Nucleoid sedimentation assessment of repair in irradiated lymphocytes. *International Journal of Radiation Biology.*, Vol. 55, No. 5, 882 (Abstract)

(ii) Deeley, J.O.T., Moore, J.L., and Mitchell, S.J., (1990). Microgel electrophoresis and nuclear lysate sedimentation measurements of DNA repair. *International Journal of Radiation Biology.*, Vol. 57, No. 6, 1268-1269 (Abstract)

(iii) Deeley, J.O.T., Mitchell, S.J., Sanders, J.A., and Moore, J.L., (1991). Microgel electrophoresis: a predictive test of radiosensitivity. *International Journal of Radiation Biology.*, Vol. 60, No. 6, 947 (Abstract)

CONTENTS

CHAPTER THREE: RESULTS

List of Abbreviations

NLS   Nuclear Lysate Sedimentation

MGE   Microgel Electrophoresis

LGT   Low gelling temperature (agarose)

NGT   Normal gelling temperature (agarose)

Gy   Gray

HF-DNA   Histone-Free DNA

ssb   Single-strand break

dsb   Double-strand break

SD   Sedimentation Distance

CTM   Comet Tail Migration

CHF   Comet Head Fluorescence

List of Tables

Table

List of Figures

Chapter One:

Introduction

1.1. The Problem of Radiosensitivity

Radiation has been used in the treatment of human cancer for almost a century. Since its introduction as a therapeutic tool, clinicians have aimed to administer radiation doses that are high enough to eradicate tumour bulk but do not cause excessive damage to the normal tissues surrounding the tumour. However, it has long been recognised that patients display diverse individual variation in the extent of damage expressed in normal tissue. The possible development of radiation-induced injuries is a limiting factor of the techniques used in radiotherapy to control and manage various malignancies. Currently, appropriate dosage regimes are determined on a basis of experience of population responses and a consensus of opinion regarding the occurrence of normal tissue damage the clinician is obliged to accept.

Acute radiation sensitivities initiating nausea, diarrhoea and skin erythema are commonly known to occur during and for some weeks after treatment and are occasionally reported to interfere with a planned treatment programme. Certain individuals display chronic reactions for example, late skin telangiectasia, excessive fibrosis and tissue necrosis causing irreversible damage so that the total dose necessary for curative radiotherapy is unobtainable (Turesson, 1989). Further, in a particular treatment regime where a standard dose is applied, some individuals have been known to present little or no adverse reaction while others will develop severe complications months or even years after treatment causing an unacceptable occurrence of associated morbidity, (Visser, 1985).

From similar observations, it has been indicated by Sabovljev *et al.* (1985) that a "safe" dose of radiation might prove to be unsafe for unusually radiosensitive individuals and a planned programme of treatment not feasible without the occurrence of major complications.

Post-Radiotherapy Complications of Cervical Cancer

The need for an "individualised" patient treatment regime is illustrated clearly when analysing the late radiation effects in normal tissue after combined irradiation for invasive carcinoma of the uterine cervix (Perez *et al.*, 1984). Different combinations of external fractionated irradiation (usually four fields to the mid plane of the pelvis) and intracavity continuous brachytherapy is common when radiation is used as the main modality in treating this disease (Joslin *et al.* 1972; Visser *et al.* 1985). However, the base of the bladder and the anterior wall of the rectum may receive an unexpectedly high dose from the intracavity sources, (Mak *et al.*, 1987). Resultant complications have been classified according to the degree of severity, (Perez *et al.*, 1984):

> **Grade 1** - Minor symptoms mainly diarrhoea, bladder and rectal irritation, responding to simple out-patient management.
>
> **Grade 2** - Major symptoms including rectal ulcer, moderate partial sigmoiditis, malabsorption syndrome, chronic cystitis and ureteral stricture, often requiring hospitalisation for diagnosis and non-surgical management.
>
> **Grade 3** - Severe complications (occurring months or years after treatment) such as small bowel perforation, rectal, sigmoid or small bowel obstruction, vesicovaginal or ureterovaginal fistula and rectal or bladder ulcer, which require major surgery or are life threatening.

In a retrospective analysis, Perez *et al.* (1984) indicate that the total percentage of patients developing Grade 2 and Grade 3 complications. These were approximately 10% and 8% respectively with a quarter of the patients demonstrating more than one sequela. They record that the most significant factor affecting the appearance of complications was the total dose of irradiation delivered to the pelvic organs. Unal *et al.* (1981) determined that an incidence of about 7% severe complications were limited only to those

patients who had received more than 35 Gy of external beam irradiation in combination with more than 9000 mg-hrs of radium (approximately 5.5 Gy). Hamberger *et al.* (1983) established that similar complications occurring in 3, 10 and 14% of patients correlated to whole pelvis dose values of 40, 50 and 60 Gy in combination with 5000-6000 mg-hrs of radium (approximately 3.5 Gy) respectively. It has been proposed by Deeley & Moore (1989) that severe complications "attributed to radiotherapy" found in approximately 5% of a large group of patients receiving 45 Gy in twenty-five external fractions and 6 Gy in four intra-cavity insertions may correlate to some of the same individuals being particularly sensitive to radiation.

Normal Tissue Damage is related to DNA Damage and Repair

The concept that certain individuals display intrinsic cellular radiosensitivity is based upon evidence that radiation damage expressed in normal tissue is largely a result of damage to the genetic material deoxyribose nucleic acid (DNA), (Coggle, 1983; Elkind, 1985; Teoule 1987; Powell & M^CMillan, 1990; Whitaker, 1992). Damage to enzymes and cell membranes may also be critical (Coggle, 1983; George *et al.* 1987; Soszynski & Schuessler, 1991) but it is thought that such effects may reveal interference with the correct functioning of DNA. As knowledge of chromatin structure and genome organisation have increased and techniques for separating chromatin into functionally distinct subfractions have advanced, accumulated evidence suggests that both DNA damage and repair display patterns of intragenomic heterogeneity (Bohr, *et al.*, 1987). Also, studies of a number of human genetic disorders, for example, xeroderma pigmentosum, Fanconi's anaemia and ataxia telangiectasia suggest that a correlation exists between defective DNA repair mechanisms and enhanced sensitivity to radiation of both patients and their isolated cells (Duckworth-Rysiecki & Taylor, 1985; Bernstein & Bernstein, 1991). Further, it has been found that mice homozygous for the *scid* mutation

3

have an increased radiosensitivity which is directly related with an inability to repair damaged DNA, (Fulop & Phillips, 1990). It is known that an error in DNA repair can cause the activation of *ras* proto-oncogenes which have a direct role in the initiation of cancer (Bohr *et al.*, 1987), an example of defective DNA repair with a biological endpoint.

Tice & Setlow (1985) have noted that cells and organisms seem to be in a delicate balance between the production of DNA damage and its repair. They commented that should the production of damage increases or the level of repair declines a new steady-state condition for DNA damage will exist. Similarly, extreme radiosensitivity to ionising radiation has been thought to result from a deficiency in the repair of radiation-induced damage (Peacock *et al.*, 1989).

1.2. Radiation-Induced DNA Damage

Ionising radiation generates DNA damage directly and/or indirectly. In the direct effect, excitation of the macromolecule occurs following the absorption and interaction of photons, electrons, protons or neutrons. Indirect action, however, involves indiscriminate multi-site attack by aqueous free radicals generated during water radiolysis (Equations 1 and 2, Allan *et al.*, 1988) which act as intermediaries in the transfer of energy to the DNA.

$$H_2O \longrightarrow H_2O^+ + e^- \qquad\qquad \text{Equation 1}$$

$$H_2O^+ + H_2O \longrightarrow OH^\bullet + H_3O^+ \qquad\qquad \text{Equation 2}$$
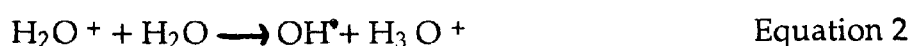
There is support for the dominance of OH radicals in initiating indirect damage to DNA (Wardman & Clarke, 1987; Blackburn & Gait, 1990; Bernstein & Bernstein, 1991) even though much oxidative damage as a consequence of

4

normal respiratory metabolism results in the production of reactive species including peroxide radicals ($HO_2^.$), superoxide radicals (O_2^-) and hydrogen peroxide (H_2O_2) (Bernstein & Bernstein, 1991). Despite debate existing as to whether damage is primarily caused by direct or indirect action, the mechanisms involved are thought to be similar. Schulte-Frohlinde et al., (1985) postulate that DNA base cation radicals formed by direct action, abstract H atoms from deoxyribose in much the same way as $OH^.$

The damage caused by ionising radiation to the physico-chemical structure of DNA assumes a variety of manifestations. For example, histones, closely associated with DNA in nucleosomes, may react with free radicals which affect the oxidation and reduction reactions of pyrimidine and purine bases (Dizdaroglu, 1992). The bases could then be modified chemically by the formation of alkyl, methyl or hydroxyl adducts; or deletion occurs if the glycosidic bonds are hydrolysed (Howard-Flanders, 1981). Adjacent pyrimidines (usually thymine) may be covalently linked as a dimer and pulled out of alignment - a typical effect of UV irradiation (Bernstein & Bernstein, 1991). Altered neighbouring bases may form inter- and intra-strand crosslinks or protein may associate tightly with the DNA in a DNA-protein crosslink, via free radical formation (Oleinick et al., 1987; Howard-Flanders, 1981). Pentoses may be attacked by hydrogen atom abstraction and phosphodiester linkages cleaved causing disruptions in the deoxyribose-phosphate backbone of DNA resulting in single (ssb) or double (dsb) strand breaks (Blackburn & Gait, 1990). Alkali-labile sites are likely to exist and can be revealed as ssb or dsb after alkali treatment (Lafleur et al., 1981). The presence of strand breaks causes a relaxation of the supercoiled higher order structure of DNA (Whitaker et al., 1991). The estimated number and type of radiation-induced lesions produced per Gy of irradiation are presented in Table 1.1.

Table 1.1. Approximate frequency of lesions induced in cellular DNA by ionising radiation (Powell & M^C Millan, 1990).

Type of Damage	Number per Diploid Genome per Gy
Double strand breaks (dsb)	40
Single strand breaks (ssb)	500-1000
Base damage	1000-2000
Sugar damage	800-1600
DNA-DNA crosslinks	30
DNA-protein crosslinks	150
Alkali-labile sites	200-300

All of the lesions outlined briefly constitute insult to the polynucleotide by disrupting base pairing and the continuity of the template which can lead to transcription termination, impairment of replication and decreased cell survival. However, dsb are generally considered to be of greater biological importance as their presence can threaten the integrity of chromatin structure resulting in potentially lethal damage, (Olive et al., 1991a; Bryant, 1984; Blocher, 1982). If not repaired, such damage may be expressed as mutations, recombinations, rearrangements, gross chromosomal abnormalities or gene amplification which affect cell function and correlate with cell death.

1.3. Repair of DNA Damage

DNA repair may be defined as cellular responses associated with the restoration of normal nucleotide sequence and the stereochemistry of DNA following damage. Even though the mechanisms involved are complex and

poorly understood, studies in yeast, bacteria and latterly, rodents and humans (Ross & Brown, 1992) have revealed sets of enzymes which survey the DNA for damage and repair it by restoring the correct nucleotide structure and sequence. A number of enzyme pathways are available to accommodate the different types and varied positioning of lesions produced in DNA.

Direct Reversal Processes

Photoreactivation

Enzymatic photoreactivation is a light-dependent process involving the use of tryptophan residues to sensitise the cleavage of cyclobutyl pyrimidine dimers formed upon exposure to UV light (280-315nm). A deficiency in the photolyase involved may be associated with the radiosensitivity of fibroblasts and lymphocytes obtained from patients with the autosomal recessive disorder, xeroderma pigmentosum (Blackburn & Gait, 1990).

Repair of O6-alkylguanine

Alkylation damage in DNA activates the synthesis of O_6-methylguanine methyl transferase which has a capability to repair O_6-alkylguanine by directly removing the methyl group and transferring it to one of its own cysteine residues. Human lymphoid cells resistant to certain alkylating agents have between ten thousand and twenty thousand copies of this enzyme per cell whereas repair-deficient cells have virtually none (Blackburn & Gait, 1990).

Excision Repair

In mammalian cells, excision repair is believed to be the most important repair mechanism and involves enzyme recognition of a modified base. There are two distinctive types of excision repair, both of which require an undamaged complementary template and appear to be error-free.

Base excision repair

Base excision repair involves two major classes of repair enzymes, N-glycosylases and AP endonucleases. The glycosylases hydrolyse the N-glycosilic bond between the damaged base and the deoxyribose moiety, and produce apurinic or apyrimidinic (AP) sites in the DNA backbone. Glycosylases may exhibit narrow substrate specificity (for example, uracil and hypoxanthine N-glycosylases) or may recognise a wide spectrum of radiolysis products (for example, endonuclease III, (Kow & Houten, 1990). AP endonucleases operate close to apurinic and apyrimidinic sites incising either 3″ to the site (Class I) or 5″ to the site (Class II). The damaged base is removed and the complementary replacement joined to the strand which is then closed by the action of DNA ligase.

Nucleotide excision repair

This repair pathway is mediated by the Uvr ABC nuclease complex which is responsible for the removal of DNA lesions that produce significant distortion of the DNA backbone (Howard-Flanders, 1981). The Uvr ABC complex has a broad substrate specificity and initiates repair by producing two incisions on either side of the lesion. The combined action of Uvr D and Polymerase I are required for the release of the damaged oligonucleotide and the resulting single-stranded gap is then enlarged from thirty to sixty nucleotides by exonuclease action. DNA Polymerase I binds to the strand and fills the gap from the 3′ end until it approaches the 5′ terminus. DNA Polymerase III then extends the process and DNA ligase completes this short-patch repair producing an accurate complementary copy of the undamaged strand.

There is evidence for convergence of the base and nucleotide excision repair pathways as the role of the Uvr ABC complex in repairing thymine glycols has been demonstrated (Kow & Houten, 1990). Any genetic defect in

8

this multi-gene repair system may lead to abnormal susceptibility to skin cancer associated with xeroderma pigmentosum (Blackburn & Gait, 1990; Bernstein & Bernstein, 1991).

Post-Replication Repair

The repair systems described above are rapid and accurate in their completion of DNA repair with high fidelity. However, if repair is slow or deficient and replication by DNA polymerase III is frustrated at the replication fork where parental strands unwind and two daughter strands are synthesised, the "SOS response" or "error-prone repair" is activated.

This response may be induced by a wide variety of damage types and occurs when a sizeable gap (possibly highly variable and over a thousand bases long) is formed opposite the lesion (for example, thymine dimer or methylated arginine). The gap can be repaired by recombination processes during which the Rec A gene-expressed protein binds to the damaged site and aligns it to the other daughter strand, an endonuclease nicks the duplex, a cross-strand exchange takes place and the upper heteroduplex is repaired by DNA Polymerase (Bernstein & Bernstein, 1991). Alternatively, the "SOS response" may be induced in which several rec A proteins bind to the single-stranded stretch of DNA. Rec A is activated as a protease towards the lex A gene protein (a multi-functional repressor of several DNA repair enzymes) and as a consequence of its hydolysis, the derepression of Uvr ABC and rec A genes occur causing increased quantities of repair enzyme production as well as a reduction in the 3' to 5' exonuclease proof-reading activity of DNA Polymerase I. Thus, DNA Polymerase III operates with decreased fidelity until the activation of rec A as a protease discontinues. At this point the "SOS repair" is rapidly switched off.

The action of each of the repair processes outlined above requiring strand cleavage, resynthesis and strand rejoining steps, is complemented by DNA topoisomerases. These enzymes alter the structural conformation of DNA and improve its accessibility to repair enzymes during the repair process. In order to achieve a state of full repair, the topoisomerases then restore the correct topological structure to the DNA superstructure.

Even though these highly accurate repair capabilities of DNA are implicit in its architecture, a defect in just one of the steps briefly outlined above is sufficient to produce a repair deficient phenotype (Ross & Brown, 1992). Errors in "rejoin fidelity" cause a lack of restoration of the damaged areas producing a "misrepaired" status which may lead to incorrect metabolic events in the cell.

1.4. Techniques to Measure DNA Damage and Repair

The repair status of cell populations after exposure to ionising radiation may be examined using a variety of *in vitro* assays based upon: (i) cell growth characteristics for example, counting the number of visually intact cells or the number of colonies remaining following irradiation, (ii) cytogenetic analysis for example, sister chromatid exchange, and (iii) cell metabolism, for example, radionuclide incorporation and dye exclusion techniques. However, all these assays include steps which are relatively time consuming and may retard the production of results for a number of weeks.

As abnormal DNA repair capability and radiosensitivity are related phenomena, it would be of considerable clinical relevance to determine repair proficiency (in terms of remaining DNA damage after repair opportunity) on the same day as sample extraction. As the majority of lesions remaining after inadequate repair can be transformed into strand breaks, a number of techniques have been developed in which remaining damage may be readily

detected. The nature of the lesion detected and the relative sensitivities of the techniques outlined below may be found in Table 1.2.

Sucrose Velocity Sedimentation

Velocity sedimentation has been used extensively since the early 1960's to determine the shape and size of many macromolecules and the factors influencing the sedimentation rate of DNA (including strand breakage). M^{C}Grath & Williams (1966) introduced a technique of releasing extracted DNA onto the top of an alkaline sucrose gradient to study single-strand breaks The alkali treatment inactivated degradative enzymes, removed proteins and separated the two strands of the double-helix. The number of strand breaks could be calculated from the size distribution of the fragmented DNA molecule throughout the gradient.

The physical properties of DNA (its size and molecular weight) and the concentration necessary for sedimentation were associated with the 'wall effect' and the collapse and gelling of gradients, (Ahnström, 1988). Further, it was found that long centrifugation times were required which caused the density gradients to destabilise. Thus, the inadequacies identified in this technique were thought unreliable for the sensitive detection of DNA damage.

Alkaline Elution

Elution techniques discriminate DNA fragment sizes by impeding the flow of alkali-treated DNA through polyvinyl chloride or polycarbonate filters with pores of 0.2μm in size. Cells are lysed on the filters and lysing solution is allowed to drip through the filters under the influence of gravity removing most molecules other than DNA. A peristaltic pump is then used to pump an alkali solution through the filters which is collected in fractions. The amount of DNA retained on the filters is plotted as a function of elution time. This

technique has been used to measure ssb, dsb, alkali-labile sites, DNA-protein crosslinks and DNA interstrand crosslinks (Kohn, 1981).

A major advantage of the alkaline elution technique is that very simple inexpensive instrumentation is required and a large number of samples may be processed simultaneously. However, this technique has been shown to be less sensitive than other DNA damage assays, (Crump et al., 1990).

Viscoelastic Measurements

Viscoelastic measurements are performed by submerging a cylindrical rotor (which is caused to rotate by an electromagnetic force) into a cell lysate in a larger cylindrical container. DNA damage initiating relaxed supercoils causes unwinding of the macromolecule and retards the rotor as it recoils from its original position. A retardation time is then determined as a function of increased hydrodynamic volume. Wun & Shafer (1982) have shown that retardation time increased with increasing dose up to about 2 Gy, from 2 to 10 Gy a plateau was reached and then above 10 Gy it decreased indicating a saturation of response. The technique seems to be sensitive at low doses in assessing DNA conformational disturbances, yet the nature of the lesions involved remain unknown.

DNA Precipitation

This technique is based upon an assay first developed by Smith (1962) to measure DNA protein binding. In precipitation assay described by Olive et al. (1988), cells are lysed in an a non-ionic detergent (2% sodium dodecyl sulphate, pH 12) followed by the addition of potassium chloride. The resultant precipitate contains protein and undamaged DNA, while DNA damaged by strand-breakage remains in the supernatant after low speed centrifugation (3500 rpm for 10 minutes). The proportion of DNA remaining in the supernatant is then used as a measure of DNA damage. The cells can be lysed

12

in neutral or alkaline solution for the estimation of dsb and ssb respectively.

There are a number of advantages of this technique including its ease and speed of performance, sensitivity for strand-break detection, and large sample handling capacity. However, the exact nature of the lesion measured remains unknown as well as the effect upon sensitivity of the presence of DNA-protein and DNA-DNA crosslinks (Olive *et al.*, 1988). Further, when performed in comparison with other methods, this technique has been shown to vary with the damaging agent being studied, (M^CMillan *et al.*, 1990).

Pulsed-Field Gel Electrophoresis

The recent advent of pulsed-field gel electrophoresis (PFGE) has dramatically extended the separation and resolution of high molecular weight DNA fragments ranging from twenty kilobase pairs to intact chromosomal DNA of more than twelve million base pairs (Erixon *et al.*, 1990) The technique is based upon the phenomenon that large DNA molecules exhibit almost size-independent mobility in agarose gel. Hence, if the molecules are forced to change their direction of migration periodically by alterations in the applied electrical field, the mobility of the DNA will depend upon the rate at which the fragments can reorientate in the changing electrical field. The actual size of the DNA fragments can then be measured directly by liquid scintillation counting of labelled DNA in gel slices, when calibrated against standards of known molecular weight (usually yeast chromosomes). The technique has been used in the study of random induction of dsb in cellular DNA and has also been used to detect such lesions as low as 2 Gy.

PFGE represents a powerful technique with the major advantage of enabling the measurement of DNA fragment size directly. However, dispute exists as to the exact nature of the quantitative analysis of electrophoretic profiles as well as concern of interference caused by lysis conditions not yielding naked DNA *per se* .

Table 1.2. Relative sensitivities of DNA damage assays

(Whitaker et al., 1991)

Assay	Lesion and dose for DNA damage detection
Sucrose velocity sedimentation	ssb > 5 Gy dsb >15 Gy
Alkaline elution	ssb 1-2 Gy dsb > 5 Gy dpc > 30 Gy base > 2 Gy
Viscoelastic	ssb 0.3-10 Gy
DNA precipitation	ssb 1-20 Gy dsb > 40 Gy
PFGE	dsb > 1 Gy

Whitaker et al. (1991) cite a number of other techniques used as standard methods in the detection of DNA damage. Examples of these include alkaline gel electrophoresis (Kovacs et al., 1990), membrane filtration (Center et al., 1970) alkaline unwinding (Ahnström et al., 1974; Rydberg, 1975), halo assay (Vogelstein et al., 1980) and high performance liquid chromatography (Srinivasan et al., 1990).

A comparison of pulsed-field gel electrophoresis, neutral sucrose gradient centrifugation and non-unwinding filter elution has indicated that these techniques yield similar estimations of DNA dsb induction despite their widely different biophysical basis (Iliakis et al., 1991). However, comparisons of techniques designed to detect changes in DNA tertiary structure, the detection of ssb or dsb, respectively, have not yielded comparative results. For the purposes of the present study, two techniques which are based upon different principles for strand break detection and display discrepancies in results so far

obtained (Deeley & Moore, 1990) have been chosen: Nuclear Lysate Sedimentation and Microgel Electrophoresis.

1.5. Nuclear Lysate Sedimentation

This technique is considered to be a sensitive procedure, detecting changes in DNA supercoiling and topological structure (van Rensburg, 1987) as well as being one of the simplest available. It is based on the lysis of isolated cells in the presence of a non-ionic detergent and high salt concentration to release a histone-free DNA complex (HF-DNA), followed by a rate zonal centrifugation in neutral sucrose gradients. The HF-DNA complex or "nucleoids" are protein-depleted-permeabilised nuclei in which DNA is organised into supercoiled loops (Stephens & Lipetz, 1983). Radiation-induced strand breaks cause a relaxation of the DNA which is associated with an alteration in sedimentation behaviour due to density changes. As the damaged DNA sediments less rapidly during centrifugation than its more compact undamaged counterpart, repair proficiency is defined as the extent the sedimentation distance of an irradiated sample after incubation resembles that of a non-irradiated sample.

The nucleoid sedimentation technique was first described by Cook & Brazell, (1976) who demonstrated that white blood cells incubated at 37°C for 5 hours post-irradiation (9.6 Gy) restored the nucleoid sedimentation distance to that of non-irradiated nucleoids. They suggested a possible application could be in screening populations for abnormal repair mechanisms. Fender & Malz, (1980) observed that a 1 hour incubation period was sufficient to restore the sedimentation distance of lymphocyte DNA from healthy donors following a 1 Gy dose. Harris *et al.*, (1985) studied hypersensitivity to gamma irradiation in patients suffering from autoimmune disease; less than 50% repair was observed when cells isolated from such patients were subjected to a 2 Gy dose

followed by a 1 hour incubation at 37°C. The same authors also studied radiosensitivity of lymphocytes in relation to donor age; a much higher proportion of lymphocytes from older donors (age 66-99) displayed deficient repair proficiency than did younger donors (age 18-63) after a 2 Gy dose and a 1 hour incubation.

Sabovljev *et al.*, (1985) studied a patient being treated for a T-cell lymphoma who was unusually sensitive to radiotherapy. There was no restoration in the sedimentation behaviour when lymphocytes irradiated *in vitro* were incubated for 1 hour prior to HF-DNA extraction. Deeley & Moore, (1989) investigated the repair proficiency of *in vitro* irradiated lymphocytes from healthy donors, new radiotherapy patients, well post-radiotherapy patients and patients with post-radiotherapy complications. After a 4.5 Gy dose, followed by a 1 hour incubation, it was observed that lymphocytes from most healthy donors, new patients and well patients showed a good repair proficiency (greater than 0.60) whereas 44% of patients with complications showed poor repair (less than 0.30).

The potential of nucleoid sedimentation as a predictive assay of DNA repair proficiency was illustrated more recently by Vaughan *et al.*, (1991) who reported a correlation between nucleoid sedimentation in tumour cells present in urine and tumour response to radiotherapy in patients with carcinoma of the bladder.

1.6. Microgel Electrophoresis

Individual cells embedded in agarose are lysed under mild alkali conditions (pH 10), subjected briefly to an electric field, stained with a fluorescent DNA-binding dye and visualised using a fluorescence microscope. The relaxed DNA structures from irradiated cells are displaced from the cell cavity site towards the anode giving the appearance of a "comet" with a head

and tail region. As the migration is more pronounced in damaged than undamaged cells, repair proficiency is measured by comparing the electrophoretic profiles (tail length and/or head intensity) of individual cells from the irradiated and incubated (37°C) samples to those of the unirradiated sample. An outline of the development of the MGE technique is found in Table 1.3.

Table 1.3 Development and comparison of MGE technique

Study	Lysis conditions	Electrophoresis Conditions	Measurement of DNA damage	Range
Östling & Johanson (1984, 1987)	Neutral (pH 9.5), SDS for 1 hr	5V/cm, 5 min EDTA/SDS (pH 9.5)	Ratio of fluorescence	Gamma rays 0-3 Gy
			Number of cones	3-400 Gy
Singh et al. (1988)	2.5M NaCl/Triton +Na-sarcosinate (pH 10) for 1hr, 20min unwinding	0.83V/cm, 20-40 min EDTA/NaOH	Tail length	X rays 0-2 Gy
Tice et al. (1990)	2.5M NaCl/Triton + Na-sarcosinate (pH 10) for 1hr, 20 min unwinding	0.83V/cm, 20-40 min EDTA/NaOH (pH 13)	Tail length	UV irradiation 6-24 J/m^2
Olive et al. (1990)	0.03M NaOH, 1M NaCl for 1hr	4V/cm, 12 min Tris/acetic acid (pH 8.3)	Tail length Tail moment	X rays 0-3 Gy 0-15 Gy
Deeley et al. (1990)	2.5M NaCl/Na-sarcosinate (pH 10) for 5 min	0.83V/cm, 30 min EDTA/NaOH (pH 13.28)	Tail length	Gamma rays 0-5 Gy
Green et al. (1992)	2.5M NaCl/Triton +Na-sarcosinate (pH 10) for 1 hr, 40 min unwinding	0.66V/cm, 24 min EDTA/NaOH	Tail length	Uvc irradiation 0-8 J/m^2
Olive et al. (1993)	1M NaCl+NaOH, 2mM EDTA for 1 hr	0.5V/cm, 1M NaCl+NaOH 2mM EDTA for 25 min	Tail moment	Etoposide 0-10µg/ml

The MGE technique is based upon an empirical method of assessing DNA damage in single cells first described by Östling & Johanson (1984). They reported that the lower damage detection limit for murine lymphoma cells was below 0.5 Gy and that a plateau in the dose-effect curve was reached at 3 Gy. Residual DNA damage was found to be present after a post-irradiation incubation of 1 hour. In 1987 the same authors found that bleomycin, in contrast to gamma irradiation, produced extreme variations in strand breakage of Chinese hamster ovary cells (CHO) grown *in vitro* - an early indication of the assay's ability to quantify heterogeneity of DNA damage within a cell population. Singh *et al.*, (1988) studied human peripheral lymphocytes that were exposed to a range of doses (0.5 to 2 Gy of X-rays) or treated with hydrogen peroxide (9.1 to 291µM). Likewise, migration patterns were relatively homogeneous among cells exposed to X-rays but heterogeneous among cells treated with hydrogen peroxide. An analysis of repair kinetics (using tail length as an indicator of damage) following exposure to 2 Gy of X-rays indicated that the bulk of DNA repair occurred within the first 15 minutes of incubation, while all of the repair was essentially complete by 2 hours after exposure.

Olive *et al.*, (1990) have used a video image analysis technique to define appropriate "features" of the comet and have quantified damage and repair in terms of a "tail moment" - the product of the amount of DNA in the tail and its mean distance of migration. In both normal and tumour cells of a murine fibroblastic tumour, they found that both cell types showed significant heterogeneity in damage induced by ionising radiation and suggested similar radiosensitivity even though the amount of damage increased linearly with dose (0-15 Gy). The technique has been modified further by Olive *et al.*, (1991a) to detect radiation-induced dsb in populations of cells exposed to X-ray doses as low as 5 Gy. Approximately 85% of the breaks were rejoined within 2 hours of irradiation in murine lung fibroblast and ovary cell lines; but in the

radiosensitive murine leukaemic lymphoblastic line, about 50% of the damage was still present 2 hours after exposure. Olive *et al.*, (1993) have also used the technique to study DNA damage induced by etoposide (a topoisomerase II inhibitor) in murine fibroblast cells. Generally, differences in DNA strand breakage between cells grown as monolayers and cells grown as spheroids correlated well to cell kill using both the MGE and DNA precipitation assays. Gedik *et al.*, (1992), have compared MGE to alkali unwinding assays to estimate the relative sensitivity of the technique. They analysed UV-C (254nm) induced DNA damage and its subsequent repair in HeLa (human transformed epithelial) cells and suggested that the MGE detects as few as 0.1 strand breaks per 10^9 daltons.

1.7. Aims of a Comparative Study

From the studies outlined above, the potential of Nuclear Lysate Sedimentation and Microgel Electrophoresis as a quick, simple and sensitive techniques for measuring DNA damage and repair in a population of cells and in individual cells is apparent. In the present study, peripheral lymphocytes were chosen as suitable cells with which to detect radiation-induced DNA damage and its subsequent repair as they are easily obtained and do not require prolonged culture *in vitro* prior to experimentation (Agarwal *et al.*, 1981). Also, lymphocytes are believed to be the most radiosensitive of non-dividing cells in the human body (Cohen & Thompson, 1986). Both NLS and MGE will be used concurrently to compare the repair proficiency of lymphocytes from: (i) healthy volunteers, (ii) new patients presenting in the clinic with cancer of the uterine cervix prior to radiation treatment, (iii) post-radiotherapy patients described as "well and complication free" and (iv) post-radiotherapy patients who have developed bowel and/or bladder complications. Patients with cancer of the cervix were considered as a suitable

patient group to study because: (i) the majority of patients are generally well and mobile, (ii) sufficient numbers of patients with post-radiotherapy complications are available for study, (iii) the expected post-radiotherapy complication rate is between 5-10% and, (iv) the post-radiotherapy complications associated with the treatment of cervical cancer are well-defined.

The aims of this study are as follows:

(i) To assess the efficiency, efficacy and reliability of NLS and MGE techniques to detect radiation-induced DNA damage and its subsequent repair in human lymphocytes.

(ii) To compare the relative sensitivities of both techniques in their detection of radiation-induced DNA damage and its subsequent repair.

(iii) To validate direct DNA damage assessment and radiation sensitivity (in terms of cell kill) using three tumour cell lines of differential radiosensitivity.

(iv) To compare the repair proficiency of lymphocytes from healthy volunteers to that of (a) new patients (pre-radiotherapy) presenting in the clinic with cancer of the uterine cervix, (b) post-radiotherapy patients described as "well and complication free" and (c) patients who have developed bowel and/or bladder complications that are attributed to radiotherapy.

This study is directed at gaining an understanding of the relationship between DNA damage, repair proficiency and radiosensitivity. The principal aim of this work is, however, to investigate the potential of the Nuclear Lysate Sedimentation and Microgel Electrophoresis techniques as quick, reliable cellular radiosensitivity assays in the identification of particularly radiosensitive individuals to prevent unnecessary post-radiotherapy complications in clinical practice

Chapter Two:

Materials & Methods

2.1. Human Peripheral Lymphocytes

The Donors Studied

Details of the donor groups studied are presented in Table 2.1. Blood samples comprising the control group were obtained from apparently healthy individuals who were not receiving prescription medication - the identity of whom was known to the operator. Blood samples from patients attending the hospital out-patient clinic were obtained with the patient's permission and at the written request of medical staff - the initial diagnosis was known but the response to radiotherapy was not known.

Table 2.1. The donor groups studied

Donor Group	Mean Age (yrs) and Range	Numbers Studied NLS	MGE CTM	CHF
Healthy males (n=20)	34.5 (22-66)	20	20	7
Healthy females (n=39)	36 (21-51)	39	31	8
New patients (n=38)	58 (21-76)	38	27	15

CTM = Comet tail migration; CHF = Comet head fluorescence

Collection of Blood Samples

A Vacutainer system (Becton-Dickenson) was used to extract 10 to 20ml of venous blood from patients and healthy volunteers. The blood was collected into 13 x 75mm evacuated blood collection tubes containing 143 units (U.S.P) of lithium heparin and kept at room temperature (about 18°C) until required. Generally, the blood was prepared for lymphocyte isolation immediately after donation.

21

Isolation of Lymphocytes from Whole Blood

The whole blood was divided into two clear sterile universal containers and mixed with equal volumes of RPMI 1640 (Gibco) medium (pH 7.4 and 18°C) containing L-glutamine, 3mM HEPES and 4.5 mM Na_2HCO_3 using a 10ml pipette. Plastic screw-top lids were secured and both containers were inverted once to ensure mixing of the blood and medium. The diluted blood was then underlayed with a 5ml cushion of Histopaque 1077 (Sigma) using a 10ml sterile syringe and 22 gauge hypodermic needle.

The diluted blood was centrifuged using a MSE Mistral 3000i temperature-controlled bench centrifuge at 500g for 30 minutes at 19°C. After centrifugation a band of cells at the plasma/cushion interface was collected using a Pasteur pipette and added to fresh RPMI 1640 medium in two 13ml plastic conical centrifuge tubes (Celcult, Sterlin). The contents of the tubes were mixed by inversion and centrifuged at 200g for 10 minutes at 19°C. After the supernatant was decanted, the cell pellet was resuspended in fresh medium and the washing procedure repeated. The resulting pellet of lymphocytes was resuspended in 5 to 7.5ml (depending upon the amount of whole blood originally drawn) of fresh RPMI 1640 supplemented with 5% foetal calf serum (Gibco).

Prepared lymphocytes were generally used the same day but when kept overnight were stored at 4°C in supplemented medium and used the following morning. Overnight storage did not seem to affect the number of mononucleated cells which fluoresced brightly in ultraviolet light following the addition of acridine orange.

Estimation of Cell Numbers

A 75μl sample of the final lymphocyte preparation was added to the same volume of an acridine orange/phosphate buffered saline (PBS) solution and cell numbers were estimated using an improved Neubauer

haemocytometer counting chamber. The cells were counted under a low power magnification (x16) using a Zeiss epi-fluorescence microscope. When viewed under ultraviolet light (using a blue filter) the viable cells fluoresced green (Frenster, 1972).

This method was used to gain an estimation of cell viability when accurate numbers of viable cells were required for experimentation and cell survival studies performed on the cell lines. However, when determining the cell numbers for sub-culturing purposes, unstained cells were counted under transmitted light.

2.2. Cell Lines

MOLT-4

The MOLT-4 cell line was established by Minowada *et al.*, (1972) from a 19-year-old male who was receiving chemotherapy for acute lymphoblastic leukaemia. The cells resemble relatively mature lymphocytes and carry surface antigens present in normal T-cells and human thymus leukaemia. MOLT-4 is an especially interesting cell line since after irradiation it shows Na^+-dependent amino acid transport (Kwock *et al.*, 1979) and reduced K^+ transport (Szekely *et al.*, 1982) which correlates with the appearance of dead cells 3 - 5 hours after the irradiation, (Szekely & Lobreau, 1985).

The cells were obtained from Flow Laboratories, Scotland (Gibco) and grown in RPMI 1640 (Gibco) containing 10% heat-inactivated foetal calf serum (Gibco) and antibiotics (0.05% streptomycin sulphate (Evans) and 0.05% sodium benzylpenicillin (Glaxo). The line was maintained in suspension culture in loosely capped upright 25cm^3 culture flasks (Nunc) at 37°C in a humidified atmosphere of 5% CO$_2$ in air. The cells were harvested every 7th day and subcultured at a seeding density of 1x10^5 cells per ml in 30ml. The population doubling time was approximately 15 hours.

DAUDI

The DAUDI cell line was first established in tissue culture by Klein *et al.*, (1968) and originated from a 16-year-old male who was receiving treatment for Burkitt lymphoma (a highly malignant disease of lymphoblasts derived from B lymphocytes). The cells are characterised by three types of chromosomal translocation which constitutively activate the c-myc oncogene by juxtaposing it to Ig coding sequences (Masucci & Klein, 1991).

The cell line was obtained from Flow Laboratories, Scotland, maintained as a 5ml suspension cultures under the same conditions as the MOLT-4 line but were subcultured every 3-4 days. The population doubling time was approximately 26.5 hours.

V79

The V79 cell line was derived from Chinese hamster lung fibroblasts and maintained as attached monolayer cultures. The cells were trypsinised and subcultured every 3 to 4 days in 5ml of Dulbecco's modified eagle medium (DMEM) containing 5% v/w foetal calf serum and 5% w/v new born calf serum and antibiotics (0.05% streptomycin sulphate and 0.05% benzylpenicillin). The cells were grown under the same conditions as the MOLT-4 and DAUDI lines. The population doubling time was approximately 18.5 hours.

Cell Survival Studies

Exponentially growing MOLT-4, DAUDI and V79 cells were harvested and resuspended in fresh culture medium to examine the effect of increasing doses of radiation on cell survival. Cell concentrations of $5x10^4$ per ml in 5ml for the V79 and DAUDI lines and in 30ml for the MOLT-4 line were dispensed into twenty-four $25cm^2$ tissue culture flasks, (Nunc). Each set of three flasks were gamma irradiated under a Caesium source at 0.5, 1, 2, 3, 5, 10 and 20 Gy

respectively, with three control flasks remaining unirradiated. The flasks were incubated at $37^{\circ}C$ in a humidified atmosphere of 5% CO_2 in air. Where possible, every twenty-four hours cell numbers were estimated in MOLT-4 and DAUDI from the mean of one full haemocytometer count (4 quadrants of a Neubauer haemocytometer counting chamber) from each of three flasks that were exposed to the same radiation dose. In V79, however, as the cells grew as an attached monolayer culture, cell numbers were estimated from the mean of three sets of ten cell counts of the number of cells growing over a fixed area ($10\mu m^2$) on the bottom of the tissue culture flasks. This was performed to avoid trypsinisation which may have caused additional damage to the cells. Cell counts were performed for up to eight days after irradiation.

The fraction of clonogenic cells surviving following gamma irradiation was determined in an independent experiment from that described above. Three hundred cells in a total 5 ml of medium were plated into three $25cm^2$ tissue culture flasks for unirradiated cells and cells that were to receive $0..5$, 1, 2, 3, 5 and 10 Gy, respectively. The flasks were incubated for seven days (5% CO_2 in air) after which the cells were fixed and stained with crystal violet. All the colonies containing 50 or more cells were scored.

2.3. The Nuclear Lysate Sedimentation Technique

An outline of the NLS technique is presented in Figure 2.1.

Formation of Linear Sucrose Gradients

Buffered sucrose solutions containing 5%, 10%, 15% or 20% sucrose respectively and 2M NaCl, 1mM EDTA-(Na), 10mM Trisma (Sigma), pH 8, and $1\mu g/ml$ of Hoechst dye 33258 (Bisbenzimide) were made up to 1 litre with distilled water, autoclaved at 15psi at $120^{\circ}C$ for 10 minutes and stored at $4^{\circ}C$ until required.

0 Gy   2 Gy

0.75 x 10⁶ lymphocytes

NP40 Detergent

nucleus   ●

2M NaCl

Histone-Free DNA

Lysate layered onto sucrose
gradients and spun at 48,000g
for 17.5 mins at 10 °C

0%

2M NaCl

Sucrose   HF-DNA band

20%

0 Gy   2 Gy   2 Gy
(+ incubation)

Assessment of DNA Damage and Repair
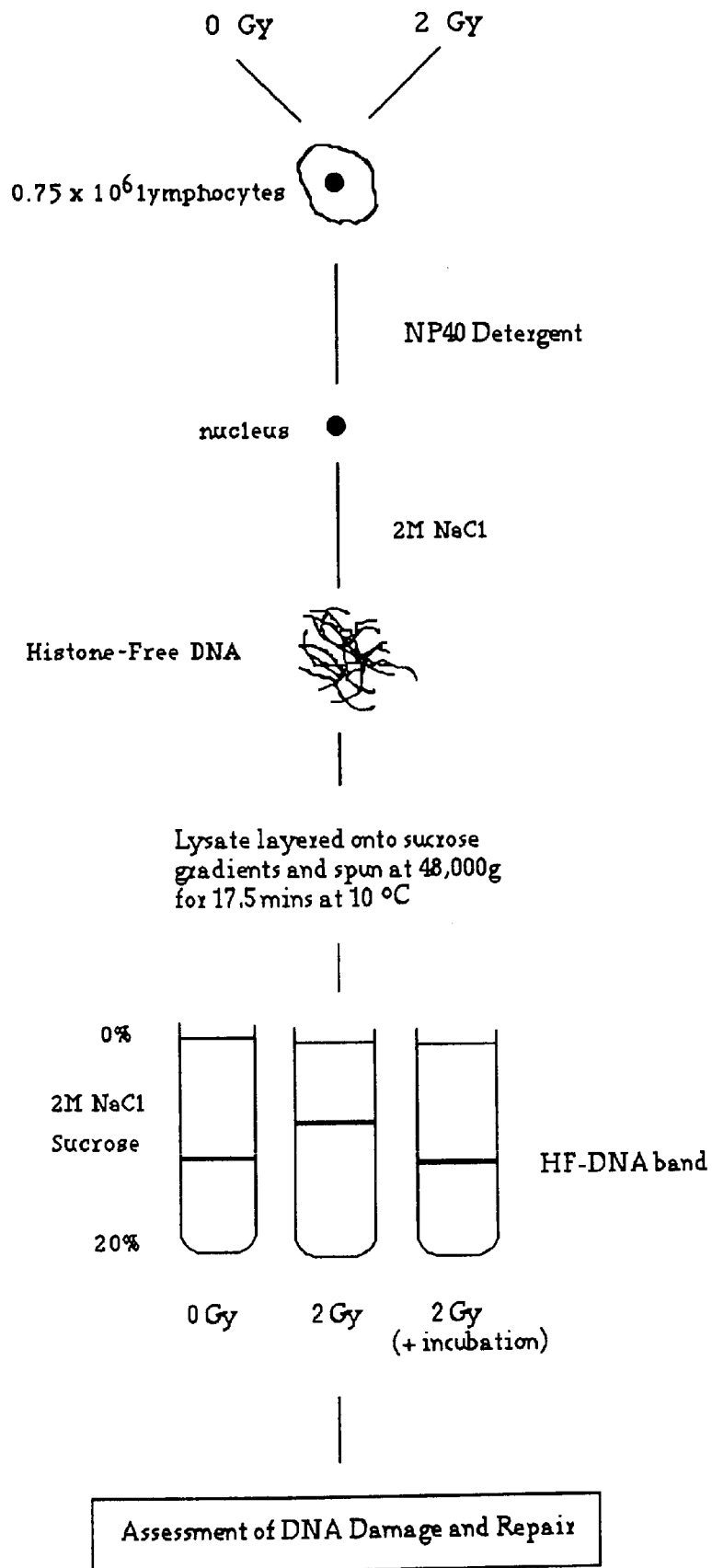
Figure 2.1. Outline of the Nuclear Lysate Sedimentation Technique.

26

Eight polycarbonate centrifuge tubes (25ml nominal capacity, cross-sectional area 2.45cm^2) were placed in a rack and capped with a needle holder containing eight blunted, large-bore (22 gauge) hypodermic needles. A 5ml calibrated polypropylene syringe was used to introduce 4ml of a 5% buffered sucrose solution into each tube. Likewise, 4ml of a 10% and 15% and finally, 5ml of a 20% sucrose solution were slowly underlayered so that the less dense solution was underlayered by a more dense solution. A stepwise gradient of 5, 10, 15 and 20% sucrose was thus formed of total volume 17ml and of 55mm in height in each of the eight tubes. The needle holder was removed, the tubes covered with "Labfilm" and left for two hours at room temperature (approximately 18°C) in order for a 5 to 20% linear sucrose gradient to generate. The tubes were then carefully placed in a refrigerator at 4°C for 30 minutes before use.

Determination of the Linear Nature of Prepared Sucrose Gradients

A Multiperpet 2115 peristaltic pump (LKB Bromma) attached to a Support elevator S9298-3 labjack was flushed with distilled water and a needle (connected to the pump via a rubber tube) was placed at the bottom of a centrifuge tube containing a prepared linear gradient. Twenty drop-fractions were collected into each well of a "multiwell" plate until all of the gradient had passed through the pump. The percentage sucrose concentration was estimated on every fifth well using a pocket refractometer to determine the refractive index of the solutions.

Irradiation Procedure

Aliquots of 0.75 x 10^6 lymphocytes from the final cell suspension were dispensed into eight 13ml plastic conical tubes. The volume of medium in each tube was made up to 1ml with 5% foetal calf serum supplemented RPMI 1640 medium so that each cell sample was irradiated in the same volume.

Dose Response Irradiation

Eight tubes containing 0.75×10^6 cells were cooled on ice for 10 minutes prior to gamma irradiation. Six tubes were then placed separately in a plastic beaker containing perpetual ice cubes and cold water and each irradiated at different doses, for example, 0.5, 1, 2, 3, 5, 10 Gy depending upon the experimental requirements. For irradiation, a beaker containing the appropriate tube was placed under a double-headed [137] Caesium source (0.66 MeV) and exposed at a dose rate of 0.92 Gy per minute. The dose rate was determined by both a Farmer dosimeter fitted with a thin walled ionisation chamber and Li^7F thermoluminescence dosimetry, conducted by the Physics Department at Velindre Hospital.

Repair Assay Irradiation

For repair studies following 2 Gy irradiation, eight tubes containing 0.75×10^6 cells were placed on ice for 10 minutes after which three tubes were irradiated on ice at 2 Gy. All eight tubes were then incubated in a waterbath at 37°C for 1 hour and then placed on ice for 5 minutes. One of the tubes that had not been previously irradiated was exposed to 4 Gy and one of the previously irradiated tubes was further irradiated at 2 Gy along with the remaining two tubes that had not been previously irradiated.

In summary, of the eight tubes, two were left unirradiated (controls), two were irradiated at 2 Gy prior to incubation (repair), two were irradiated (2 Gy) directly after incubation (damage), one tube was irradiated before and after incubation (2 Gy split-dose) and the final tube irradiated for 4 Gy after the incubation period (4 Gy damage).

Isolation and Centrifugation of Lymphocyte HF-DNA

Immediately after the final irradiation all eight tubes were centrifuged at 200g for 5 minutes at 4°C. The tubes were returned to the ice bath (containing perpetual ice cubes and water), supernatants discarded and the

pellets resuspended in the residual liquid by gentle agitation of the tubes. 2 ml of ice-cold "Nonidet reagent" (NP40) (0.25% w/v Nonidet P40 (Sigma), 0.25M sucrose and 3.3mM $CaCl_2$) was added to each tube and incubated on ice for 10 minutes. NP40 is a non-ionic detergent which gently lyses the plasma membrane releasing intact nuclei.

The resultant nuclei were harvested by bench centrifugation at 500g for 3 minutes at 4°C. The supernatants were discarded, and the pellets resuspended in the residual liquid by agitation of the tubes. The nuclear material of each sample was released by the addition of 0.5ml of lysis reagent (2M NaCl, 1mM EDTA-$(Na)_2$, 10mM Trisma, pH 8). The resulting clear viscous suspensions (containing HF-DNA) were immediately layered, using a 1ml disposable wide-bore plastic pipette, just below the surface of the appropriate 17ml 5-20% linear sucrose gradient.

The eight polycarbonate centrifuge tubes containing gradients were sealed with individual aluminium screw-on caps each with an "O" ring seal and loaded carefully into an 8 x 25ml aluminium alloy fixed angle rotor centrifuge head. The head was positioned in a MSE 65 superspeed Mark 2 ultracentrifuge and spun for 17.5 minutes at 42000g (an average of 28000 rpm) at 10°C. Typically, there was an initial run up time of 4.5 minutes and run down time of 9.5 minutes on either side of the centrifuge run.

Visualisation of the HF-DNA Complex

After centrifugation, the HF-DNA bands were visualised using long-wave ultraviolet illumination (365nm) in a 4°C dark room. The positions of the fluorescent bands of HF-DNA/Hoechst dye complex were examined and the middle of each band marked. The bands were photographed through a Kodak gelatin 2B ultra-violet barrier filter, using 35mm FP4 (Ilford) film rated at 125 ASA. The position of each band was measured, in millimetres, from the centre of the mark to the bottom of each

centrifuge tube against a 5 centimetre scale on a right-angled perspex stand.

The ratio of the HF-DNA sedimentation distances of irradiated cells compared to that of the HF-DNA sedimentation distances of unirradiated cells was used as a measure of damage. Likewise, the repair proficiency of irradiated cells was expressed as the ratio of the shift in sedimentation distance of HF-DNA extracted from irradiated cells incubated for 1 hour at 37°C compared to the shift in sedimentation distance of HF-DNA from unirradiated cells (see equation below). Full restoration of the HF-DNA complex to the original state was indicated by a repair proficiency of 1.0 with less than 1.0 indicating a less proficient repair.

Thus:

$$\text{Repair Proficiency} = \frac{\text{('Repair' SD) minus ('Control' SD)}}{\text{('Damage' SD) minus ('Control' SD)}} - 1$$

where SD=sedimentation distance (mm)

2.4. The Microgel Electrophoresis Technique

An outline of the MGE technique is presented in Figure 2.2.

Preparation of Microscope Slides

Aliquots of the final lymphocyte preparation or the cell culture sample were dispensed into a 13ml plastic tube and placed in a water bath at 37°C for at least 30 minutes before use. Cell counts usually ranged from 1×10^5 to 1×10^6 per ml. Three 8ml glass test tubes containing aliquots of 0.5% normal gelling temperature (NGT) agarose (BDH), and aliquots of 1% and 0.5% low-gelling temperature (LGT) agarose, type vii (Sigma) prepared in sterile calcium and magnesium-free phosphate buffered saline (PBS), were placed in

Microscope slide with layer of normal gelling temperature agarose

Cells in low gelling temperature agarose layered onto a prepared microscope slide

5 min in lysis solution

Formation of comets after 30 mins electrophoresis (25V, 300mA)

-ve

+ve

Neutralisation of lysis and electrophoresis buffers, staining with a fluorescent dye and visualisation using fluorescence microscopy

Figure 2.2. An Outline of the Microgel Electrophoresis Technique

a 50cm^3 beaker of water and heated to boiling point on a Rodwell monotherm hotplate stirrer. The aliquots (usually 2 to 4ml) of both types of agarose were prepared previously in phosphate buffered saline and refrigerated at 4°C until required.

After having reached boiling point, the LGT agarose was cooled to 37°C before mixing with cells. Meanwhile, 150μl of the 0.5% NGT agarose was pipetted as a thin horizontal streak across the centre of three pre-cleaned fully-frosted microscope slide and a No.1 Chance propper coverslip (22 x 50mm) was held at an angle of 45° and gently slipped over the agarose to form a smooth layer beneath the coverslips. The layer of agarose across the surface of the slides was then allowed to set by placing the slides on an ice tray for a 30 seconds. The layer of 0.5% NGT agarose was used as a base for the firm attachment of a second layer of agarose containing cells. The second layer was formed by first mixing approximately 5x10^4 cells with an equal volume of 1% LGT agarose at 37°C. The coverslips were removed from the microscope slides and a 75μl sample of the cell/agarose mixture was dispensed as a streak across the base layer of agarose and a coverslip was placed on each slide. The slides were placed horizontally on an ice-cooled metal tray for 30 seconds to allow solidification of the gels. After gently removing the coverslips, the slides were covered with a third layer of 75μl 0.5% LGT agarose (maintained at 37°C until required), the coverslips replaced and the slides kept in small humidified plastic boxes at 4°C for 10 minutes prior to irradiation. A longitudinal section of a prepared microscope slide is shown as a diagrammatic representation in Figure 2.3.

Irradiation Procedure

The irradiation procedure for the microgel technique was similar to that of the nuclear lysate technique for both dose response and repair assays. The irradiations were performed separately from those of the nuclear lysate
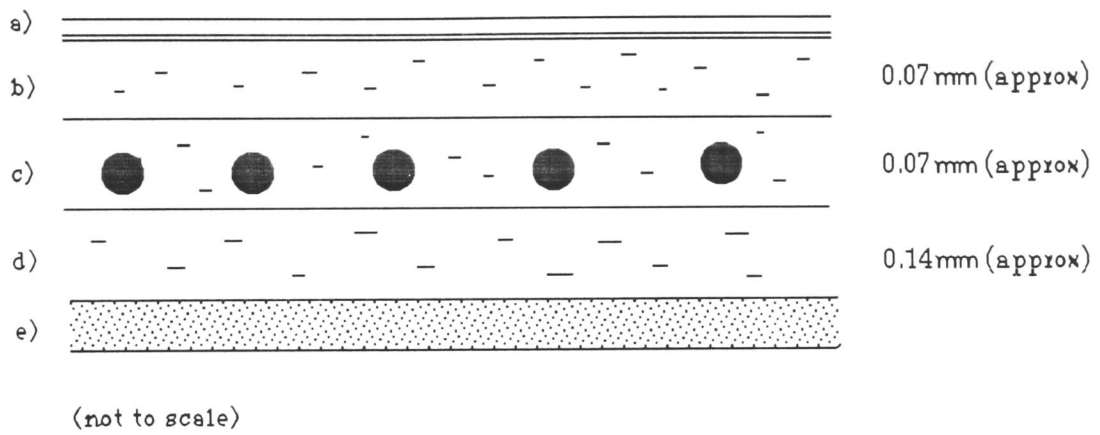
a) No. 1 (22 x 50mm) glass cover slip

b) 75µl LGT agarose

c) 75µl LGT agarose and nutrient medium containing lymphocytes

d) 150µl NGT agarose

e) 76 x 25mm fully frosted microscope slide

Figure 2.3. Diagramatic representation of a prepared microscope slide.

technique with the appropriate cooled slides placed in the centre of the double-headed ^{137}Cs source to ensure as little radiation scatter as possible. For the repair assay, the slides were kept in small humidified plastic boxes and placed in a 5% CO_2 in air humidified incubator at 37°C.

Lysis and Electrophoresis Conditions

Immediately after the final irradiation, the slides were immersed in an ice-cold lysing solution (30% w/v sodium sarcosinate, 2.5M NaCl in de-ionised water and adjusted to pH 10 with 2M NaOH) for 5 minutes to lyse the plasma and nuclear membranes and remove histone proteins from the DNA. The slides were gently removed from the lysis solution using forceps and placed in a row in a horizontal DNA sub cell (Biorad) electrophoresis chamber containing about 1500ml of fresh electrophoresis buffer (0.3M NaOH, 1mM EDTA in de-ionised water, pH 13.3). The voltage and current were set prior to adding the slides by adjusting the level of buffer in the chamber. Typically, the buffer was about 0.5cm above the slides and electrophoresis was conducted for 30 minutes at 25V (0.862V/cm) using a compact electrophoresis power supply EPS 500/400 (Pharmacia Fine Chemicals).

Each of the above steps were conducted under dim orange light (Ilford filter S902) to prevent any additional DNA damage by ultraviolet light from fluorescence strip lighting and sunlight.

Staining and Visualisation of Comets

After electrophoresis, the slides were placed horizontally on a tray and flooded slowly with a neutralisation buffer (0.4M Tris, pH 7.5) to remove alkali and detergents which may interfere with ethidium bromide staining. After 5 minutes the neutralisation buffer was drained off the slides and 75µl of 2% ethidium bromide constituted in distilled water was placed onto each slide. The slides were covered with clean glass coverslips and placed in humidified

3 4

containers to prevent any shrinkage of the gels. Generally, the slides were viewed immediately after staining; although overnight storage did not affect the appearance of DNA migration patterns.

Observations were made using a Leitz Dialux 20 fluorescence microscope fitted with a band pass exciting filter 530-560nm, a beam splitting mirror with reflection short pass filter of 580nm and a suppression long pass filter of 580nm (the N2 filter block) using a low magnification (x16) objective lens. The comets were visualised under green light as red areas of particulate matter. Generally, about 10-15 comets were present per field under a total magnification of x200

Comet Analysis

Measurements of the length of comet "tails" and the fluorescence intensity of comet "heads" were recorded as indicators of DNA damage and repair.

Photography

A Leica (R3 MOT Electronic) camera loaded with Ilford HP5 negative film was attached to the fluorescence microscope and each slide was scanned at random using a 16x objective lens. Fields containing a suitable number of comets (for example, 10 or more) that were well spaced from each other and at the same depth in the gel were photographed. Usually six exposures of each slide were taken. The film was exposed for about 30 seconds and push - processed for 10 minutes in Kodak D76 developer at 20°C (nominal rating 800ASA).

The photomicrograph negatives were viewed on an X-ray light box and comet length measurements made using a pair of dividers. The comet tail length was defined as the distance from the centre of the comet head to the visible end of the comet tail. If heads only were present, the whole diameter of the head was taken and then divided by two. The measurements

were recorded in millimetres and converted to microns from a previous calibration. Damage was determined as the increase in the length of the material drawn towards the anode in relation to that of the control. Repair proficiency was calculated from the ratio of the shift in comet tail migration after a irradiation to the shift in comet tail migration after irradiation and a 1 hour incubation at 37°C (see equation below).

Repair proficiency = $\dfrac{\text{('Repair' CTM) minus ('Control' CTM)}}{\text{('Damage' CTM) minus ('Control CTM')}}$ — 1

where CTM = Comet tail migration

Photometry

A Leitz MPV compact photometer was connected to the fluorescence microscope as a complete attachment unit. Fluorescence was measured at 525nm using a Phloemopak filterblock filter and mirror system. The emitted light from individual comets passed the selection filter and thus the intensity of ethidium bromide bound to single-stranded DNA giving red fluorescence was recorded. The readings were taken over a fixed area (using a x25 objective lens and x250 total magnification) judged from the relative size of the head area of the comets on the control slide. Five readings of the background intensity were taken in the vicinity of the comets, fifty comets were chosen at random on each slide and the fluorescence intensity of the comet head measured.

Radiation-induced DNA damage was expressed as the decrease in the fluorescence intensity of the head area of comets from irradiated cells compared to the control. Repair proficiency was calculated from the shift in fluorescence intensity of comet heads of irradiated cells incubated at 37°C for 1 hour, compared to the shift in fluorescence intensity of comet heads from irradiated cells comprising the "damage" sample (see equation below).

3 6

Repair proficiency = $\dfrac{\text{('Repair' CHF) minus ('Control' CHF)}}{\text{('Damage' CHF) minus ('Control' CHF)}} - 1$

where CHF = comet head fluorescence

Chapter Three:

Results

3. 1. PRELIMINARY STUDIES

Initial studies suggested that NLS and MGE determine repair proficiency to a similar extent but that the assessment of DNA damage may differ (Deeley *et al.*, 1990). Prior to running both techniques concurrently, to compare the extent of DNA damage and repair detected, preliminary work was performed to examine the nature, sensitivity and reliability of NLS and MGE.

Nuclear Lysate Sedimentation

3.1(a). *Linear Nature of Sucrose Gradients*

The linear nature of the sucrose concentration in the gradient was estimated from refractometer readings of fractions, collected dropwise, from a 5-20% sucrose gradient. The gradient was linear (Figure 3.1.) except for the presence of a "cushion" of high and low sucrose concentration at the bottom and top of the column respectively.

Generally, sedimentation distances of HF-DNA, isolated from lymphocytes and tumour cell lines (unirradiated and irradiated), ranged from 10 to 34mm from the top of the gradient. Figure 3.2. shows that over this range there was a good linear fit to the data ($r^2 = 0.967, p < 0.001$), suggesting that the gradients were suitable for the estimation of radiation-induced DNA damage following low exposure to radiation.

3.1(b). *HF-DNA Band Stability and Reproducibility*

Following lysis ('NP40' and 2M NaCl) and centrifugation (48,000g av.), material from nuclei (obtained from 0.75×10^6 human lymphocytes) passed through a 55mm high 0-20% linear sucrose gradient containing Hoechst dye forming a distinct band of HF-DNA. This was approximately 2mm in thickness and fluoresced brightly when illuminated in long wave ultraviolet light (365nm).
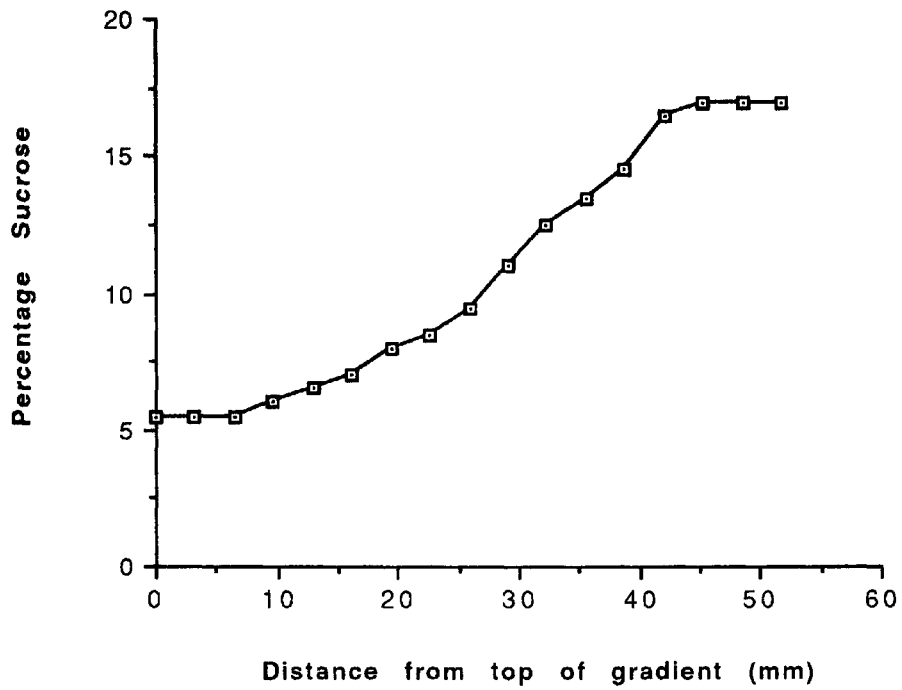
Figure 3.1. Linear nature of 5-20% sucrose gradients. Fractions were collected into 20 drop aliquots and the sucrose concentration of every 5th fraction estimated using a pocket refractometer.
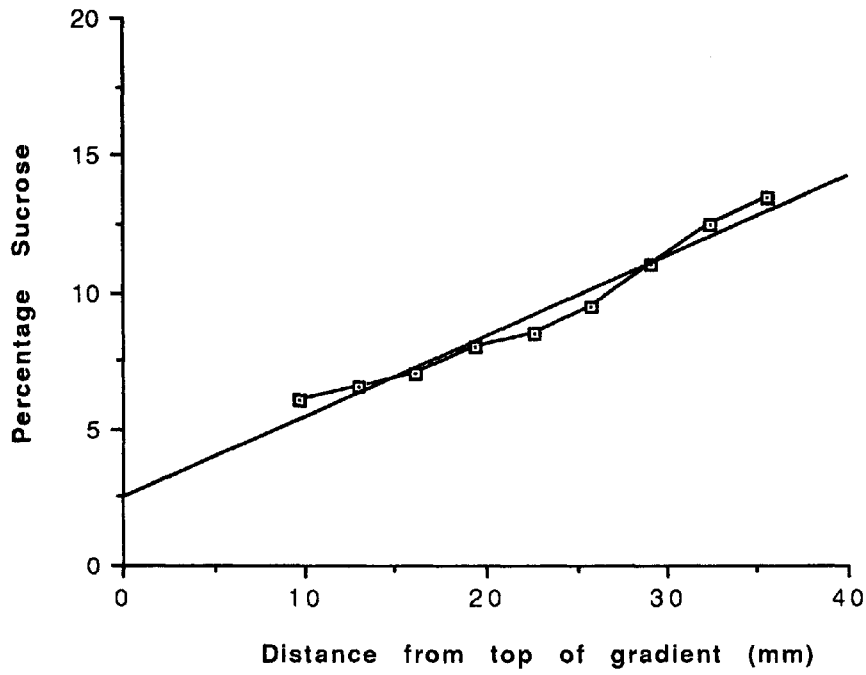
Figure 3.2. Derived from Figure 3.1 to show the linearity of sucrose concentration in the region of the gradient where the majority of post-irradiation shifts in sedimentation distance were recorded (r^2=0.967, slope=0.30, $p < 0.001$).

The diagrammatic representation in Figure 3.3. illustrates that HF-DNA was sensitive to physical shearing. As the stability of HF-DNA bands was dependent upon operator handling and a gentle pipetting technique, the reproducibility of sedimentation distances of HF-DNA layered by the same operator was examined on an intra-sample and an inter-gradient basis (Table 3.1.). Small variation (CV < 14%) was found in the sedimentation distances of unirradiated HF-DNA in each of the four donors. Similar variation was found in the sedimentation distances of irradiated HF-DNA in donor c. Again, small variation was observed when the sedimentation distances of unirradiated HF-DNA were compared in three separate centrifugation runs (donor d). Thus, the gentle transfer of nuclear lysate onto the top of sucrose gradients did not appear to damage the HF-DNA and good reproducibility was produced on an intra-sample and inter-gradient basis.

3.1(c). Damage Effect of Gamma Irradiation on HF-DNA

A reduction in the sedimentation distance of HF-DNA following gamma irradiation has been attributed to damage caused to the compact DNA supercoiled structure. The presence of a single or double strand break in a supercoiled loop or domain causes a relaxation in the DNA within that domain. In consequence there is a decrease in density of the HF-DNA, which is reflected as a reduction in sedimentation distance (van Rensburg et al., 1989). Figure 3.4. shows that, for a healthy donor, there was a dose-related decrease in the sedimentation distance of the HF-DNA from in vitro irradiated lymphocytes over the range 0.5-10 Gy. Typically, there was a linear dose response in sedimentation behaviour as shown in Figure 3.5. The shift in sedimentation distance per Gy shown in Figure 3.6. illustrates that the dose response is linear over low doses (0.5-2 Gy) but is non-linear over the higher range.

A dose of 2 Gy was chosen as a determinant of DNA damage as: (i) nuclear lysate sedimentation measurements are sensitive in the 2 Gy range, (ii) 2
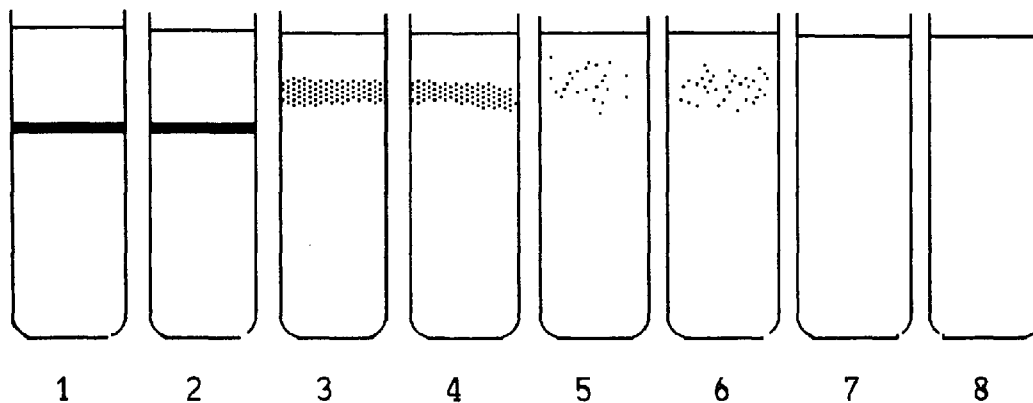
(a) 1&2: Well-defined HF-DNA bands with high sedimentation distance

(b) 2&4: Less compact HF-DNA bands with low sedimentation distance

(c) 5&6: Fragmentation of HF-DNA without discernable band

(d) 7&8: No HF-DNA bands observed

Figure 3.3. Shearing forces and HF-DNA band stability in 8 unirradiated lymphocyte populations $(0.75 \times 10^6$ cells) from the blood sample of a healthy donor. Cells were lysed and treated as follows prior to normal layering and centrifugation: normal layering technique (1&2); 2 gentle agitations with a pasteur pipette (3&4); 4 vigorous agitations with a pasteur pipette (5&6) and 2s vortex using a bench mixer (7&8).

Table 3.1. Reproducibility of unirradiated and irradiated (2 Gy) lymphocyte HF-DNA band sedimentation distances.

Donor	Gradient	Mean sedimentation Distance (mm ± 1 SD)	Coefficient of variation (%)
a	1	26.29 ± 1.22 (n=7)	4.64
b	2	22.12 ± 1.30 (n=8)	5.88
c	3	22.81 ± 2.81 (n=8)	12.32
c*	4	23.50 ± 2.57 (n=6)	10.94
d	5	8.40 ± 1.14 (n=5)	13.57
d	6	10.25 ± 1.26 (n=4)	12.29
d	7	9.40 ± 0.89 (n=5)	9.47

n = number of HF-DNA bands measured in each centrifugation run; * = lymphocytes irradiated (2 Gy) prior to HF-DNA extraction; CV = 14.24% for inter-gradient HF-DNA bands in donor d with no significant difference between gradients ($p > 0.06$ at 95% significance level in one-way analysis of variance).
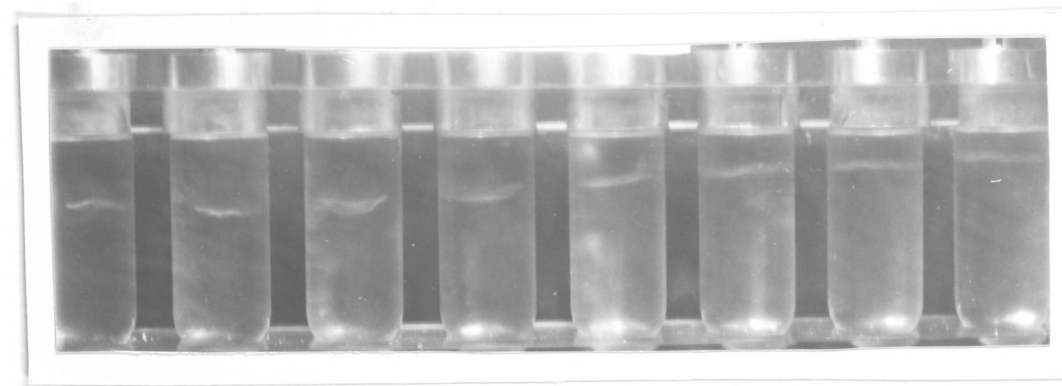
Figure 3.4. Gamma irradiation response (0.5-10 Gy) of lymphocytes from an apparently healthy donor. The fluorescent bands in the first two tubes on the left of the photograph represent the sedimentation distance of unirradiated HF-DNA. The next six tubes (left to right) represent the sedimentation distance of HF-DNA after exposure to 0.5, 1, 2, 3, 5, and 10 Gy respectively.
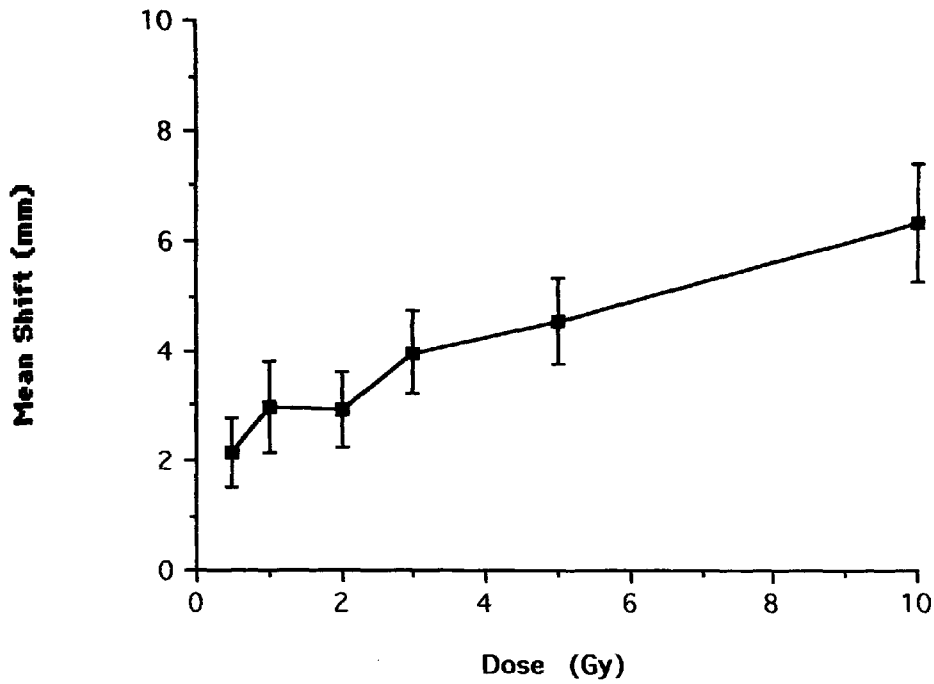
Figure 3.5. Effect of gamma irradiation (0.5-10Gy) on the sedimentation distance of peripheral lymphocyte HF-DNA obtained from nine apparently healthy donors. Each point represents the mean shift in sedimentation distance between unirradiated and irradiated HF-DNA from the nine donors at each dose respectively. The range bars indicate standard error of the mean.
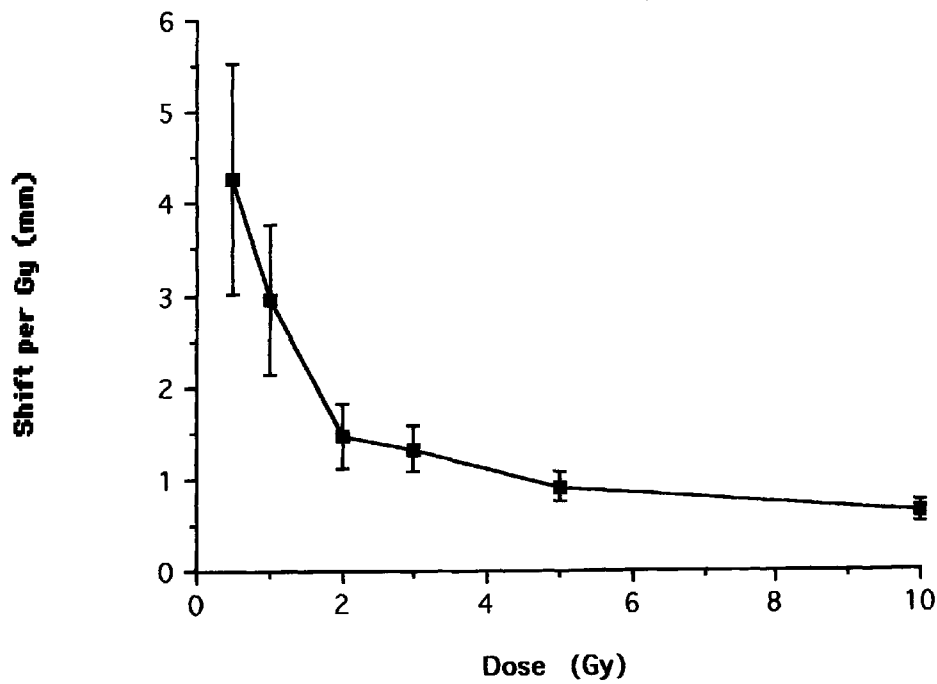
Figure 3.6. The response per Gy of lymphocyte HF-DNA from the same nine donors as Figure 3.5. Each point was derived by dividing the mean shift in sedimentation distance by the radiation dose received. The standard error of the mean is shown.

45

Gy produces a measurable shift in the sedimentation distance between unirradiated and irradiated HF-DNA and, (iii) 2 Gy administered at a high dose rate (0.92 Gy/minute) is a clinically relevant dose of gamma radiation. To maximise the '2 Gy shift' (the difference in HF-DNA sedimentation distance between unirradiated cells and cells irradiated with 2 Gy), various centrifugation times were investigated. Figure 3.7. shows that under the conditions employed there was an optimum centrifugation time of 17.5 minutes. It had previously been shown that these centrifugation conditions were the most suitable, (J.O.T. Deeley, personal communication).

3.1(d). Restoration of HF-DNA Structure

A restoration of the sedimentation distance of HF-DNA extracted from irradiated cells approaching that of HF-DNA from unirradiated cells can be demonstrated following a post-irradiation incubation at $37^{\circ}C$. The post-incubation restoration in sedimentation distance is indicative of DNA conformational changes associated with repair (Cook & Brazell, 1976). To study repair proficiency, the relative sedimentation distances of duplicate samples of: (i) unirradiated ('control'), (ii) irradiated ('damage'), and (iii) irradiated with a 1 hour incubation at $37^{\circ}C$ ('repair') were compared. Repair proficiency was expressed as the ratio in sedimentation distance of HF-DNA extracted from irradiated cells (incubated for 1 hour at $37^{\circ}C$) compared with the sedimentation distance travelled by HF-DNA from unirradiated cells. Full repair was indicated by a repair proficiency of 1.0 or greater, a less proficient repair was indicated by a repair proficiency of less than 1.0. Figure 3.8. shows that the nuclear lysate sedimentation repair assays of human lymphocyte HF-DNA from two different healthy donors expressed good and poor repair capacity respectively after a 2 Gy irradiation.

The association between post-incubation restoration of irradiated HF-DNA sedimentation distance and DNA repair activity was investigated.
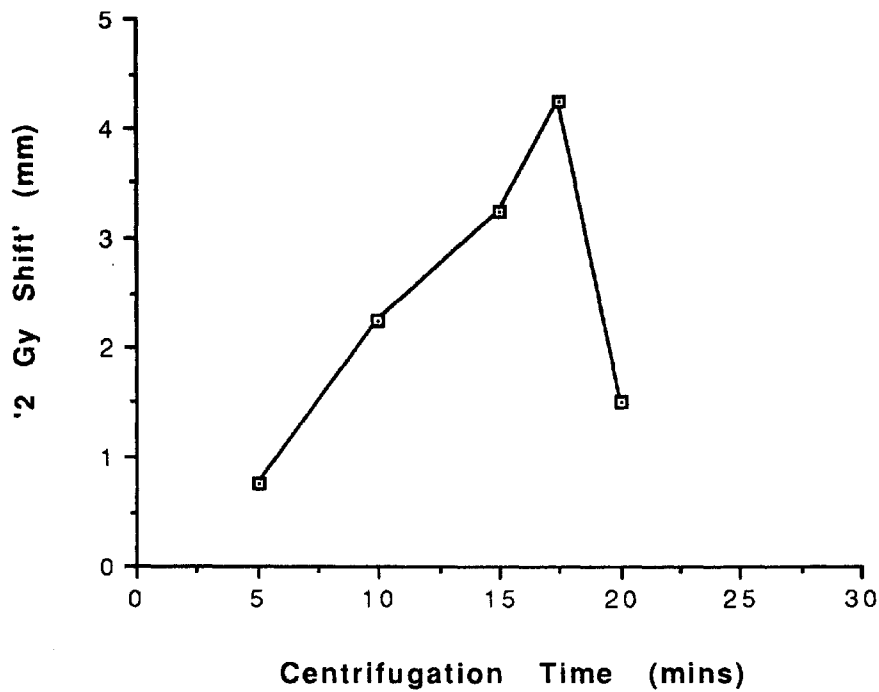
Figure 3.7. The effect of centrifugation time on the '2 Gy shift' of HF-DNA. A sample of human peripheral lymphocytes from an apparently healthy donor was used for five separate centrifugation runs at 48,000g (27500 rpm) for 5, 10, 15 17.5 and 20 minutes, respectively. Each point on the graph represents the '2 Gy shift' derived from the difference between the means of 2 unirradiated and 2 irradiated HF-DNA sedimentation distances.

Good Repair
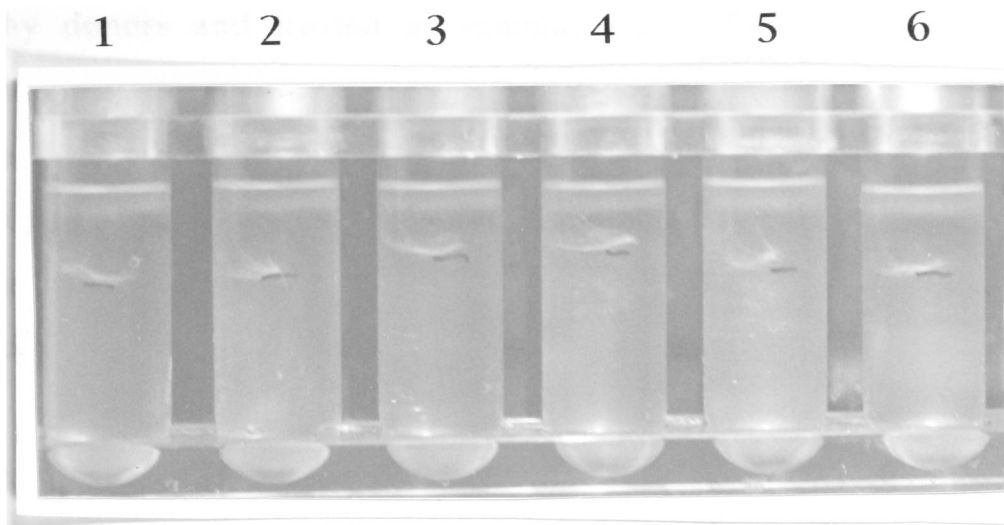
Poor Repair
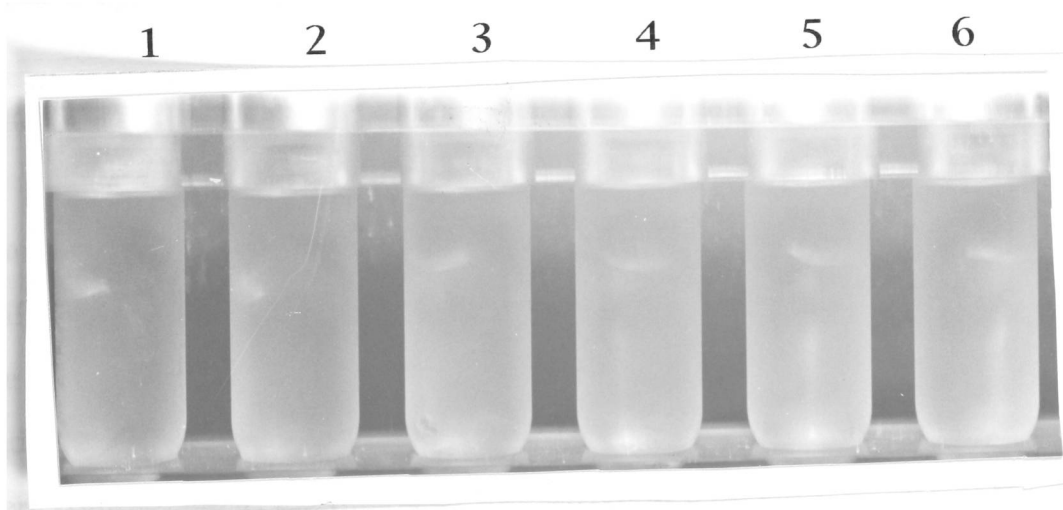
Figure 3.8. Expressions of good and poor repair proficiency. The six tubes in the photographs represent the HF-DNA bands of unirradiated (tubes 1 and 2), irradiated (tubes 3 and 4) and irradiated (2 Gy) followed by an incubation for 1 hour at 37°C (tubes 5 and 6) lymphocyte DNA extracted from two individual donors Figure 3.8(a) illustrates a good repair proficiency with the mean sedimentation distance of irradiated and incubated HF-DNA (tubes 5 and 6) approaching that of the unirradiated sample (tubes 1 and 2). Figure 3.8(b) shows a poor repair proficiency with the mean sedimentation distance of the irradiated and incubated sample resembling that of the irradiated sample (tubes 3 and 4).

Lymphocyte samples were isolated and examined on separate days from seven healthy donors and treated as summarised in Table 3.2. The similar sedimentation distances of unirradiated lymphocytes maintained at 4°C or 37°C indicated that DNA supercoiling was not affected by a decrease in temperature to 4°C for 1 hour. Post-incubation restoration of the sedimentation distance of irradiated HF-DNA to that of the equivalent unirradiated sedimentation distance was dependent upon the incubation temperature. Lymphocytes incubated at 37°C after 2 Gy irradiation expressed similar sedimentation distances to unirradiated lymphocytes, unlike those maintained at 4°C. Thus, the temperature-dependent restoration of HF-DNA sedimentation distance was associated with changes in DNA supercoiling and appeared to be related to repair enzyme activity.

3.1(e). Reproducibility of Nuclear Lysate Sedimentation

Repeat tests on three apparently healthy donors were performed to examine the variation in unirradiated or basal sedimentation distance, '2 Gy shift' and repair proficiency on an intra-sample basis (Table 3.3.). For each donor, the inter-gradient variation in unirradiated (CV < 10%), irradiated (CV < 17%) and irradiated with incubation (CV < 21%) HF-DNA sedimentation distances were comparable to the inter-gradient variation with CV < 14.24% in Table 3.1. The basal sedimentation distances agreed within 0.5mm in all of the measurements for donor a and in two out of three out of the measurements for donors b and c. Likewise the '2 Gy shift' measurements agreed within 0.25mm in two out of three of the measurements for each donor. Good repair proficiency was reproduced in all three centrifugation runs for donor a (ranging from 0.71-1.00) and in two out of three runs in donors b and c (ranging from 1.21-1.80 and 0.71-0.79, respectively). It remains unclear why one of the repair proficiency estimates disagreed in both donors b and c. Generally, the extent of variation

Table 3.2. Effect of incubation temperature on HF-DNA sedimentation distance of human lymphocytes after 2 Gy gamma irradiation.

Treatment of lymphocytes	Mean sedimentation distance (mm ± 1SD)
Unirradiated & maintained for 1 hr at 4°C	19.86 ± 3.67
Unirradiated & incubated for 1 hr at 37°C	19.86 ± 3.80
Irradiated following 1 hr at 37°C	15.25 ± 4.09
Irradiated & maintained for 1 hr at 4°C	16.86 ± 2.62
Irradiated & incubated for 1 hr at 37°C	19.54 ± 2.31

For each of the seven donors, a single centrifugation tube was used for samples that were unirradiated and maintained at 4°C or 37°C whereas two tubes were used for samples receiving other irradiation and incubation treatments.

Table 3.3. Intra-sample variation in basal sedimentation distance, '2 Gy Shift' and repair proficiency of lymphocyte HF-DNA in three apparently healthy donors.

Donor	Centrifugation Run	Mean Basal Sedimentation Distance (mm)	Mean '2Gy Shift' (mm)	Repair Proficiency
a	1	18.00	4.00	1.00
	2	17.75	4.25	0.71
	3	17.50	5.75	0.83
b	1	18.50	2.50	0.60
	2	19.00	3.50	1.21
	3	23.00	3.75	1.80
c	1	21.50	4.75	0.05
	2	21.00	3.50	0.71
	3	25.50	3.50	0.79

For each donor three separate centrifugation runs were performed consecutively on the same day on lymphocyte preparations originating from the same sample. In each centrifugation run, mean basal sedimentation distance, '2 Gy shift' and repair proficiency were derived from repeat HF-DNA band measurements, the largest difference between which was 3mm.

51

between repeat tests on an individual suggests that the procedure is reasonably reproducible.

Repeat tests were also performed on three apparently healthy donors to examine the variation in basal sedimentation distance, '2 Gy shift' and repair proficiency on an inter-sample basis (Table 3.4.). For each donor, the inter-gradient variation in unirradiated (CV < 28%), irradiated (CV < 32%) and irradiated with incubation (CV < 32%) HF-DNA sedimentation distances was generally larger than: (i) the inter-gradient variation of CV < 14.24% in Table 3.1 and (ii) the inter-gradient variation in unirradiated, irradiated and irradiated with incubation HF-DNA sedimentation distances described above in the intra-sample variation study (Table 3.3.). Generally, for each donor (with the exception of samples 1 and 2 in donor a), variation was apparent in basal sedimentation distances. In donors a and b differences in basal sedimentation distance of 8.25mm and 12mm respectively were observed between samples. This may indicate that the technique detects changes in the degree of supercoiling present in unirradiated lymphocyte DNA. The '2 Gy shift' measurements agreed within 1.25mm for all the donors with the exception of sample 2 in donor a. Repair proficiency was similar in two out of three of the samples in donor a (ranging from 0.45-0.50) and in all of the three samples in donor b (ranging from 0.44-0.55) and donor c (ranging from 0.86-1.07). However, repair proficiency in donor a decreased from 1.00 on week 1 to 0.50 and 0.45 by week 20 and 46, respectively. This perhaps indicates that repair proficiency may vary over a period of weeks in some individuals but remain constant in others. Overall, the small extent of variation in '2 Gy shift' and repair proficiency between repeat tests over a period of weeks, however, suggests that the procedure is reasonably reproducible on an inter-sample basis.

52

Table 3.4. Inter-sample variation in lymphocyte HF-DNA basal sedimentation distance, '2 Gy shift' and repair proficiency in samples received over a period of months from three apparently healthy donors.

Donor	Centrifugation Run and Week of Sample	Mean Basal Sedimentation Distance (mm)	Mean '2 Gy Shift' (mm)	Repair Proficiency
a	1 (wk 1)	13.50	5.00	1.00
	2 (wk 20)	14.00	2.00	0.50
	3 (wk 46)	22.25	5.50	0.45
b	1 (wk 1)	13.75	2.25	0.44
	2 (wk 18)	18.00	3.50	0.50
	3 (wk 21)	25.75	2.75	0.55
c	1 (wk 1)	19.00	3.50	1.00
	2 (wk 17)	14.25	3.75	1.07
	3 (wk 18)	16.50	3.50	0.86

In each centrifugation run mean basal sedimentation distance, '2 Gy shift' and repair proficiency were derived from repeat HF-DNA band measurements, the largest difference between which was 3mm.

3.1(f). *Summary*

Nuclear Lysate Sedimentation is a simple, rapid and sensitive technique that detects changes in DNA supercoiling associated with DNA damage and repair. Preliminary investigations have shown the technique to be:

> (i) capable of detecting the effect of radiation-induced DNA damage over a range of 0.5-20 Gy.

> (ii) sensitive in the clinically relevant 2 Gy range.

> (iii) suitable for estimating the repair proficiency of DNA after
> a dose of 2 Gy

> (iv) reasonably reproducible on an intra- and inter-sample basis.

The potential of NLS as an *in vitro* assay of radiation sensitivity is apparent. However, the technique only detects radiation-induced DNA damage and its subsequent repair as a population response in a large number (0.75×10^6) of cells. Nuclear Lysate Sedimentation was therefore studied in conjunction with Microgel Electrophoresis, a technique with the novel ability to detect DNA damage and repair in single cells.

Microgel Electrophoresis

3.1(g). *Gel Casting and Cell Distribution*

A simple casting technique (described in Section 2.4.) was used to embed approximately 1×10^5 single cells in LGT agarose on a microscope slide. Typically, cells were distributed evenly throughout the agarose (as shown in Figure 3.9) which would allow the formation of well-spaced comets after electrophoresis. Even though there was often a poor dispersal of cells around the edge of the slide, alterations in the casting technique or in the volume of agarose/cell suspension mixture would generally cause a less even cell distribution over the centre of the slide.

3.1(h). *Damage Effect of Gamma Irradiation on HF-DNA of Single Cells*

Microscopic examination of individual cells embedded in agarose and subjected to lysis, electrophoresis and staining with a fluorescent dye (ethidium bromide), revealed a "comet" consisting of a brightly fluorescent "head" and a less intense "tail" region. The migration of DNA from the cell cavity site toward the anode is related to the amount of damage sustained by the cell. An increase in comet tail migration of HF-DNA following gamma irradiation has been associated with the induction of single and double strand breaks and the resulting relaxation of DNA within supercoiled domains (östling & Johanson, 1987). Consequently, the DNA is readily disposed to migrate towards the anode during electrophoresis .

The extent of radiation-induced DNA damage (expressed as a dose-related increase in comet tail migration) was assessed by both (i) comet length measurements taken from photomicrograph negatives and (ii) comet head intensity using a fluorescence microscope photometer. To minimise any error due to fading when using comet head fluorescence as an indicator of DNA damage, the fluorescence intensity of unirradiated and irradiated comet heads was

55
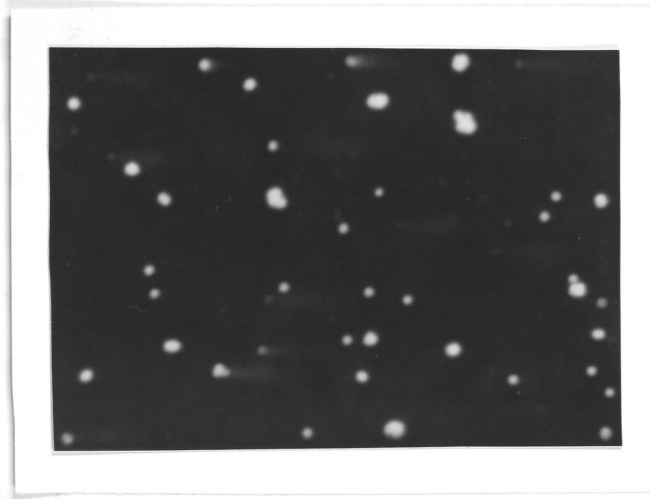
Figure 3.9. The distribution of comets, embedded in agarose, in a typical microscope slide examined in this study. The photograph shows human lymphocytes, stained with acridine orange, (total magnification x100) prior to lysis and electrophoresis.

recorded over time. Figure 3.10. shows that over 24 hours there was a decrease in comet head intensity in the comets of unirradiated cells but not in the comets of irradiated cells. After the first hour of staining, there was no significant difference in the intensity of unirradiated or irradiated comet heads ($p > 0.1$ and $p > 0.4$, respectively using a one-tailed unpaired t test). However, between the first and second hour of staining, a significant decrease in intensity was found in both unirradiated and irradiated comet heads ($p < 0.02$ and $p < 0.01$, respectively). Thus, comet head fluorescence readings were taken manually immediately after staining. The time of illumination and the time between measurements were standardised in order to obtain similar fading in a measuring sequence.

Dose Response to Gamma Irradiation

Figure 3.11. shows that there is a dose-related increase in comet tail migration when lymphocytes from a healthy donor were irradiated over the range 0.5-10 Gy prior to lysis. The photographs indicate that an increase in comet tail migration is accompanied by a decrease in the fluorescence intensity of the comet head as increased amounts of fragmented DNA move out of the cell cavity site towards the anode with increasing radiation dose. Figure 3.12 shows that there is a linear dose response in the increase in comet tail migration and in the decrease in comet head fluorescence with increasing radiation dose over the range 0.5-10 Gy. The 'shift per Gy' in comet tail migration and comet head fluorescence in Figure 3.13. indicates that in MGE, DNA damage is detected (i) as a linear increase in the shift in comet length over 0.5-2 Gy but as a non-linear increase in the shift in comet length over 2-10 Gy and (ii) as a linear increase in the shift in comet head fluorescence over 0.5-3 Gy but as a non-linear increase in the shift in comet head fluorescence over 3-10 Gy.

A dose of 2 Gy was chosen as a determinant of DNA damage as, (i) MGE measurements were sensitive in the 2 Gy range, (ii) 2 Gy produced a measurable shift in the comet tail migration and comet head fluorescence between
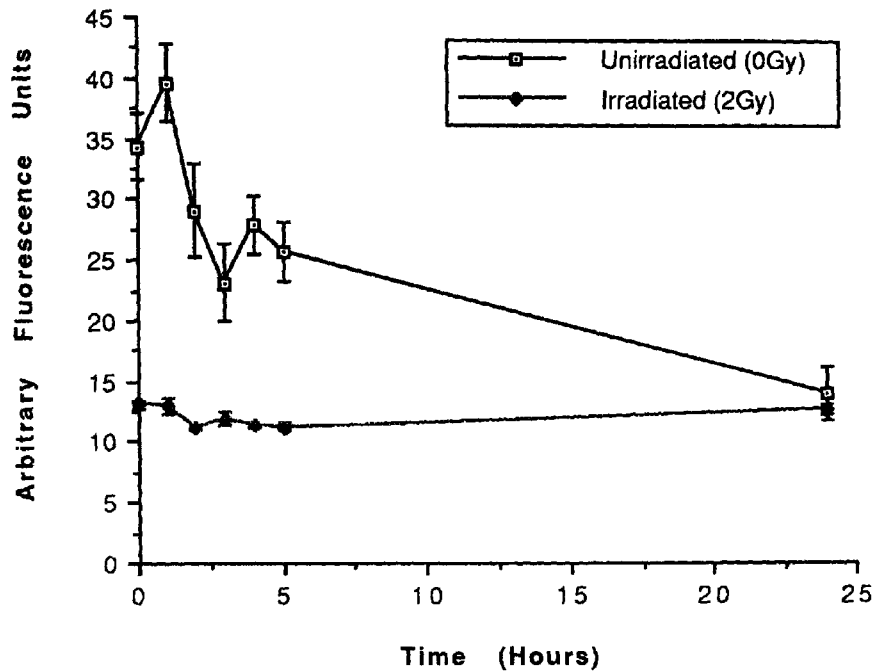
Figure 3.10. Relative decrease in fluorescence intensity of comet heads from unirradiated and irradiated (2 Gy) populations of the same lymphocyte sample over time. Each point was derived, using a microscope photometer, from the mean of 25 random readings minus the mean of 5 random background readings. The vertical bars shown represent the standard error of the mean. To ensure significant decrease in head intensity did not occur whilst recording the initial 25 readings, 25 readings of a single unirradiated and irradiated comet head were performed in the first 4 minutes of the experiment. The resultant mean readings for the unirradiated and irradiated heads were 44.57 ± 0.32. and 14.91 ± 0.75 standard deviations respectively. Samples were stored in the dark at 4°C between readings.

Dose Response

0 Gy

0.5 Gy

1 Gy
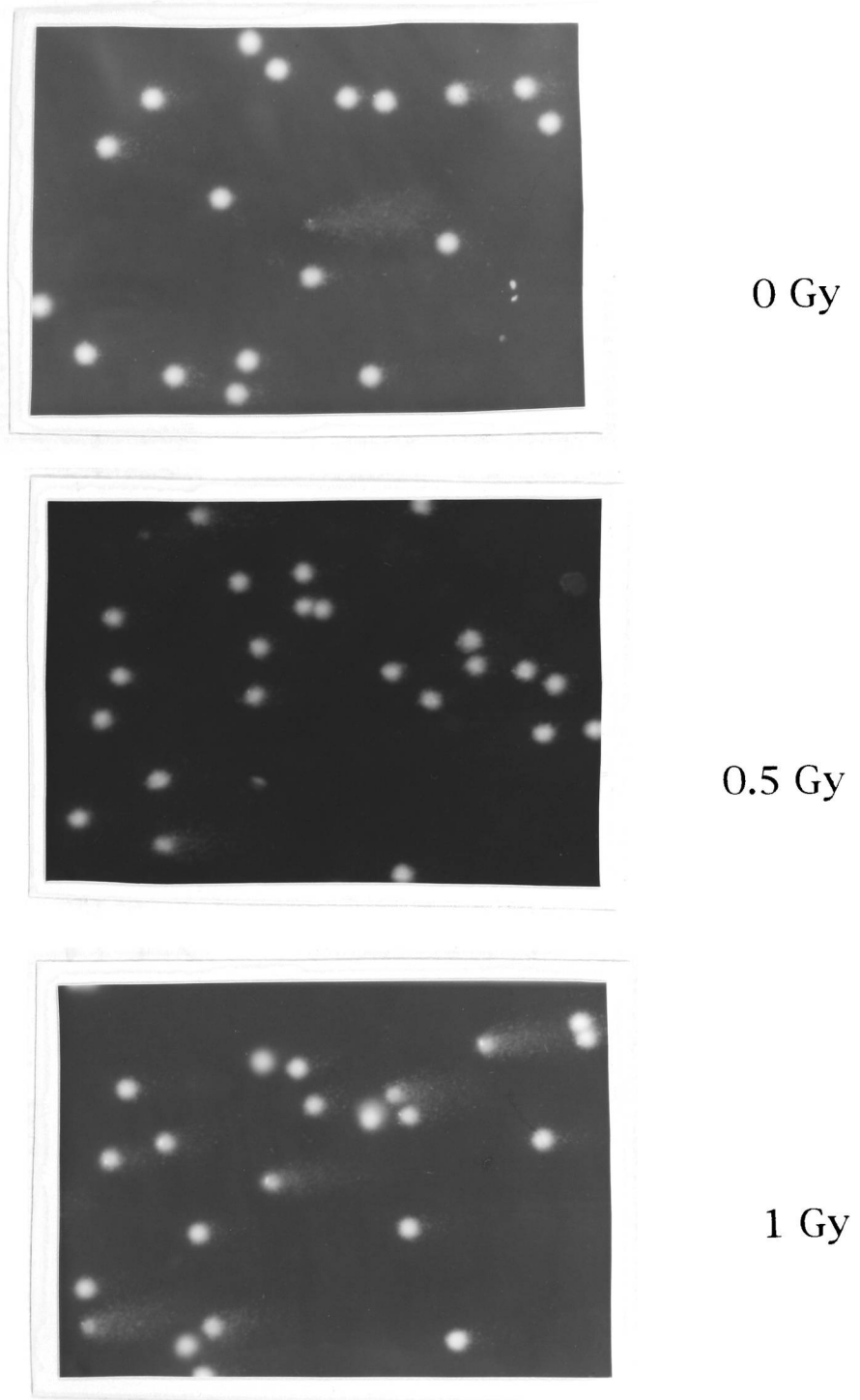
Figure 3.11. Response of a single lymphocyte sample from an apparently healthy donor to gamma irradiation over a range of 0.5-10 Gy. Each of the photographs represents the comets visualised after staining with a fluorescent dye following 0, 0.5 1, 2, 3, 5, and 10 Gy of gamma irradiation, respectively.

Dose Response

60

2 Gy
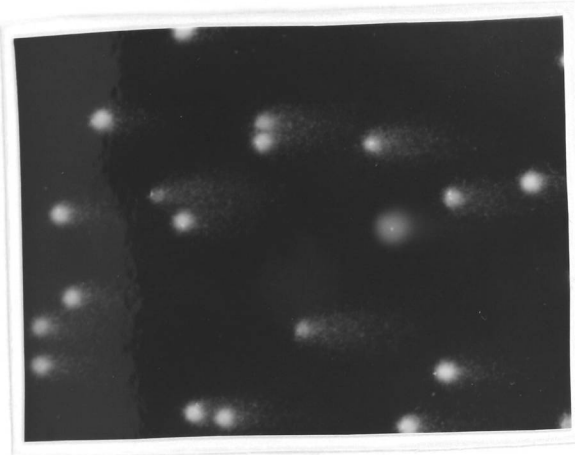
3 Gy

5 Gy
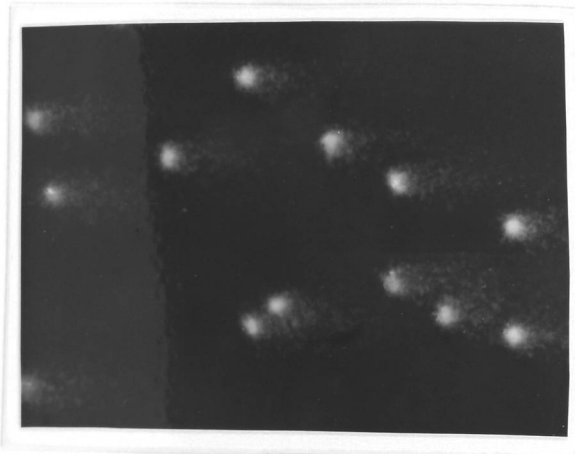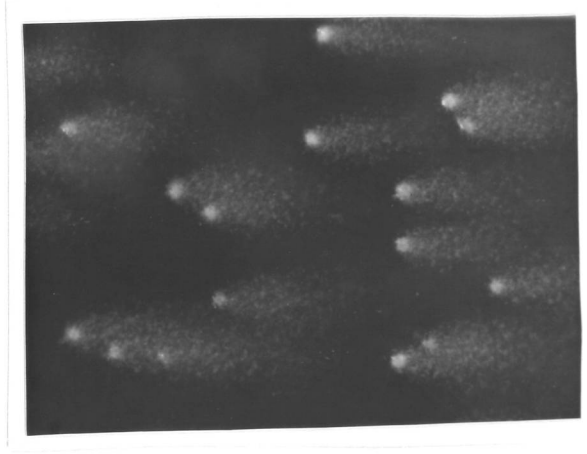
10 Gy

Figure 3.11. continued
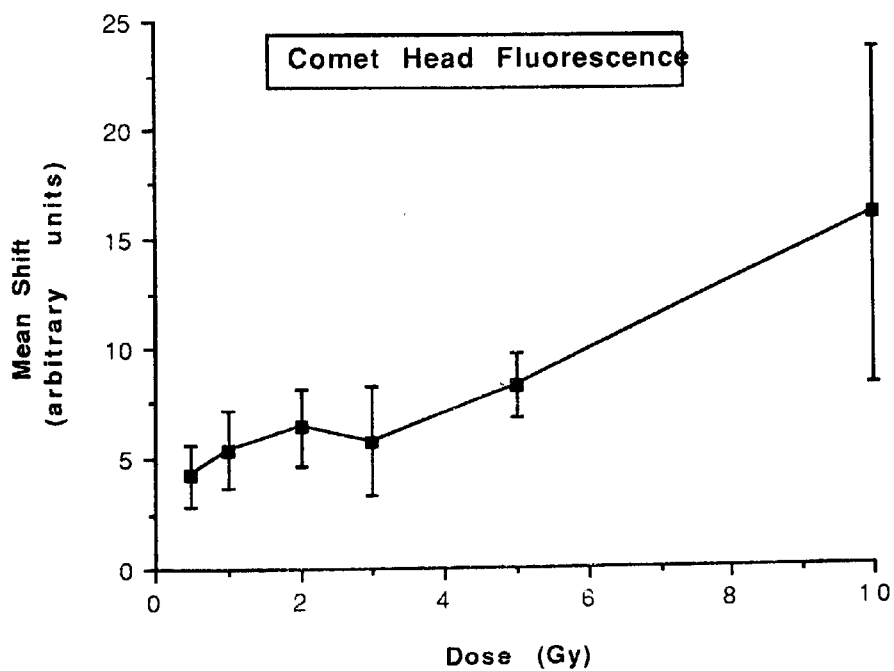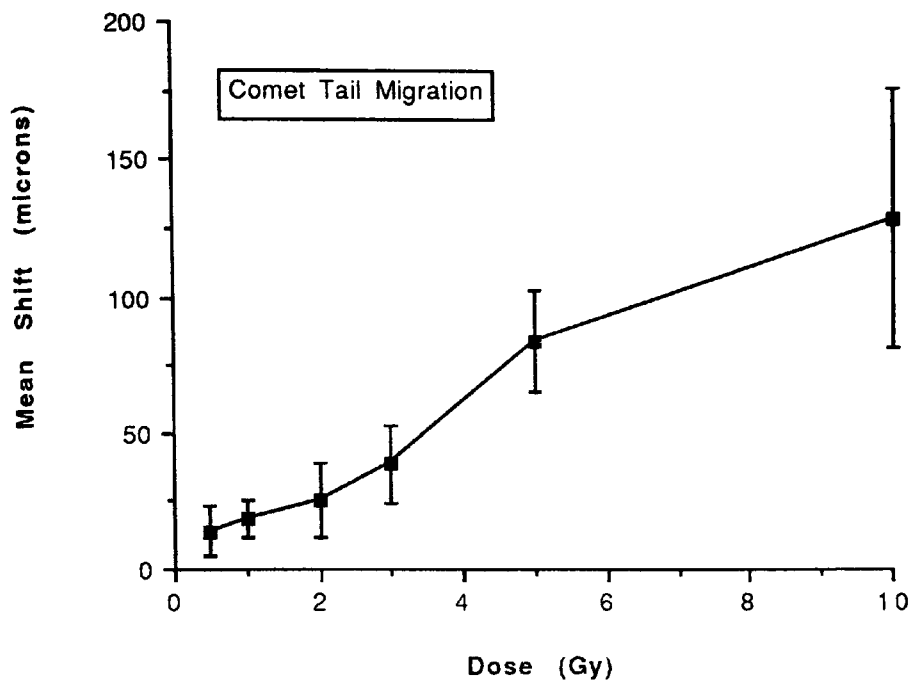
Figure 3.12. Increase in comet tail migration and decrease in comet head fluorescence of HF-DNA over 0.5-10 Gy. Comet tail measurements were taken of lymphocyte DNA obtained from eight healthy donors and comet head fluorescence readings were taken of lymphocyte DNA obtained from seven healthy donors. Vertical distribution bars refer to the S.E.M.

61
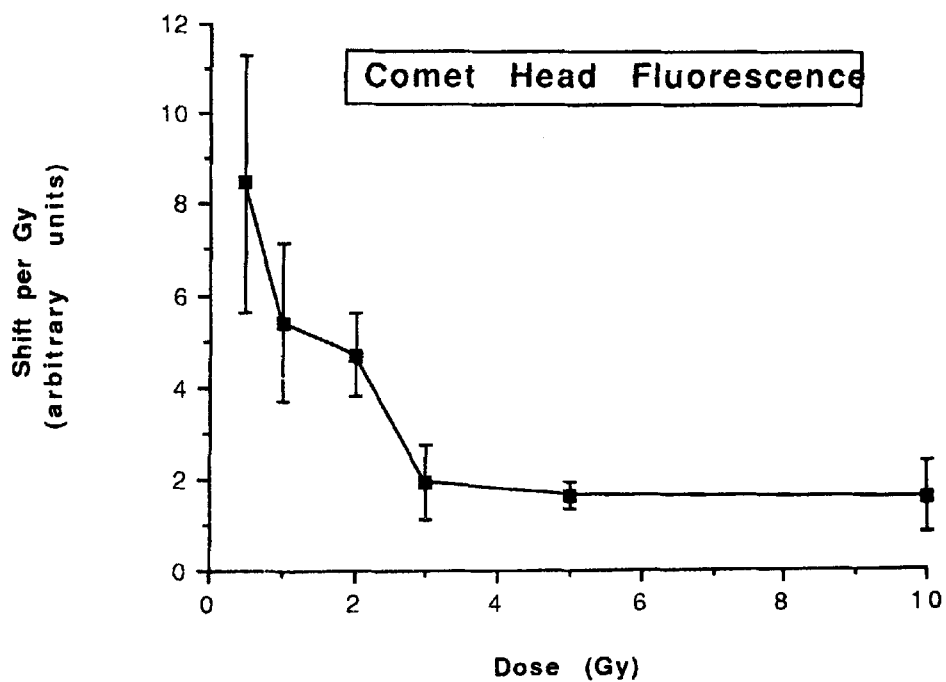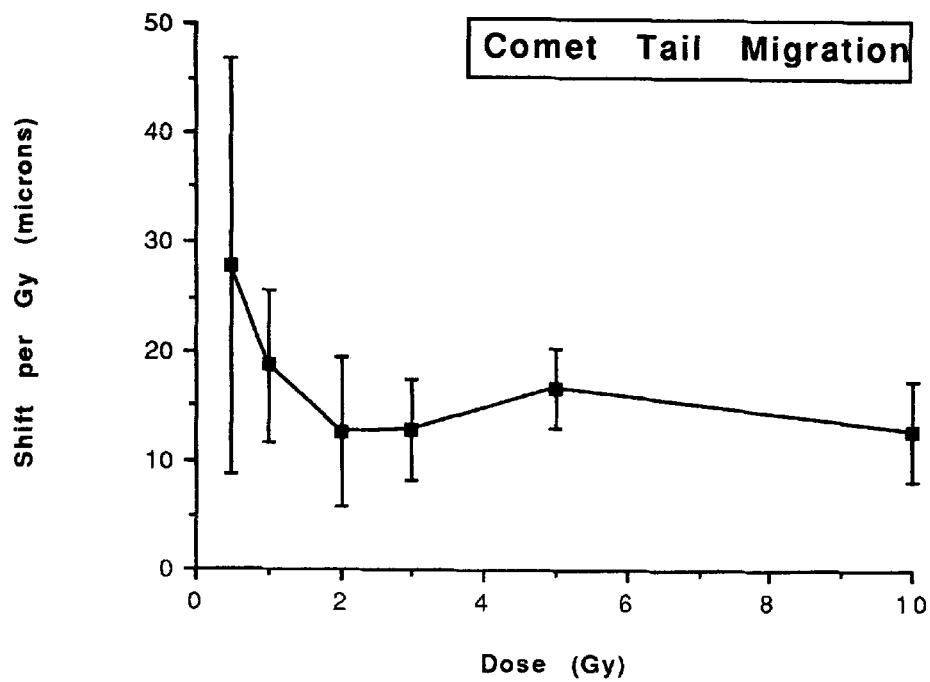
Figure 3.13. Mean shift per Gy over 0.5-10 Gy. The shift per Gy was obtained by dividing the shift in comet tail migration or the shift in comet head fluorescence by the radiation dose received by lymphocyte DNA derived from the same individuals as Figure 3.12.

unirradiated and irradiated HF-DNA and (iii) the response of DNA to a clinically relevant dose of radiation can be compared in NLS and MGE.

To maximise the '2 Gy shift', various electrophoresis times were investigated. Figure 3.14. shows that, under the conditions employed, the optimum electrophoresis time was 30 minutes. Electrophoresis times of 10 or 20 minutes produced only small comets tails in irradiated cells whereas an electrophoresis time of 40 minutes caused comet tails to form in unirradiated as well as irradiated cells thus reducing the '2 Gy shift'.

3.1(i). Effect of Lysis Conditions on DNA Damage Expression

The extent of comet tail migration was dependent on the dose of radiation received and the length of electrophoresis time (Figures 3.12. and 3.14., respectively). Olive et al. (1992) have shown that lysis conditions also influence the extent of DNA migration. In the present study, the effect of lysis conditions on DNA damage expression was examined using the lysis and alkali unwinding conditions of Singh et al. (1988). Figure 3.15. shows the effect of varying lysis times on the length of comet tail migration of lymphocyte DNA from two donors. In both cases, significant differences in comet length were found (using a one-tailed unpaired t test) between lymphocytes exposed to lysis buffer for 5 and 15 minutes ($p < 0.0001$ and $p < 0.0001$, respectively) and between lymphocytes exposed to lysis buffer for 15 and 30 minutes ($p < 0.0001$ and $p < 0.001$, respectively). A significant difference in comet length was also found between 5 and 60 minutes lysis exposure in donor 1 ($p < 0.003$). However, after 15, 30 and 60 minutes exposure to lysis buffer, the increase or decrease in comet length (compared to comets of lymphocytes exposed to lysis for 5 minutes) was also accompanied by a decrease in the number of comets present in the six randomly selected photomicrograph negatives. Figure 3.16. shows the effect of lysis time and alkali unwinding time on the comet tail migration of lymphocyte DNA. The combined effect of lysis and alkali unwinding buffer exposure (for 10 or 20

63
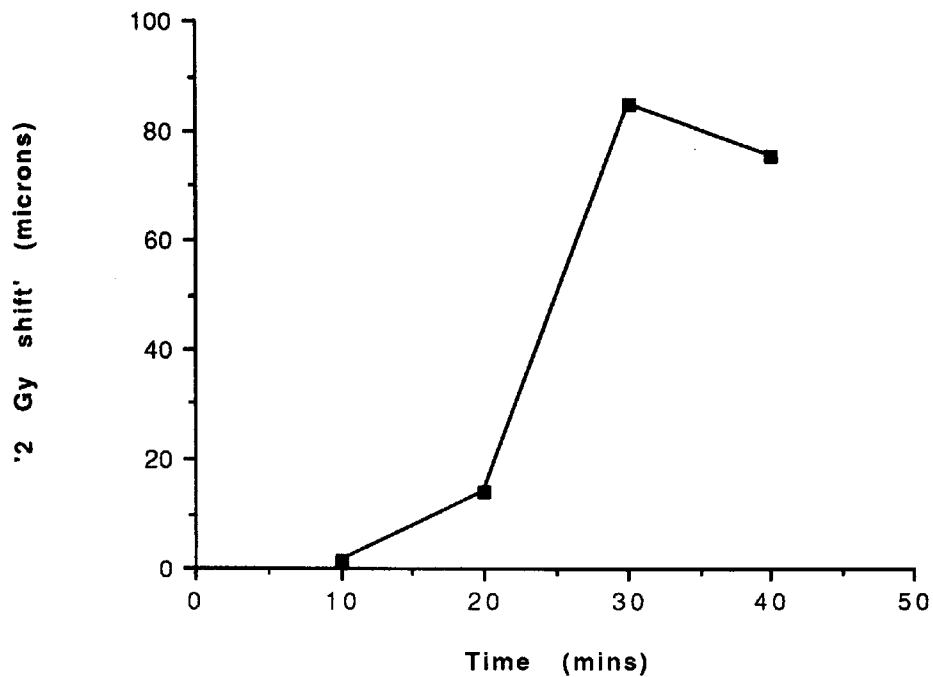
Figure 3.14. Effect of electrophoresis time on the '2 Gy shift' between unirradiated and irradiated comet tail length. Peripheral lymphocytes were obtained from a single volunteer and batches of slides containing unirradiated and irradiated cells were electrophoresed separately for 10, 20, 30 and 40 minutes, respectively. Each point was derived from the mean of approximately 50 irradiated comet length measurements minus the mean of 50 unirradiated comet length measurements. S.E.M. 's were loss than 15% for unirradiated and irradiated comet lengths in each electrophoresis run.
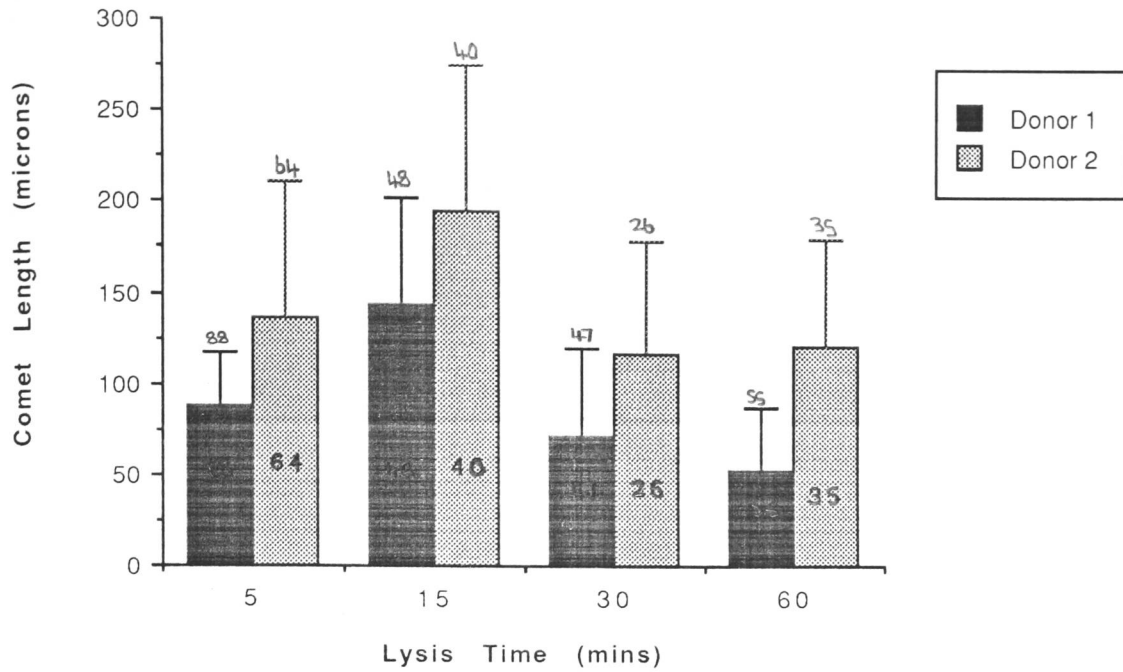
Figure 3.15. Effect of lysis time on comet tail length of lymphocyte DNA from two healthy donors after exposure to 1Gy gamma irradiation. Each stack represents mean comet length with range bars corresponding to the respective standard deviation. The figures inserted into each stack represent the number of comets observed and measured in six photomicrograph negatives (6 x 8.64cm^2) for each lysis time. The mean unirradiated comet length and number of comets measured were 71.83 ± 50.72, n=70 and 78.02 ± 15.10, n=72 for donors 1 and 2 respectively.
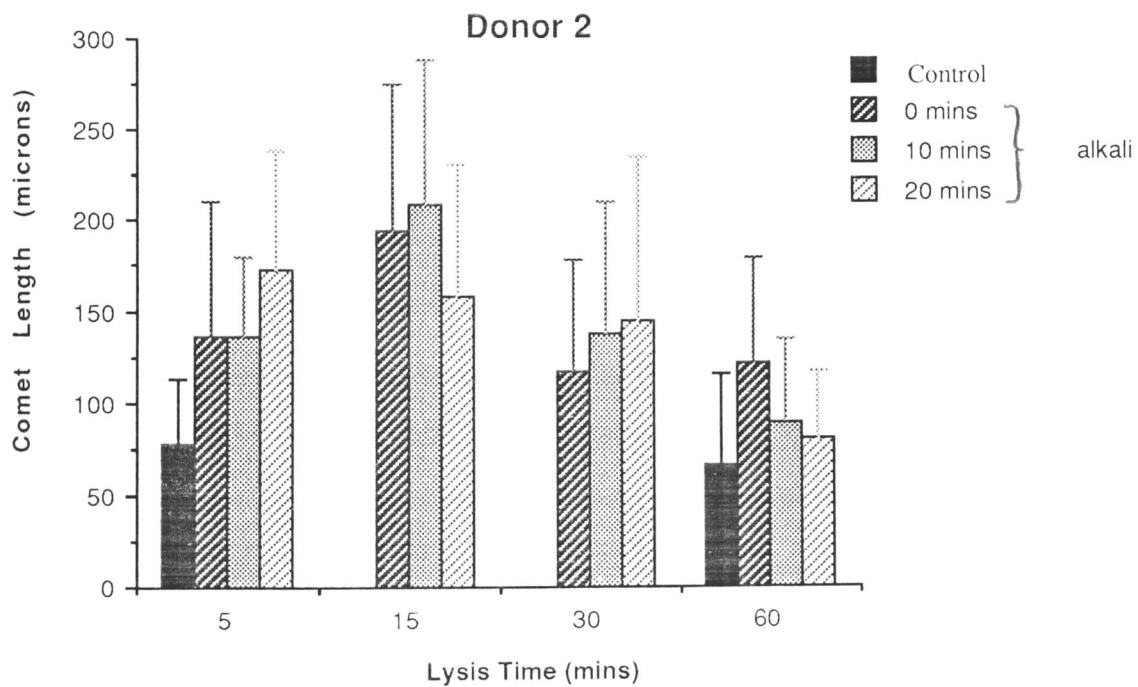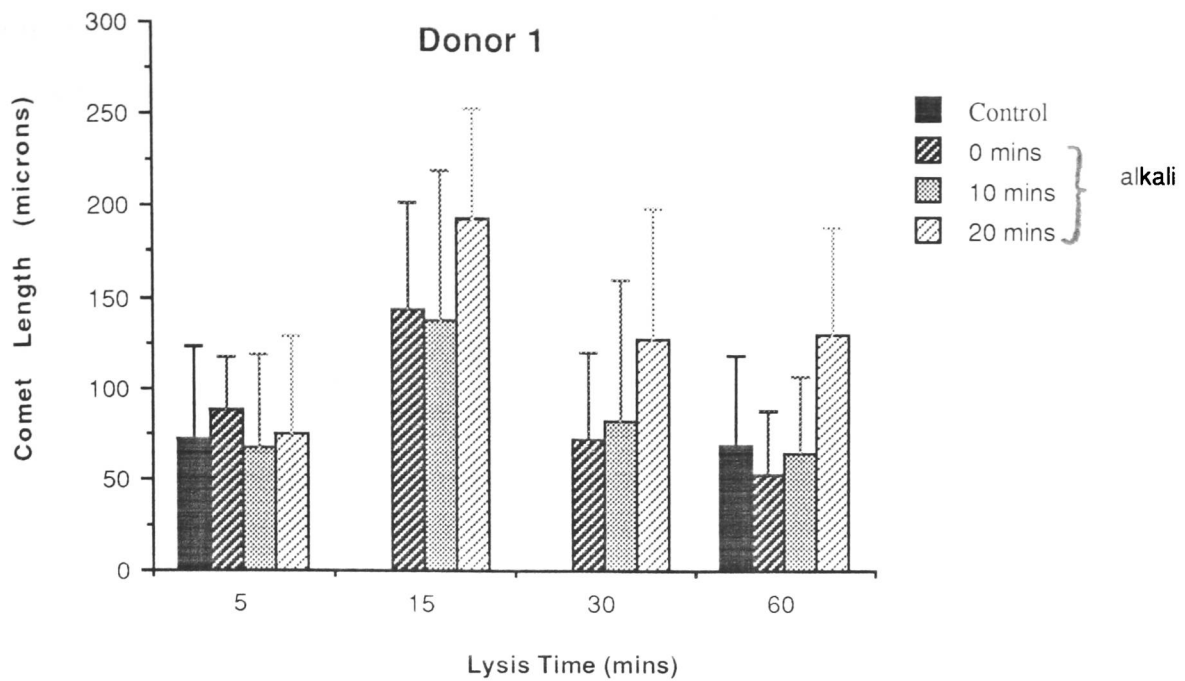
Figure 3.16. The effect of lysis time and alkali unwinding time on the comet tail migration of lymphocyte DNA from the same donor samples as Figure 3.15. The cells were subject to 1 Gy gamma irradiation and exposed to electrophoresis buffer (pH > 13) for 0, 10 or 20 minutes prior to electrophoresis. Control samples comprised of unirradiated cells that were subject to either 5 minutes lysis without unwinding or 60 minutes lysis with 20 minutes unwinding. Each stack represents the mean comet tail length measurements (ranging from 26-88 comets measured over six photomicrograph negatives) with range bars corresponding to standard deviations.

66

minutes) also generally produced an increase in comet length between 5 and 15 minutes lysis and a decrease in comet length between 15 and 60 minutes lysis as seen in Figure 3.15. Vijayalaxmi *et al.* (1992) observed an increase in comet length after 60 minutes lysis and 20, 40 and 60 minutes exposure to alkali, respectively. They attributed the increase in comet length to the production of single-stranded DNA and the consequent detection of single strand breaks and alkali-labile sites. Whilst long lysis times (60 minutes) and unwinding times (20 minutes) may improve the detection of alkali-labile sites and occult single-strand breaks, it was found in the present study that when lymphocytes from the two donors in Figure 3.16. were lysed for more than 5 minutes and exposed to alkali for 10 or 20 minutes, there was at least a 30% decrease in the number of comets observed in six photomicrograph negatives.

Singh *et al.* (1988) recommended, for human lymphocytes, a lysis time of 60 minutes with an added unwinding time of 20 minutes. To test this recommendation, the number of comets observed over a fixed area, the mean comet length and the heterogeneity of comet lengths were compared when lymphocytes were exposed to (i) lysis for 5 minutes without alkali unwinding or to (ii) lysis for 60 minutes with 20 minutes alkali unwinding (Table 3.5.). There were no significant differences (using a one-tailed paired *t* test) in the number of comets observed from unirradiated or irradiated lymphocytes that were exposed to either 5 minutes lysis without alkali unwinding or 60 minutes lysis with 20 minutes alkali unwinding. However, the number of comets visualised from both unirradiated and irradiated lymphocytes, were reduced in four out of six of the donors after 60 minutes lysis and 20 minutes unwinding as compared to 5 minutes lysis without unwinding. Even though there was no significant difference in the mean comet lengths between unirradiated and irradiated lymphocytes exposure to either 5 minutes lysis without unwinding or 60 minutes lysis with 20 minutes unwinding, lymphocytes lysed for 5 minutes without unwinding consistently produced a mean increase in comet tail length after a 1

Table 3.5. The number of comets observed, mean comet length and heterogeneity of comet length in lymphocyte DNA exposed to either 5 minutes lysis without unwinding or 60 minutes lysis with 20 minutes unwinding.

Donor	Radiation Dose	Number of Comets		Mean Comet Length +/-1 SD (um)		Heterogeneity (Range to SD ratio)	
		5 mins lysis	60 mins lysis	5 mins lysis	60 mins lysis	5 mins lysis	60 mins lysis
1	0 Gy	70	40	71.83 ± 50.72	69.31 ± 49.17	3.44	2.23
	1 Gy	88	40	87.51 ± 29.23	130.87 ± 57.69	5.30	3.02
2	0 Gy	63	100	40.66 ± 6.20	89.06 ± 72.99	4.69	3.05
	1 Gy	70	43	48.79 ± 18.78	107.84 ± 72.99	3.61	2.79
3	0 Gy	50	42	91.77 ± 52.85	141.33 ± 56.72	2.75	3.07
	1 Gy	46	34	103.38 ± 30.40	118.48 ± 35.82	3.18	3.25
4	0 Gy	51	39	80.54 ± 50.14	121.19 ± 48.40	3.09	3.00
	1 Gy	49	52	104.35 ± 48.98	101.06 ± 59.44	2.57	3.26
5	0 Gy	40	41	153.72 ± 99.70	124.68 ± 85.38	2.43	2.72
	1 Gy	21	32	170.56 ± 97.57	74.73 ± 46.08	2.68	2.73
6	0 Gy	72	41	78.02 ± 34.46	65.82 ± 50.34	3.65	3.46
	1 Gy	67	41	135.91 ± 74.34	81.70 ± 35.24	3.13	3.02

Heterogeneity of comet lengths was calculated from the ratio of the range to the standard deviation; values below 2 or greater than 6 indicate that the data are extremely homogeneous or heterogeneous, respectively (Statview II, 1991)

Gy irradiation unlike those lysed for 60 minutes with 20 minutes unwinding. There was no significant difference (using a two-tailed paired t test) in the heterogeneity of comet lengths for lymphocytes lysed under both conditions.

The effect of lysis and unwinding time on the shift in comet tail migration over the range of 0.5-5 Gy is shown in Figure 3.17. For both lysis conditions, no significant differences were present in the numbers of comets observed or in the comet length of the unirradiated samples ($p > 0.19; p > 0.12$, respectively using a one-tailed paired t test). However, significant differences ($p < 0.01$, one-tailed paired t test) were present between the dose responses produced from the differing lysis conditions. At doses between 2 and 5 Gy, the mean shift in comet length was greater in lymphocytes subject to 5 minutes lysis without unwinding than those subject to 60 minutes lysis with 20 minutes unwinding. Further, at 5 Gy it was apparent that the lymphocytes exposed to lysis for 5 minutes without alkali unwinding produced a larger mean shift and more variation in comet length than lymphocytes exposed to lysis for 60 minutes with 20 minutes alkali unwinding.

It was concluded that the modified lysis conditions (5 minutes lysis without unwinding) rather than those of Singh $et\ al.$ (1988) (60 minutes lysis with 20 minutes alkali unwinding) were more appropriate to employ for the following reasons: (i) Prolonged lysis exposure may induce additional damage to DNA (Figure 3.15.), (ii) The decrease in comet numbers observed when lysis times were greater than 5 minutes suggests that highly damaged comets were not detectable (Figure 3.15.), (iii) The loss of heterogeneity of comet types that were observed at 60 minutes lysis with unwinding compared to 5 minutes lysis without unwinding suggests a decrease in the sensitivity of damage expression and (iv) The differences in the dose response observed over 0.5-5 Gy between the two lysis conditions (Figure 3.17.). Further, the implementation of a 5 minute lysis exposure without alkali unwinding produces an rapid and sensitive estimation of radiation-induced DNA damage in single cells.

69
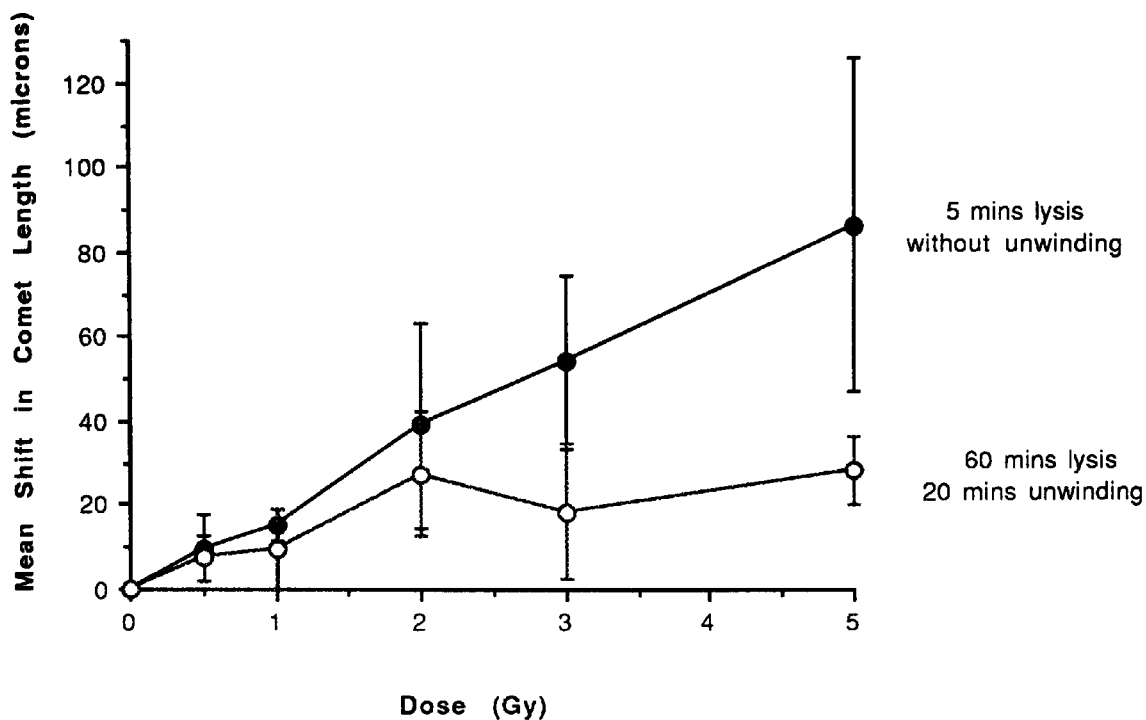
Figure 3.17. Effect of lysis and unwinding time on the shift in comet tail migration in a 0-5 Gy dose response. The graph represents the mean shift in comet tail migration (between approximately 50 unirradiated comets and approximately 50 comets produced at each radiation dose) of lymphocyte DNA extracted from four healthy donors. The cells of each donor were lysed for either 5 minutes without unwinding or for 60 minutes with a 20 minute unwinding time prior to electrophoresis. The four experiments were performed on separate days but both sets of slides were electrophoresised concurrently for each donor. The range bars indicate the S.E.M. for the four experiments.

70

3.1(j). *Restoration of the HF-DNA structure*

Olive *et al.* (1991) have suggested that a decrease in comet tail length following the incubation of irradiated cells at 37°C was indicative of the repair of radiation-induced DNA damage. Likewise, in the present study, the reduction of comet length and the restoration of comet head fluorescence to that of unirradiated cells could also be interpreted as an indication of DNA repair. The repair of radiation-induced DNA damage was studied in single cells by incubating irradiated (2 Gy) lymphocytes for 1 hour at 37°C prior to electrophoresis. The relative mean comet tail length (and mean comet head fluorescence) of approximately 50 comets in each of three slides: (i) unirradiated ('control'), (ii) irradiated ('damage'), and (iii) irradiated with incubation ('repair') was compared. The repair proficiency of irradiated cells was calculated from the ratio of the difference in comet tail length (or comet head fluorescence) between unirradiated and irradiated and incubated cells to the difference between unirradiated and irradiated cells (Section 2.4.). Full repair was indicated by a repair proficiency of 1.0 or greater, a less proficient repair was indicated by a repair proficiency of less than 1.0. Figure 3.18. shows the MGE repair assays of human lymphocyte HF-DNA from donors who expressed either good or poor repair proficiency after a 2 Gy *in vitro* irradiation of their isolated lymphocytes. The photographs show that in both donors a and b: (i) mainly comet heads were present after lysis and electrophoresis of their unirradiated lymphocytes and, (ii) a mixture of comets with bright heads and short tails and, comets with smaller and less bright heads with long tails were present after 2 Gy irradiation. Photograph 3, however, shows that after incubation, the comets resemble the comet heads of the unirradiated lymphocytes in donor a (indicating good repair) and that the comets resemble the comets of the irradiated lymphocytes in donor 2 (indicating poor repair).

71

(a) Good Repair
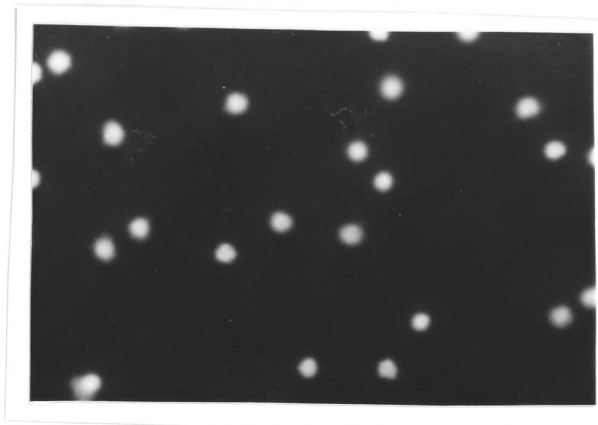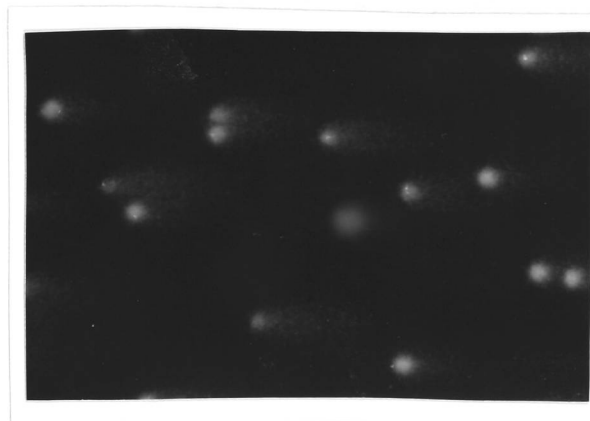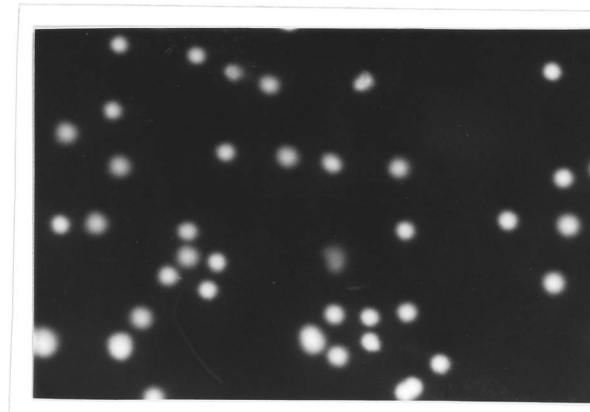
Figure 3.18. Expressions of good and poor repair proficiency in two individuals using MGE as a DNA repair assay. Each set of three photographs represent separate microscope slides containing unirradiated, irradiated (2 Gy) and irradiated and incubated comets respectively, from the DNA of individual lymphocytes. In donor a, the reduction in comet tail migration following a 1 hour incubation at 37°C after a 2 Gy irradiation illustrates good repair whereas in donor b, a similar comet tail migration in the irradiated and incubated sample as in the irradiated sample suggests a poor repair proficiency.

(b) Poor Repair
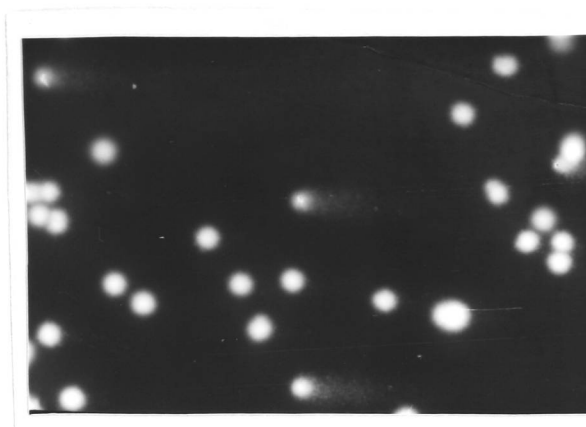
1
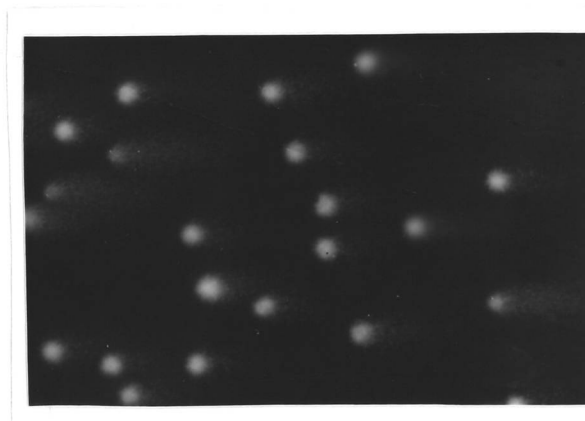
2
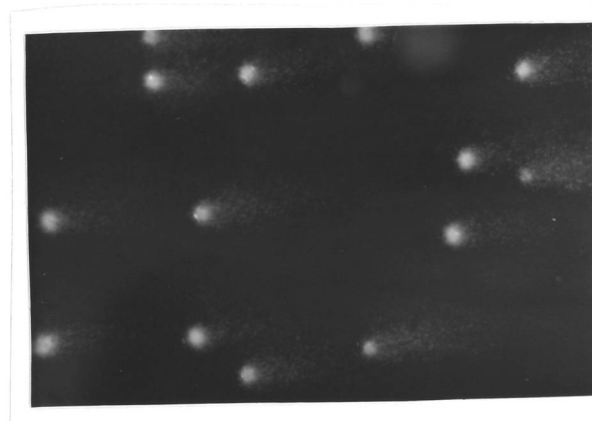
3

Figure 3.18. continued

3.1(k). Reproducibility of Microgel Electrophoresis

Triplicate electrophoresis runs were performed on two apparently healthy donors to examine the variation in unirradiated (basal) comet tail length, '2 Gy shift' and repair proficiency on an intra-sample basis (Table 3.6.). It was found that there were significant differences between electrophoresis runs (at 95% significance level, using a one-way analysis of variance) in: (i) Basal comet length, irradiated comet length and irradiated and incubated comet length in donor a ($p < 0.02$) and in (ii) Basal comet length and irradiated comet length in donor b ($p < 0.0001$). However, mean basal comet tail length agreed closely in all of the electrophoresis runs of donor a and in runs 1 and 2 of donor b and the '2 Gy shift' agreed within $5\mu m$ in two out of three runs in both donors. Repair proficiency also agreed in two out of three of the runs for both donors. Even though some variation in repair proficiency was observed, DNA repair activity was detected in each electrophoresis run for both donors. Overall, it was thought that this investigation indicated that the procedure was probably reproducible on an intra-sample basis.

Repeat tests were also performed on three apparently healthy donors over a number of weeks to examine the variation in basal comet tail length, '2 Gy shift' and repair proficiency on an inter-sample basis (Table 3.7.). It was found that, over a period of weeks, there were significant differences between the separate electrophoresis runs (at the 95% significance level, using a one-way analysis of variance) in: (i) Unirradiated, irradiated and irradiated and incubated comet lengths in donors a and b ($p < 0.0001$) and in (ii) Irradiated and irradiated and incubated comet lengths in donor c ($p < 0.0001$). Also, the mean basal comet length and mean '2 Gy shift' varied by at least 20% between each of the electrophoresis runs in all the donors. However, repair proficiencies were consistently good in the three samples of donor a and donor b. In donor c, good but variable repair proficiencies were produced on week 1 and week 9 with a

Table 3.6. Intra-sample variation in basal comet tail length, '2 Gy shift' and repair proficiency of lymphocyte HF-DNA in two apparently healthy donors.

Donor	Electrophoresis Run	Mean basal comet length (μm +/- 1SD)	Mean '2 Gy Shift' (μm)	Repair Proficiency
a	1	155.27 ± 50.53	80.34	1.42
	2	128.55 ± 70.28	54.01	0.68
	3	118.10 ± 73.96	58.27	0.56
c	1	92.35 + 57.50	54.21	0.78
	2	91.38 + 42.20	99.90	0.41
	3	190.70 + 39.11	56.92	1.23

For each donor, three separate electrophoresis runs were performed consecutively on the same day on lymphocyte preparations originating from the same venous blood sample. In each electrophoresis run, basal comet tail length, '2 Gy shift' and repair proficiency were derived from the mean of approximately 50 comet measurements.

Table 3.7. Inter-sample variation in lymphocyte HF-DNA basal comet tail length, '2 Gy shift' and repair proficiency in separate blood samples received over a period of months from three apparently healthy donors.

Donor	Electrophoresis run and week of sample	Mean basal comet length (μm +/- 1SD)	'2 Gy Shift' (μm)	Repair Proficiency
a	1 (wk 1)	77.44 ± 51.50	83.44	0.81
	2 (wk 18)	45.88 ± 13.36	39.11	0.92
	3 (wk 44)	90.99 ± 31.75	43.17	0.95
b	1 (wk 1)	98.93 ± 53.24	30.20	0.58
	2 (wk 3)	72.60 ± 9.29	86.93	0.67
	3 (wk 53)	115.58 ± 22.07	65.82	0.88
c	1 (wk 1)	138.42 ± 50.34	66.40	0.59
	2 (wk 4)	113.64 ± 59.44	48.79	0.11
	3 (wk 9)	83.44 ± 56.72	28.46	1.00

In each electrophoresis run, basal comet tail length, '2 Gy shift' and repair proficiency were estimated from the mean of approximately 50 comet tail measurements of unirradiated, irradiated and irradiated and incubated lymphocytes.

poor repair proficiency produced on week 4. These results indicate that in some individuals, over a period of weeks, basal DNA damage and the extent of radiation-induced damage may differ but that repair proficiency may remain constant (donors a and a, for example). Overall, it was thought that inter-sample reproducibility could probably be demonstrated in individuals expressing a consistent DNA repair capacity but may not be demonstrated in individuals who exhibit differential radiation responses over a period of weeks (donor c, for example).

3.1(l). *Summary*

Microgel Electrophoresis is a simple, rapid and sensitive technique that detects changes in comet tail migration and comet head fluorescence associated with DNA damage and repair. The present study has shown the technique to be:

(i) capable of detecting radiation-induced DNA damage over a range of 0.5-10 Gy.

(ii) sensitive at clinically relevant doses of 2 Gy.

(iii) suitable for estimating the repair proficiency of DNA after a dose of 2 Gy.

(iv) Reproducible on an intra- and inter-sample basis.

Like Nuclear Lysate Sedimentation, Microgel Electrophoresis has potential as an *in vitro* assay of radiation sensitivity. Both techniques were, therefore, compared to determine their relative usefulness in the determination of radiation-induced DNA damage and its subsequent repair (as a population response and as a response in single cells) in concurrent lymphocyte samples obtained from the same donors.

3.2. COMPARATIVE STUDIES

The ability of NLS and MGE to detect radiation-induced DNA damage and its subsequent repair has been demonstrated. Therefore, the relationship between sedimentation distance, comet tail migration and comet head fluorescence as indicators of DNA damage and repair ability was compared.

3.2.1. Dose response to Gamma Irradiation

The effect of gamma irradiation on human lymphocyte HF-DNA over a range of 0.5-10 Gy was examined in NLS and MGE. (Section 3.1(c). and 3.1(h).). There was a dose-related reduction in the sedimentation distance and comet head fluorescence and a dose-related increase in the comet tail migration of HF-DNA. Figure 3.19. shows that with increasing radiation dose there was a positive linear correlation between the shift in sedimentation distance and either the shift in comet tail migration ($r^2 = 0.938$, $p < 0.01$) or the shift in comet head fluorescence ($r^2 = 0.734$, $p < 0.01$). A similar correlation was also found between the increase in shift in comet tail length and the decrease in comet head fluorescence with increasing radiation dose ($r^2 = 0.667$, $p < 0.02$). To determine the lowest dose at which a significant shift in sedimentation distance, comet length and comet head fluorescence occurred, paired comparisons were made between the control data and each dose using a one-tailed paired Student's t test. A significant difference was observed at 0.5 Gy in sedimentation distance ($p < 0.01$) and comet head fluorescence ($p < 0.02$) and at 1 Gy in comet tail migration ($p < 0.01$).

The relative sensitivity of NLS and MGE as indicators of DNA damage was determined from the 'ratio of the shift per Gy' in sedimentation distance, comet tail length and comet head fluorescence of HF-DNA over the dose range 0.5-10 Gy (Figure 3.20.). At 1 Gy the detection of DNA damage as shift per Gy was similar in sedimentation distance, comet tail migration and comet head fluorescence. At 2 Gy however, more damage per Gy was expressed in MGE
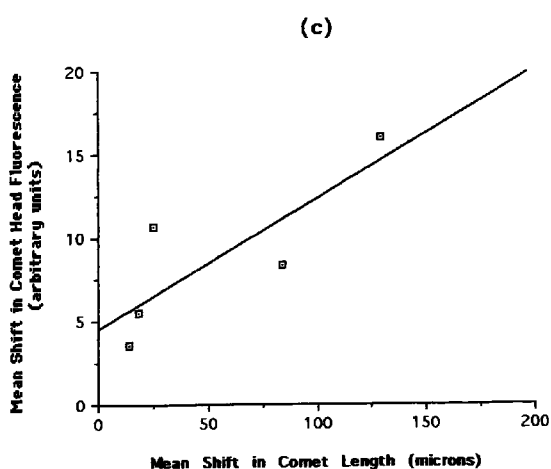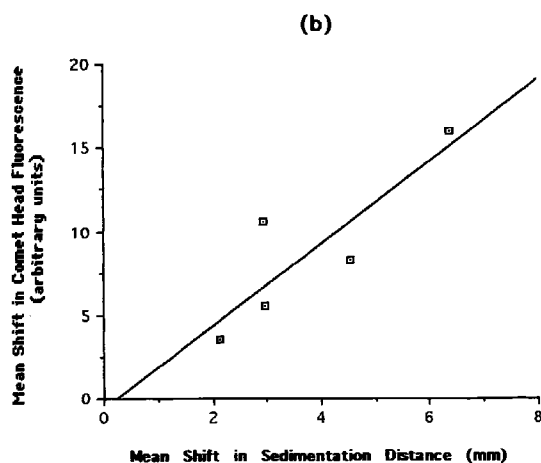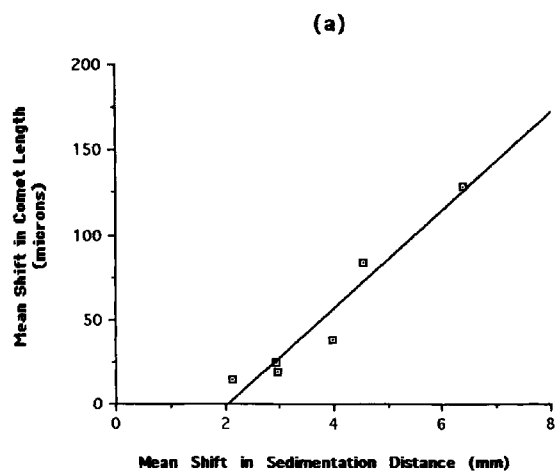
Figure 3.19. Comparison of the increase in sedimentation distance with the increase in comet length (a), or the decrease in comet head fluorescence (b); and comparison of the increase in comet length with the decrease in comet head fluorescence (c) over 0.5-10 Gy. Each point on the graphs represents the mean shift in sedimentation distance of lymphocyte HF-DNA from nine healthy donors, the mean shift in comet length of eight donors and the mean shift in comet head fluorescence of seven healthy donors after 0.5, 1, 2, 3, 5, and 10 Gy respectively. The same donors were used in both techniques. Graph (a) r^2=0.938, slope=2.93, p < 0.01), Graph (b) r^2=0.734, slope=2.47, p <0.01), Graph (c) r^2=0.667, slope=7.85, p <0.02).
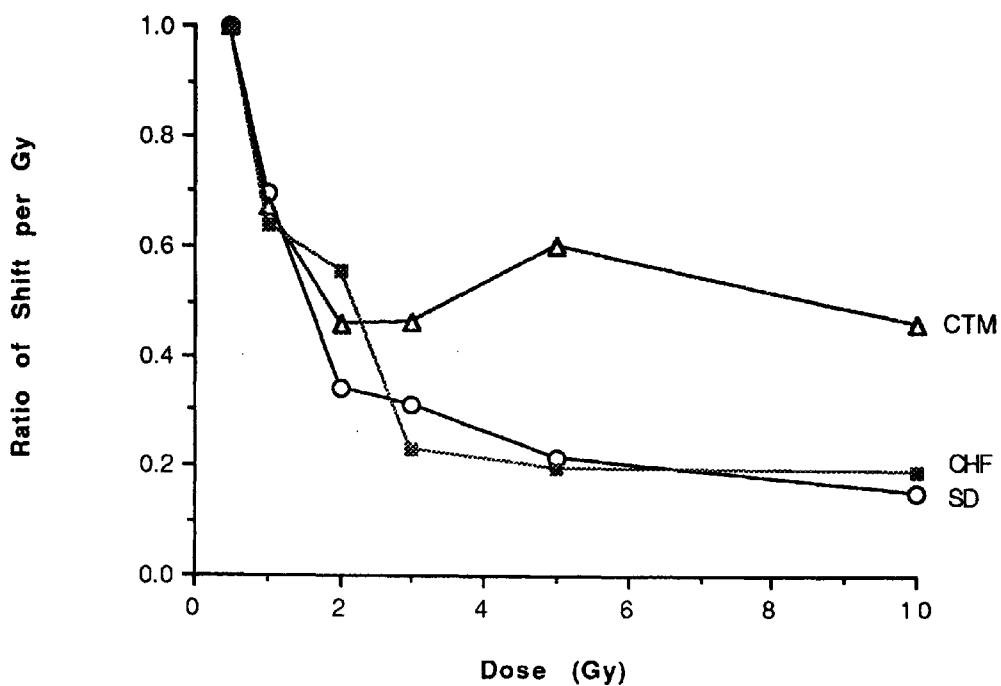
Figure 3.20. Comparison of the 'ratio of the shift per Gy' in sedimentation distance, comet length and comet head fluorescence of lymphocyte HF-DNA over a 0.5-10 Gy range. The 'ratio of the shift per Gy' was calculated from the mean shift per Gy after 1, 2, 3, 5 and 10 Gy respectively, divided by the mean shift per Gy after 0.5 Gy. HF-DNA was obtained from the same healthy donors as Figure 3.19a, b and c. CTM = Comet Tail Migration; CHF = Comet Head Fluorescence; SD = Sedimentation Distance.

rather than NLS. Over 3-10 Gy more DNA damage was detected per Gy using comet length rather than sedimentation distance or comet head fluorescence as an indicator of DNA damage.

3.2.2. Split -Dose Recovery

The ability of cells to repair DNA damage between two doses of radiation (separated by a 1 hour incubation at 37°C) was investigated using the NLS technique. The effect of a single dose (2 Gy) and a split-dose (2 Gy plus 1 hour at 37°C followed by 2 Gy) on the shift in sedimentation distance of lymphocyte HF-DNA was investigated in fifty-six apparently healthy donors. The amount of DNA repair between the two radiation doses was calculated from the shift in sedimentation distance after a single 2 Gy dose divided by the shift in sedimentation distance after a split 2 Gy dose. The relationship between the extent of DNA repair that had occurred during the incubation period between the two doses of radiation to the repair proficiency, calculated from an irradiated (single 2 Gy dose) and incubated sample, was then examined.

Figure 3.21.(a) shows that there was a linear relationship between the shift in sedimentation distance of HF-DNA after a single 2 Gy dose and after a single 4 Gy dose ($r^2 = 0.589$, slope $= 1.06$, $p < 0.001$). The figure indicates that in most samples the mean shift in sedimentation distance was greater after a single 4 Gy dose than after a single 2 Gy dose. Figure 3.21.(b) shows that there was a similar linear relationship as shown in Figure 3.21.(a) between the shift in sedimentation distance of HF-DNA after a split 2 Gy dose and after a single 4 Gy dose ($r^2 = 0.576$, slope $= 0.97$, $p < 0.001$). This indicates that DNA repair was occurring between the two doses of the split-dose. Figure 3.21.(c) shows that there was also a linear relationship between the 2 Gy shift and the split-dose 2 Gy shift ($r^2 = 0.507$, slope $= 0.77$, $p < 0.001$). The figure indicates that generally more damage was present after the 2 Gy split-dose than after the 2 Gy single dose (intercept = 1.27). However, as the ratio of the 2 Gy shift to the split-dose shift was less than 1
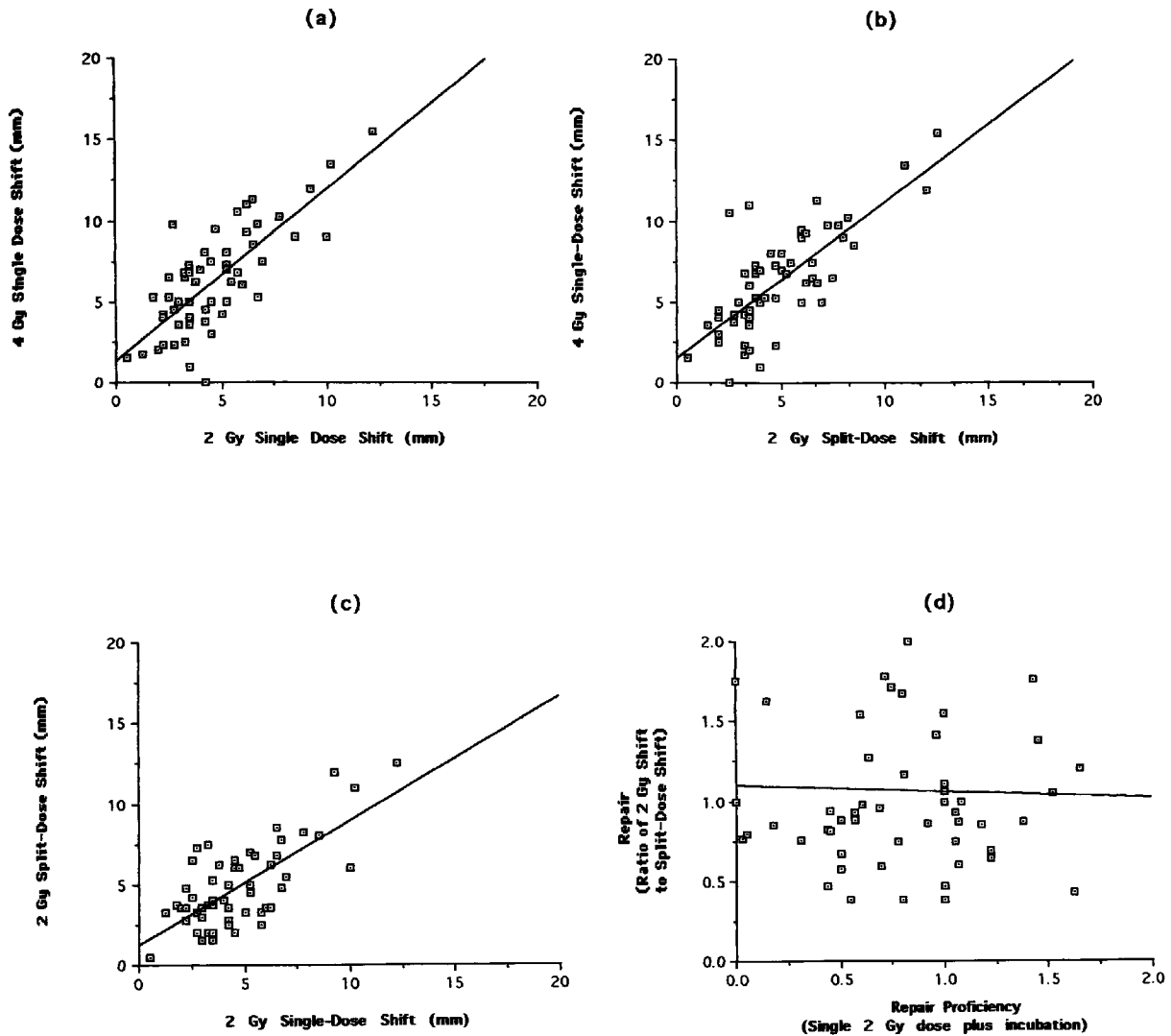
Figure 3.21. Comparison of single dose and split-dose shift in sedimentation distance of irradiated lymphocyte HF-DNA isolated from fifty-six healthy donors. Graph (a) shows the relationship between the 2 Gy single dose and the 4 Gy dose, where r^2=0.589, slope=1.06, p < 0.001. Graph (b) shows the relationship between the 2 Gy split-dose and the 4 Gy single-dose, where r^2=0.576, slope=0.97, p < 0.001. Graph (c) shows the relationship between the 2 Gy single dose and the 2 Gy split-dose, where r^2=0.507, slope=0.77, p < 0.001. Graph (d) shows the relationship between repair proficiency after a single 2 Gy dose and after a split- 2 Gy dose (r^2=0.001). Significant differences were found (using a one-tailed paired t test) between the 2 Gy and 4 Gy shift (p < 0.0001) and the 2 Gy split shift and the 4 Gy shift (p < 0.0001), respectively. No significant difference was found (using a one-tailed paired t test) between the 2 Gy single dose shift and the 2 Gy split-dose shift (p > 2). A significant difference was found (using a two-tailed paired t test) between DNA repair (derived from the ratio of the 2 Gy shift and the 2 Gy split-dose shift) and repair proficiency (p < 0.003).

(slope = 0.77) it was concluded that less than 100% repair was occurring during the incubation period between the two doses of radiation. However, the percentage repair occurring between the two doses of radiation was significantly different from the repair proficiency (p < 0.003, using a two-tailed paired t test) derived from irradiated and incubated HF-DNA from the same lymphocyte sample. Figure 3.21.(d) shows that there was a lack of linear correlation between the two estimates of DNA repair (r^2 = 0.001). when the repair proficiency after the single dose (derived from an irradiated and incubated sample) was compared to the repair proficiency after a split-dose (derived from the ratio of the 2 Gy shift. It was concluded that estimates of DNA repair (derived from split-dose recovery and from remaining DNA damage after repair opportunity) may differ in the NLS technique as the type of DNA damage present immediately after irradiation (for example, strand breakage) may differ to the type of DNA 'damage' remaining after repair opportunity (for example, DNA rewinding).

3.2.3.DNA Repair Over Time

The NLS and MGE techniques were used to investigate the repair pattern over time of radiation-induced DNA damage in six healthy donors following 2 Gy gamma irradiation (Figure 3.22.). After 5 minutes of a post-irradiation incubation period, generally more repair was observed in NLS (0.56 ± 0·41 (mean and standard deviation)) than in MGE (0.28 ± 0·48 in comet tail migration and 0.14 ± 0·16 in comet head fluorescence). After 30 minutes incubation all of the donors expressed a repair proficiency greater than 0.50 with mean repair proficiencies increasing to 1.10 ± 0.57 in sedimentation distance, 1.20 ± 0·29 in comet tail migration and 0.82 ± 0.26 in comet head fluorescence. After 60 minutes incubation, mean repair proficiency estimations were similar to those after 30 minutes incubation at 1.07 ± 0.27 in NLS, 0.82 ± 0.44 (comet tail migration) and 0.79 ± 0.23 (comet head fluorescence) in MGE. Broadly speaking, both techniques detected a rapid cellular response to radiation-induced DNA damage during the

82
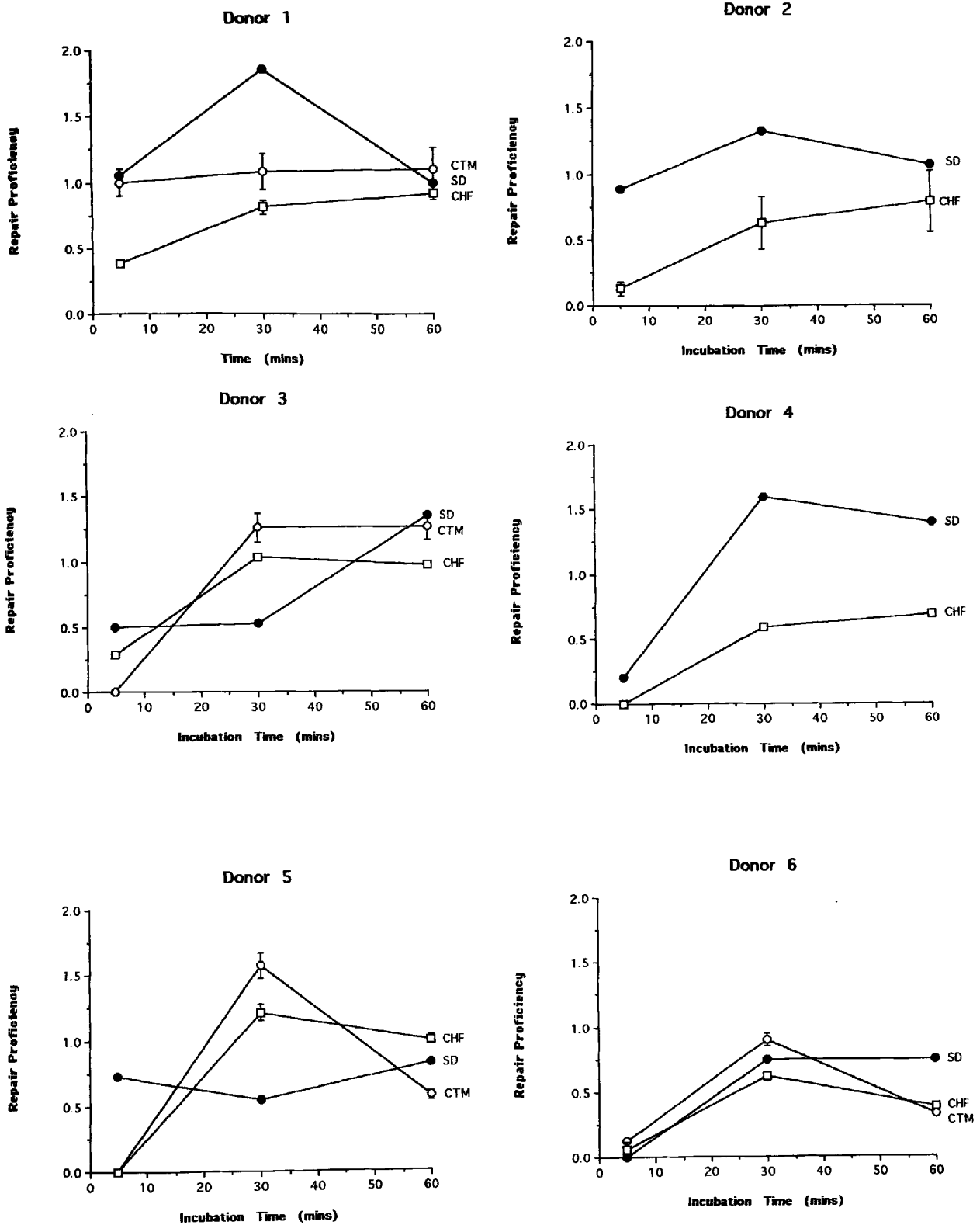
Figure 3.22. Effect of post-irradiation incubation time on the repair proficiency of lymphocyte DNA extracted from six healthy donors. Repair proficiency was calculated from three irradiated and incubated samples (5, 10 and 30 minutes, respectively) and a single unirradiated and irradiated (2 Gy) sample. Following a 2 Gy dose, the shift in sedimentation distance, comet tail migration and comet head fluorescence of the six donors had a CV of 27%, 37% and 32% respectively. Error bars, where apparent, represent the standard error of the mean. SD = Sedimentation Distance; CTM = Comet Tail Migration; CHF = Comet Head Fluorescence.

first 30 minutes and a slower response between 30-60 minutes of a 60 minute incubation period. Some donors exhibited a greater repair proficiency after 30 minutes incubation than after 60 minutes incubation. This effect was observed in both NLS (donor 1) and MGE (donors 5 and 6) and indicates that: (i) the bulk of DNA repair activity occurred and in some cases was complete within the first 30 minutes of post-irradiation incubation and (ii) the techniques could detect topological changes of the DNA superstructure during the repair process.

In donors 1, 3 and 5 similarities between repair proficiency derived from comet tail migration and comet head fluorescence were observed but differences in the time course of repair events were apparent between the NLS and MGE techniques. This observation indicates that the techniques may differ in their sensitivity to density changes which occur in the DNA during the post-irradiation repair process.

3.2.4. Repair Proficiency and Age of Donor

Harris et al. (1986) showed that lymphocytes extracted from older donors (66-99 years) display an increased frequency of spontaneous chromosomal aberrations than younger donors (18-62 years). Thus, NLS and MGE were used to investigate the relationship between the extent of basal DNA damage and repair proficiency (following exposure to 2 Gy and a post-irradiation incubation at 37°C for 1 hour) to donor age. Figure 3.23. shows that there was no linear correlation between donor age and the extent of repair proficiency derived from the sedimentation distance, comet tail length or comet head fluorescence of HF-DNA. Even though the donor group comprised healthy subjects (age range 22-51 years) as well as patients with cancer of the cervix (age range 21-76 years), no significant differences were found between donor age and DNA repair proficiency in the two groups using a one tailed paired Student's t test).

84

(a) Sedimentation Distance

(b) Comet Tail Migration

(c) Comet Head Fluorescence

(d) Sedimentation Distance

(e) Comet Tail Migration

(f) Comet Head Fluorescence
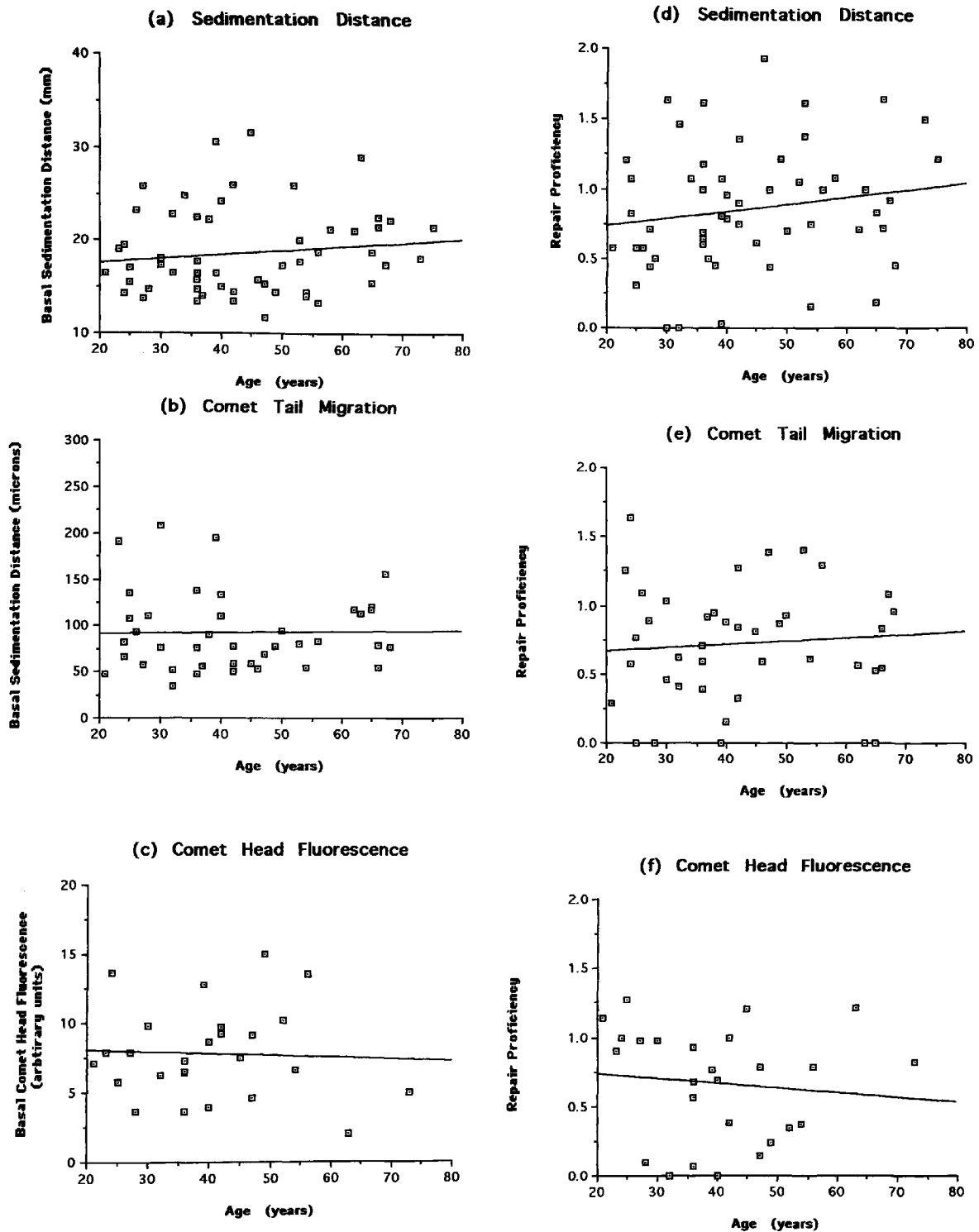
Figure 3.23. The relationship of donor age to basal DNA damage and DNA repair proficiency. Basal DNA damage and repair proficiency was estimated from the sedimentation distance, comet tail migration and comet head fluorescence of HF-DNA extracted from the lymphocytes of a group of healthy donors and cancer patients. Donor age and basal DNA damage: Graph (a) $r^2=0.018$, graph (b) $r^2=0.000$ and graph (c) $r^2=0.0102$. Donor age and repair proficiency: Graph (d) $r^2=0.029$, graph (e) $r^2=0.002$ and graph (f) $r^2=0.010$.

3.2.5. *Relationship between Basal DNA Damage, Radiation-induced DNA Damage and Post-irradiation Repair in NLS and MGE*

The relationships between: (i) basal DNA damage, (ii) radiation-induced DNA damage and (iii) post-irradiation DNA repair at 37°C were investigated in NLS and MGE using donor and patient lymphocyte samples.

In NLS the correlation between the basal sedimentation distance, basal comet tail migration and basal comet head fluorescence of lymphocyte HF-DNA and '2 Gy shift' is shown in Figure 3.24. Positive linear relationships were observed between the basal sedimentation distance and basal comet head fluorescence and '2 Gy shift'. However, no significant relationship between basal comet tail migration and '2 Gy shift' was observed. A rapid sedimentation behaviour and bright comet head fluorescence intensity of basal HF-DNA are indicators of a compact DNA superstructure at the time of analysis. If the DNA is undamaged (that is without relaxation of the supercoiled structure due to single strand breaks, for example), then the effect of radiation-induced DNA damage may be more apparent than that which occurs if some degree of damage is already present. The lack of correlation between basal comet tail migration and '2 Gy shift' is probably due to using comet length alone as an indicator of DNA damage as the measurements rely upon how far broken DNA has migrated rather than the total amount of DNA that has migrated from the comet head.

The relationship between basal HF-DNA sedimentation distance, comet tail migration and comet head fluorescence and repair proficiency are shown in Figure 3.25. No linear relationship was observed between basal superhelical density as indicated by sedimentation distance, comet tail migration and comet head intensity and repair proficiency.

Sedimentation distance, comet tail migration and comet head fluorescence of lymphocyte HF-DNA were also used to examine the relationship between DNA damage induction and DNA repair proficiency (Figure 3.26.). No significant linear correlations were observed between the post-irradiation shift in

(a) Sedimentation Distance

(b) Comet Tail Migration

(c) Comet Head Fluorescence
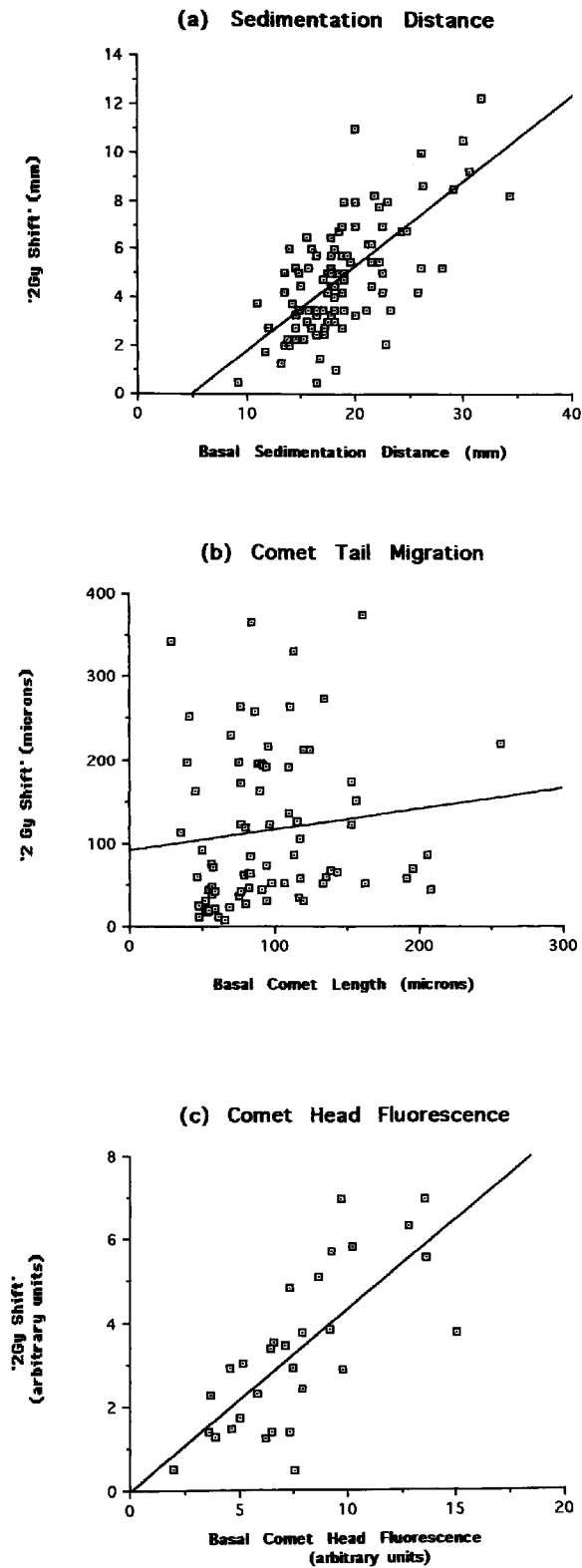
Figure 3.24. Comparisons of the relationship between basal (unirradiated) HF-DNAdamage and '2 Gy shift'. Both donor and patient samples comprised the study from which 97 sedimentation distance, 78 comet tail length and 30 comet head fluorescence results were gained. The ratio of donor to patient samples remained constant. (ns=non-significant). Graph (a) r^2=0.468, slope=0.35, $p < 0.001$. Graph (b) r^2=0.015, slope=0.25, ns. Graph (c) r^2=0.532, slope=0.44, $p < 0.001$.

(a) Sedimentation Distance

(b) Comet Tail Migration

(c) Comet Head Fluorescence
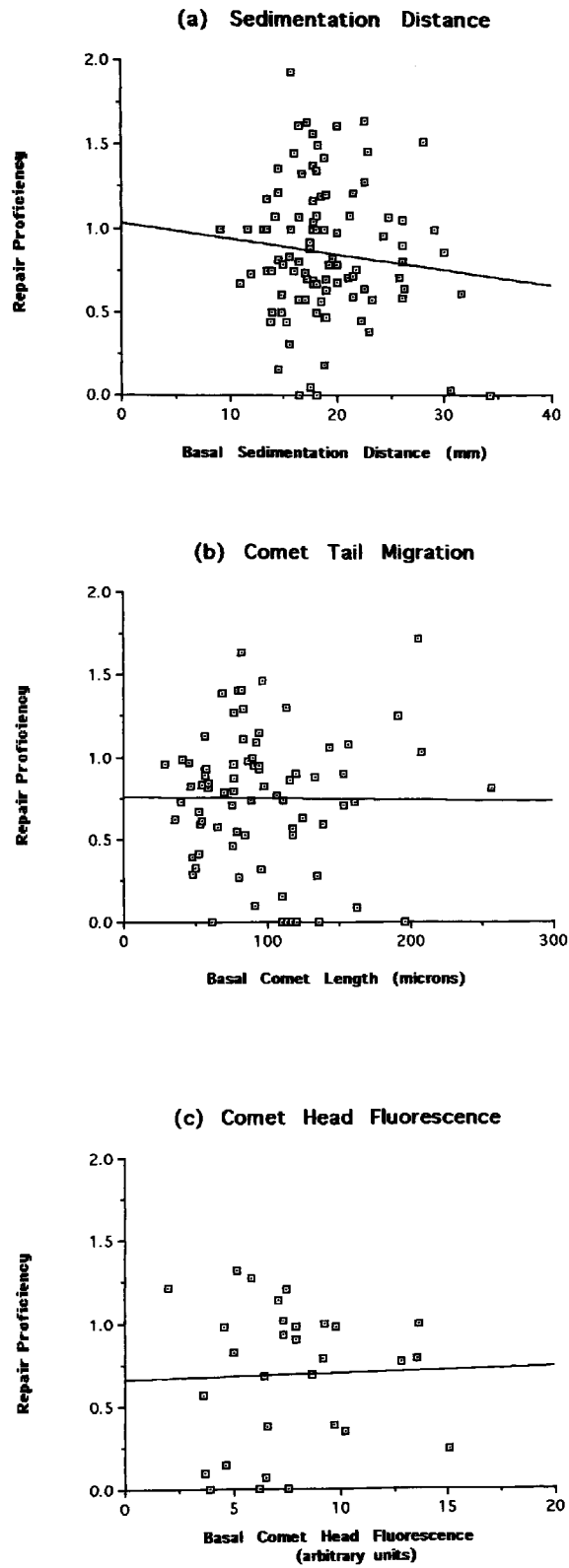
Figure 3.25. Comparisons of the relationship between the '2Gy shift' and repair proficiency derived from sedimentation distance, comet tail migration and comet head fluorescence of HF-DNA from donors and patients as Figure 3.24. Graph (a) r^2=0.011, ns, Graph (b) r^2=0.00, ns, Graph (c) r^2=0.001, ns.
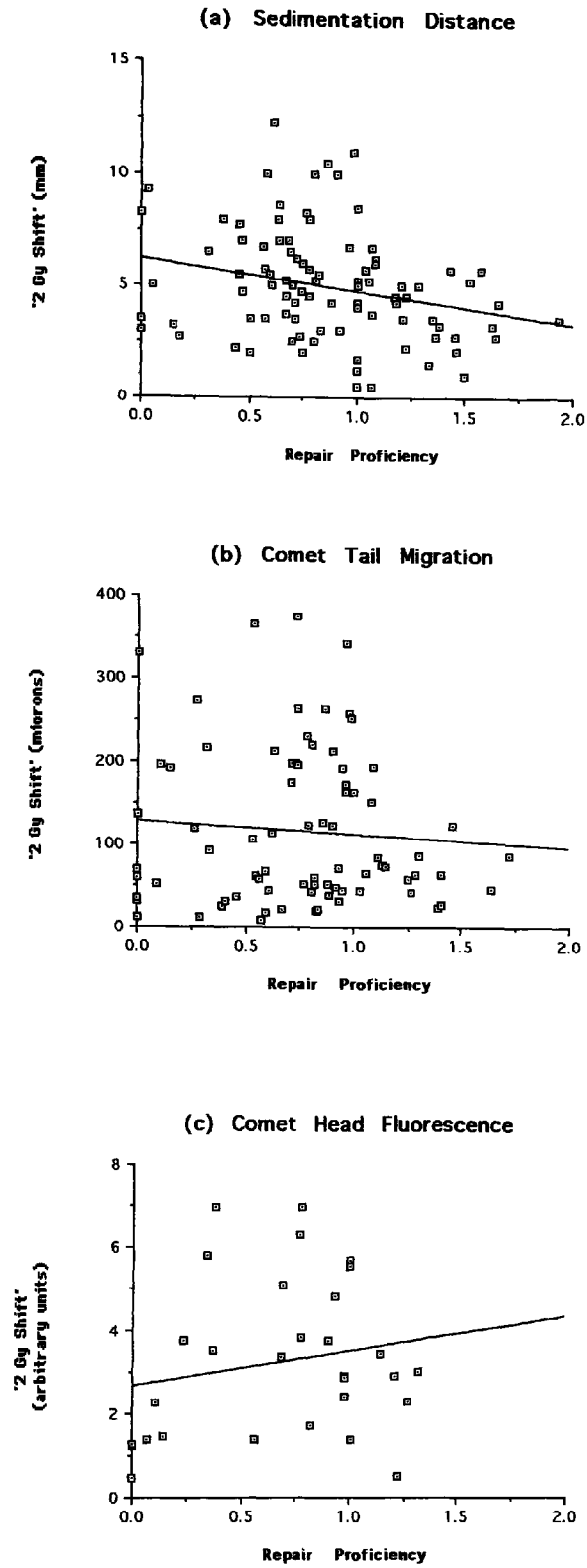
Figure 3.26. Comparisons of the relationship between the '2 Gy shift' and repair proficiency derived from sedimentation distance, comet tail migration and comet head fluorescence of HF-DNA from donors and patients as in Figure 3.24. Graph (a) r^2=0.063, ns; Graph (b) r^2=0.005, ns; Graph (c) r^2=0.036, ns.

sedimentation distance, comet tail migration and comet head fluorescence and the respective repair proficiencies.

From the above sedimentation and electrophoretic analyses, the following assumptions were made:

(i) The effect of radiation-induced DNA damage is more apparent when unirradiated DNA has a compact superstructure (as indicated by a rapid sedimentation distance and bright comet head fluorescence).

(ii) The unirradiated superhelical density of DNA (as indicated by sedimentation distance, comet tail migration and comet head fluorescence) is independent of repair proficiency

(iii) DNA repair activity is independent of the extent of DNA damage induction at the 2 Gy level.

3.2.6. Comparisons of Sedimentation Distance, Comet Tail Migration and Comet Head Fluorescence as indicators of DNA Damage and Repair Status

Both the NLS and MGE techniques have been shown to detect the presence of radiation-induced DNA damage and its subsequent repair following incubation at 37°C. The relationship between the two techniques was examined by comparing: (i) basal DNA damage, (ii) '2 Gy shift' and (iii) repair proficiencies derived from changes in the sedimentation distance, comet tail migration and comet head fluorescence of HF-DNA from healthy donors and patients with cancer of the cervix. When the sedimentation distance of basal HF-DNA was compared to basal comet length or basal comet head fluorescence, or when basal comet length was compared to basal comet head fluorescence, no significant linear relationships were observed (Figure 3.27.). It seems that no estimation of the extent of basal damage in unirradiated DNA can be made from composite assessments of HF-DNA sedimentation and migration behaviour in the NLS and MGE techniques. However, the assessment of basal DNA damage in an individual is reliant upon absolute measurements of sedimentation distance,

90
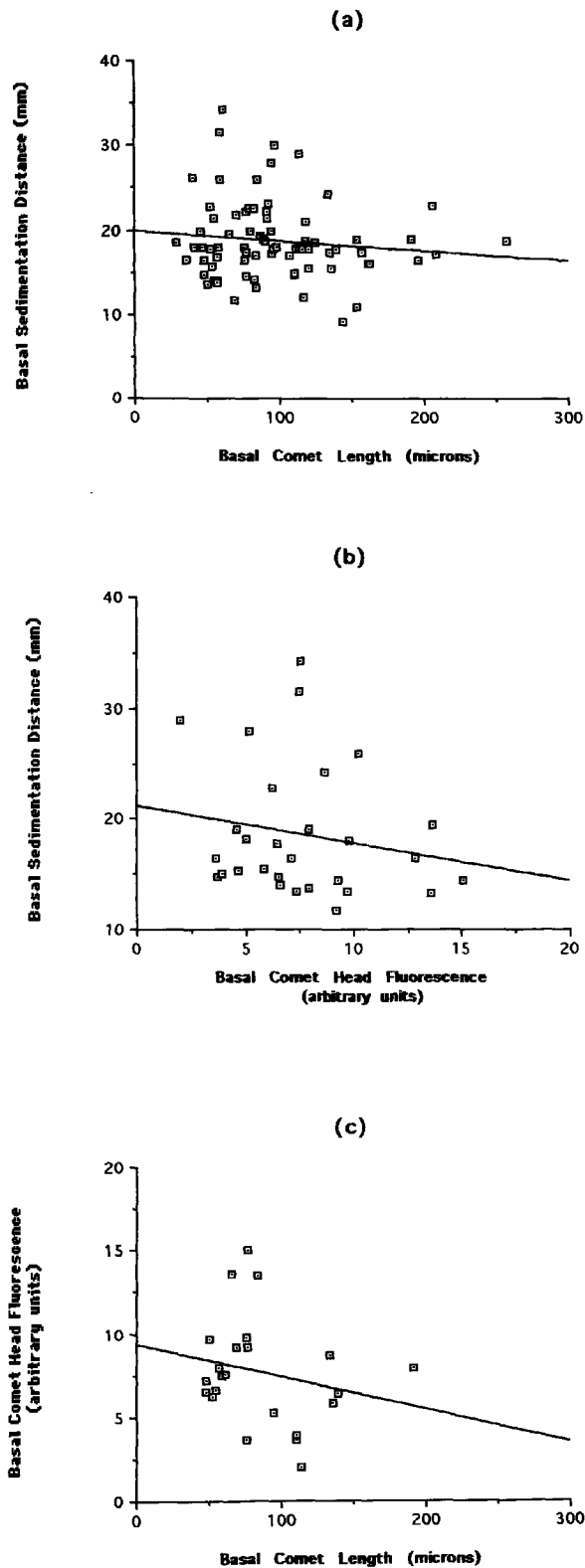
Figure 3.27. Comparisons of basal DNA damage status derived from sedimentation distance, comet tail migration and comet head fluorescence of HF-DNA from unirradiated donor and patient lymphocytes. Graph (a) compares comet tail migration to sedimentation distance where $r^2=0.012$, ns; Graph (b) compares comet head fluorescence to sedimentation distance where $r^2=0.033$, ns; Graph (c) compares comet head fluorescence to comet tail migration where $r^2=0.05$, ns.

comet tail migration and comet head fluorescence rather than a relative shift (like the '2 Gy shift', for example). Further, absolute measurements of sedimentation distance, comet tail migration and comet head fluorescence may be differentially sensitive to changes that occur to DNA higher order structure which are associated with cellular function or quiescent DNA damage.

In both techniques, the shift in sedimentation distance, increase in comet tail migration or decrease in comet head fluorescence after 2 Gy gamma irradiation was significant in the donor and patient groups ($p < 0.0001$, one-tailed paired Student's t test). This indicates that radiation-induced DNA damage is detected in both techniques. However, there was a poor linear correlation when the shift in sedimentation distance was compared to shift in comet tail migration or to the shift in comet head fluorescence; or when the shift in comet tail migration was compared to the shift in comet head fluorescence as shown in Figure 3.28.

A significant difference was also found (in the same donor and patient groups) between the increase sedimentation distance, reduction in comet tail migration and increase in comet head intensity of HF-DNA following a 1 hour post-irradiation incubation period at 37°C ($p < 0.001$, one-tailed paired Student's t test). Thus, it was assumed that a post-damage restoration or repair of the DNA structure occurs during incubation at 37°C which is detected by each of the three methods. However, Figure 3.29. shows that poor linear relationships were found when the repair proficiencies of lymphocyte HF-DNA derived from sedimentation distance were compared to repair proficiencies derived from comet length or comet head intensity; or when the repair proficiencies derived from comet length and comet head fluorescence were compared. Even though large amounts of scatter were present in each graph when individuals with repair proficiencies greater than 0.50 were compared, the graphs indicate that both assays and the three methods of detection were effective in detecting individuals with poor repair proficiency (less than 0.50).
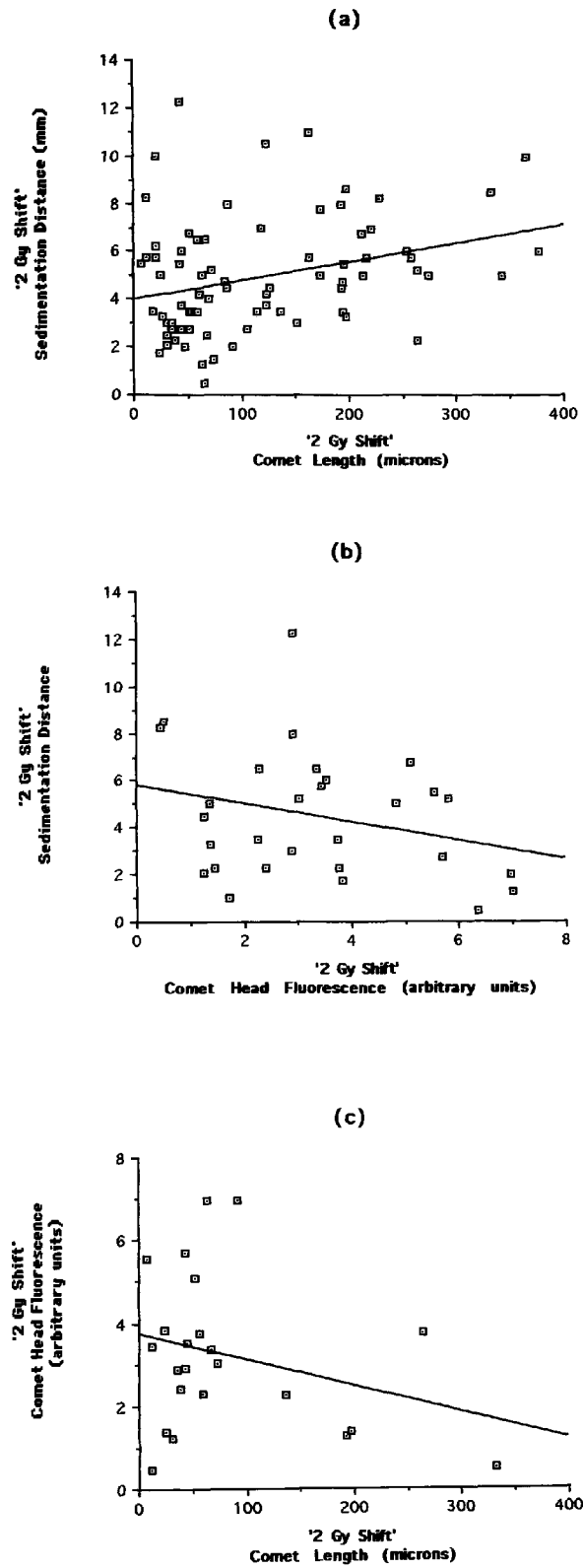
Figure 3.28. Comparisons of the '2 Gy shift' of HF-DNA from donors and patients using sedimentation distance, comet tail migration and comet head fluorescence as indicators of DNA damage. Figures 3.28a and b refer to sedimentation distance compared to comet tail migration and comet head intensity, where $r^2=0.095$, ns and $r^2=0.075$, ns respectively. Figure 3.28c refers to comet tail migration compared to comet head intensity where $r^2=0.083$, ns..
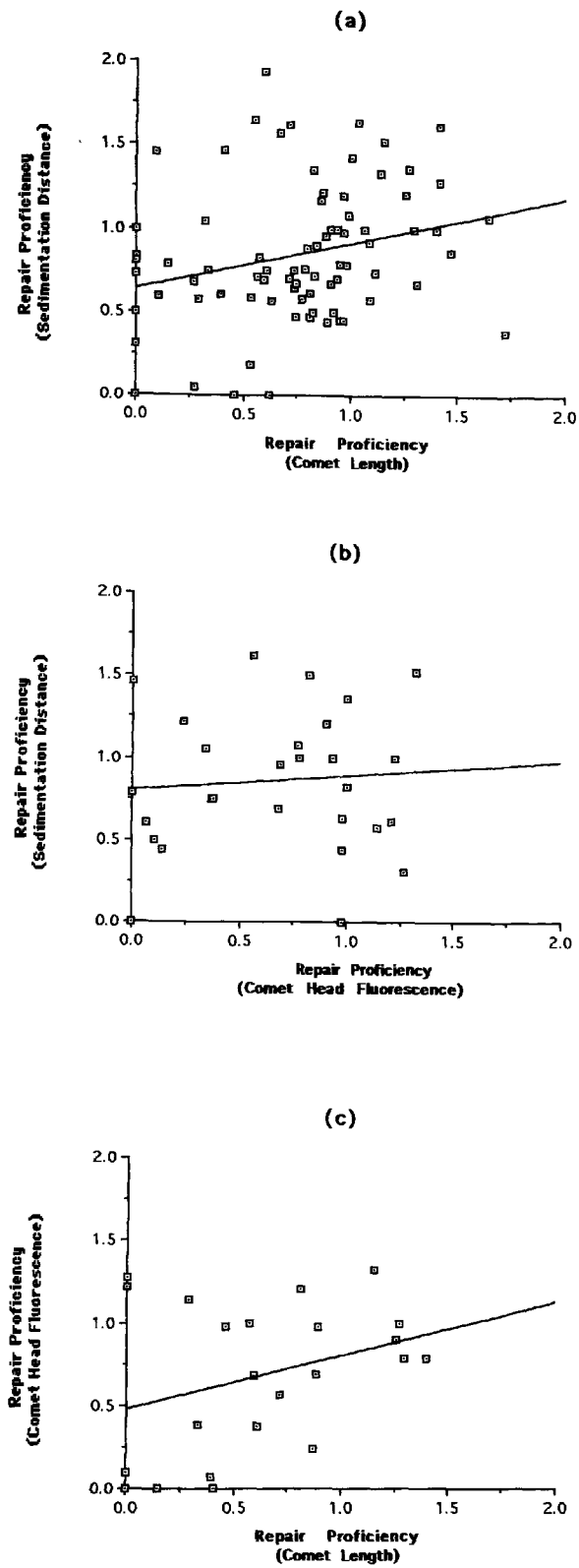
Figure 3.29. Comparative repair proficiencies between sedimentation distance and comet tail migration (Graph (a) where r^2=0.074, ns), sedimentation distance and comet head fluorescence (Graph (b) where r^2=0.007, ns) and comet tail migration and comet head fluorescence, (Graph (c) where r^2=0.0105, ns).

94

From the above analyses, it seems that even though the NLS and MGE techniques both detect damage and repair states of the DNA superstructure, they have been shown to differ in the detection of basal DNA damage the extent of radiation-induced DNA damage and repair assessment.

3.2.7.Summary

Nuclear Lysate Sedimentation and Microgel Electrophoresis have been compared as potential *in vitro* assays of radiosensitivity. From the above investigations the following conclusions were drawn:

(i) Similar dose response curves were found over 0.5-10 Gy from the decrease in sedimentation distance, increase in comet tail migration and decrease in comet head fluorescence of irradiated HF-DNA (Figure 3.19.).

(ii) The techniques showed similar sensitivities in DNA damage detection at doses lower than 2 Gy with changes in comet length as the most sensitive measure of increasing DNA damage at doses higher than 2 Gy (Figure 3.20.).

(iii) The techniques may differ in their sensitivity to changes which occur to the DNA superstructure during the post-irradiation repair process (Figure 3.22.).

(iv) DNA repair activity seems to be independent of basal DNA damage and the extent of '2 Gy shift' (Figures 3.24 and 3.25., respectively).

(v) NLS and MGE differ in their estimates of basal DNA damage, radiation-induced DNA damage and the extent of DNA repair (Figures 3.27., 3.28. and 3.29., respectively).

(vi) Both NLS and MGE have the ability to identify individuals with a poor repair proficiency (Figure 3.29.).

The techniques have been shown to differ in their detection of DNA damage and its subsequent repair. However, to investigate these differences, the relationship between cell survival and DNA damage and repair was studied.

3.3. CELL LINES

The relationship of DNA damage and repair (as detected by NLS and MGE) to cellular radiosensitivity (expressed as a reduction in the total number cells in a population after irradiation) was compared in three cell lines. The MOLT-4, DAUDI and V79 cell lines were chosen as model systems as they are known to display differential sensitivity to radiation. MOLT-4 has been ranked as highly radiosensitive (Szekely & Lobreau, 1985), DAUDI as less radiosensitive than MOLT-4 (Hanson, J.A., personal communication) and V79 as relatively radioresistant (Okayasu & Iliakis, 1992).

3.3.1. *Dose response of MOLT-4, DAUDI and V79 to Ionising Radiation*

The growth curves of unirradiated MOLT-4, DAUDI and V79 cells grown in tissue culture are shown in Figure 3.30. The graph shows that there were similarities in the growth characteristics of the three cell lines in that:

(i) A lag phase in cell division was present between Day 0 and Day 1 of culture.

(ii) The cells entered exponential growth between Day 1 and Day 6 in MOLT-4, between Day 1 and Day 5 in DAUDI and between Day 1 and Day 4 in V79.

(iii) Each cell line entered a plateau phase of cell division, after Day 6 in MOLT-4, after Day 5 in DAUDI and after Day 4 in V79.

The population doubling times for MOLT-4, DAUDI and V79 were found to be 15, 26.5 and 18.5 hours, respectively.
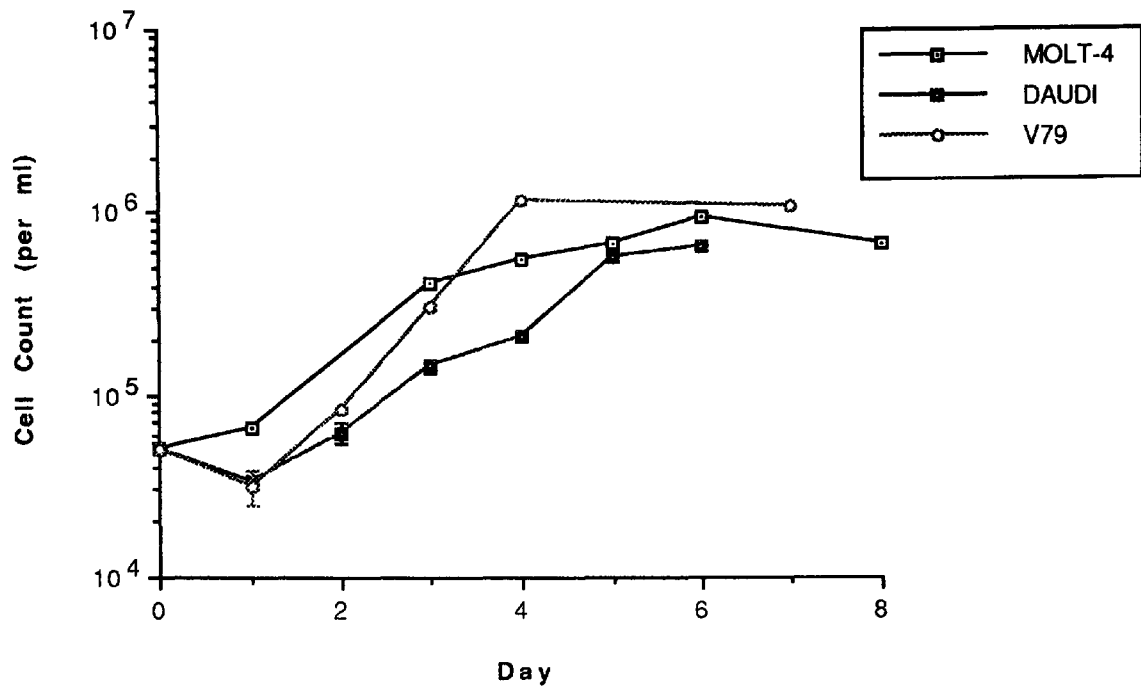
Figure 3.30. Growth curves of unirradiated MOLT-4, DAUDI and V79 cell lines grown in tissue culture flasks with MOLT-4 and DAUDI as suspension cultures and V79 as a monolayer culture. Each of the cell lines were maintained in culture for the duration of the experiment without a medium change. Each point on the graph was derived from pooled estimates of haemocytometer cell counts from 3 flasks with error bars (where apparent) representing the standard error of the mean.

The population growth characteristics of MOLT-4, DAUDI and V79 cell lines were examined over a series of days after exposure to a doses of gamma irradiation ranging from of 0.5-20 Gy. The experiment was performed as described in Section 2.2. The cell population growth characteristics of MOLT-4, DAUDI and V79 cell lines over a dose range of 0.5-20 Gy are presented in Figure 3.31. The graphs indicate that:

(i) The unirradiated cells of MOLT-4, DAUDI and V79, after a short cell division delay (between Day 0 and Day 1), expressed exponential growth. Cell numbers ranged from $5x10^4$ to approximately $1x10^6$ cells per ml between Day 0 and Day 6 of the study.

(ii) There was an increase in total cell number up to 2 Gy in MOLT-4, up to 3 Gy in DAUDI and up to 10 Gy in V79.

(iii) The rate of cell population growth generally decreased with increasing radiation dose. A slower growth rate than unirradiated cells was observed after 1 and 2 Gy in MOLT-4, after 2 and 3 Gy in DAUDI and after 5 and 10 Gy in V79.

(iv) Cell population growth was inhibited after 3 Gy in MOLT-4, after 5 Gy in DAUDI and after 20 Gy in V79. This indicated that, at the respective doses, reproductive cell death had occurred or that the population numbers were maintained by the rapid cell division of radioresistant subpopulations.

(v) The sharp increase in cell numbers between Day 3 and 4 after 1 and 2 Gy in MOLT-4, after 3 Gy in DAUDI and after 5 Gy in V79 indicated that at the respective doses for the three cell lines, cell division delay had occurred which was then followed by a period of rapid cell division.

Overall, it was concluded from the graphs in Figure 3.31. that: (a) MOLT-4 was the most radiosensitive, (b) V79 was the least radiosensitive and (c) DAUDI was less radiosensitive than MOLT-4 but more radiosensitive than V79. The differential sensitivities of MOLT-4, DAUDI and V79 to gamma radiation were apparent on Day 3 when the number of surviving cells counted after exposure to 0.5-20 Gy was expressed as a ratio of the number of cells present in the respective
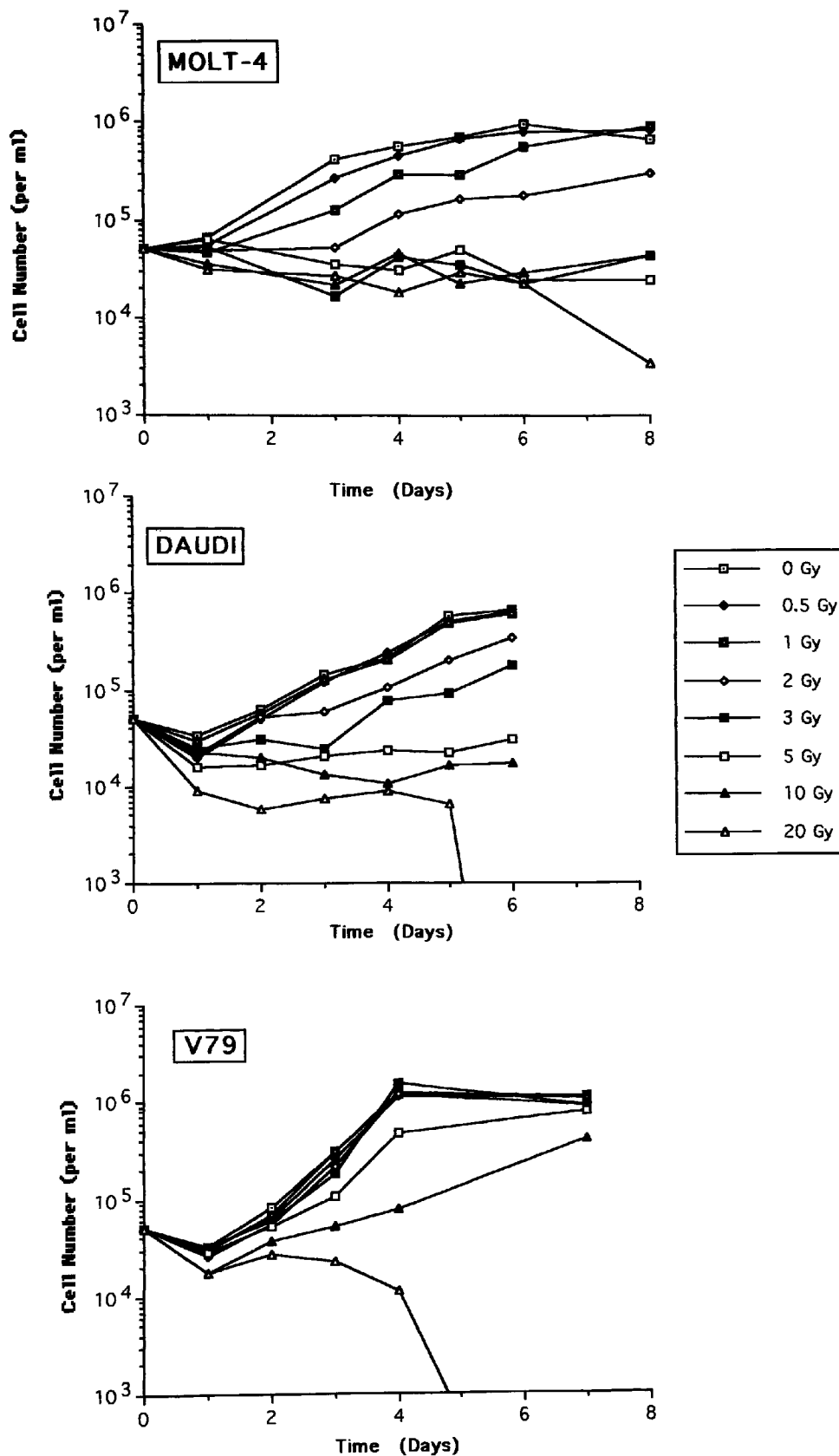
Figure 3.31. Population growth characteristics of the MOLT-4, DAUDI and V79 cell lines following 0-20 Gy gamma irradiation. Each point on the graph was estimated from one full haemocytometer count (4 quadrants) of cells stained with acridine orange taken from each of three tissue culture flasks in MOLT- 4 and DAUDI and from the number of visually intact cells growing over a fixed area on the bottom of each flask in V79. On Day 8 in V79, cell numbers were estimated from haemocytometer counts. The standard error of the mean was less than 15% of the cell counts for each dose.

unirradiated MOLT-4, DAUDI or V79 cell populations (Figure 3.32). The graph shows that on Day 3 there was a similar decrease in the surviving fraction between 0.5-5 Gy in MOLT-4 and DAUDI even though the number of cells counted relative to the unirradiated cell population were consistently less in MOLT-4 than DAUDI. The shoulder on the graph between 0.5-5 Gy in V79 indicates that a greater proportion of cells were present relative to the unirradiated population in V79 than in MOLT-4 and DAUDI. The differential sensitivities were also apparent after 10 Gy. However, after 20 Gy the surviving fraction of cells was about 10% of the number of cells in the unirradiated population for each of the three cell lines. D_{37}values (the dose required to reduce the surviving fraction to 37% of the original count *when the cells were in exponential* derived from the data in the *growth* figure were found to be 0.79, 2.19 and 4.66 Gy for the MOLT-4, DAUDI and V79 lines, respectively.

In addition to haemocytometer counts (which detect the number of visually intact cells), clonogenic assays (which detect the number of cells with the ability to divide and form colonies) were also performed to examine the differential radiation response of the three cell lines. Figure 3.33. shows that the dose response curve in V79 was generally steeper in the clonogenic assay than in the cell count assay. For example, after 5 Gy the number of cells surviving were reduced by 10% whereas the number of colonies were reduced by 40%. This indicates that (particularly at doses higher than 3 Gy) radiation mainly inhibits the clonogenic potential of V79 cells without causing cell death. Clonogenic assays were also performed on the MOLT-4 and DAUDI cell lines but it was not possible to assess the clonogenic potential of these cell lines due to poor plating efficiencies.

The NLS and MGE techniques were used to compare the differences in radiation sensitivity observed in MOLT-4, DAUDI and V79 with the extent of initial DNA damage induction and repair proficiency over a 0.5-10 Gy dose response. Figure 3.34.(a) shows that in NLS the effect of increasing radiation dose
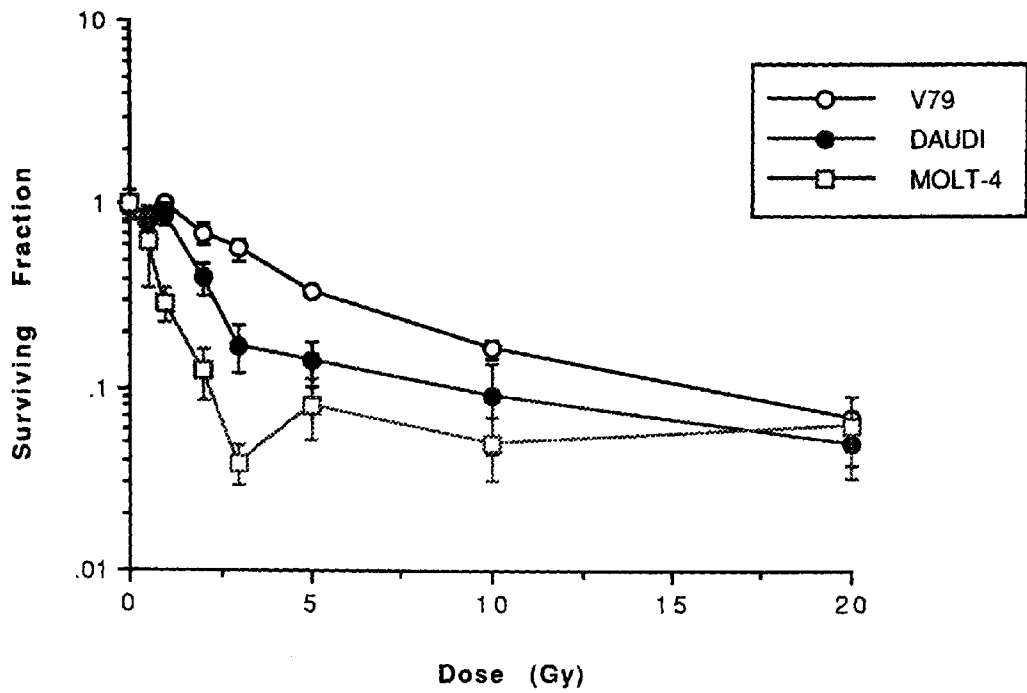
Figure 3.32. Surviving fraction of MOLT-4, DAUDI and V79 cell lines Day 3 after irradiation (0.5-20 Gy). Data points were derived from Figure 3.31. with error bars representing standard error of the mean.
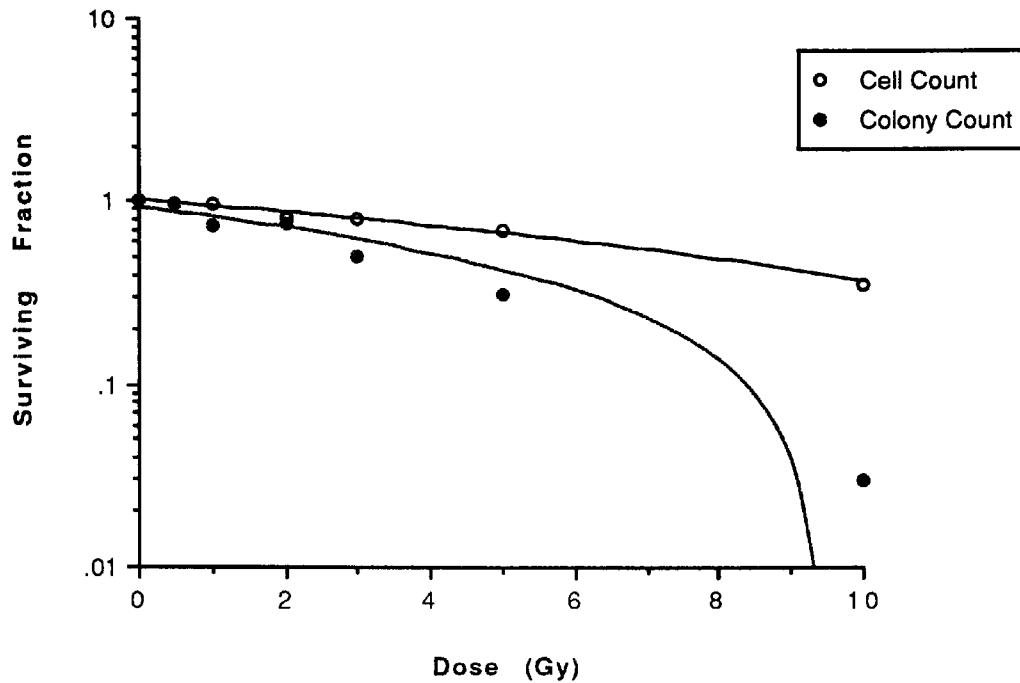
Figure 3.33. Dose response (0, 0.5 1, 2, 3, 5 and 10 Gy) of V79 using cell survival and clonogenic assays. Both cell and colony counts were performed (as previously described) on the 7th day following irradiation. For cell count estimations, each point was derived from 1 haemocytometer count (4 quadrants) from 3 flasks for each dose and for colony counts, triplicate flasks were counted for each dose (plating efficiency 23-26%). The standard error of the mean was less than 15% for the cell survival and colony forming assays. For cell counts, $r^2=0.986$, $p < 0.001$; Colony counts, $r^2=0.924$, $p < 0.001$.

(a) Sedimentation Distance

(b) Comet Tail Migration
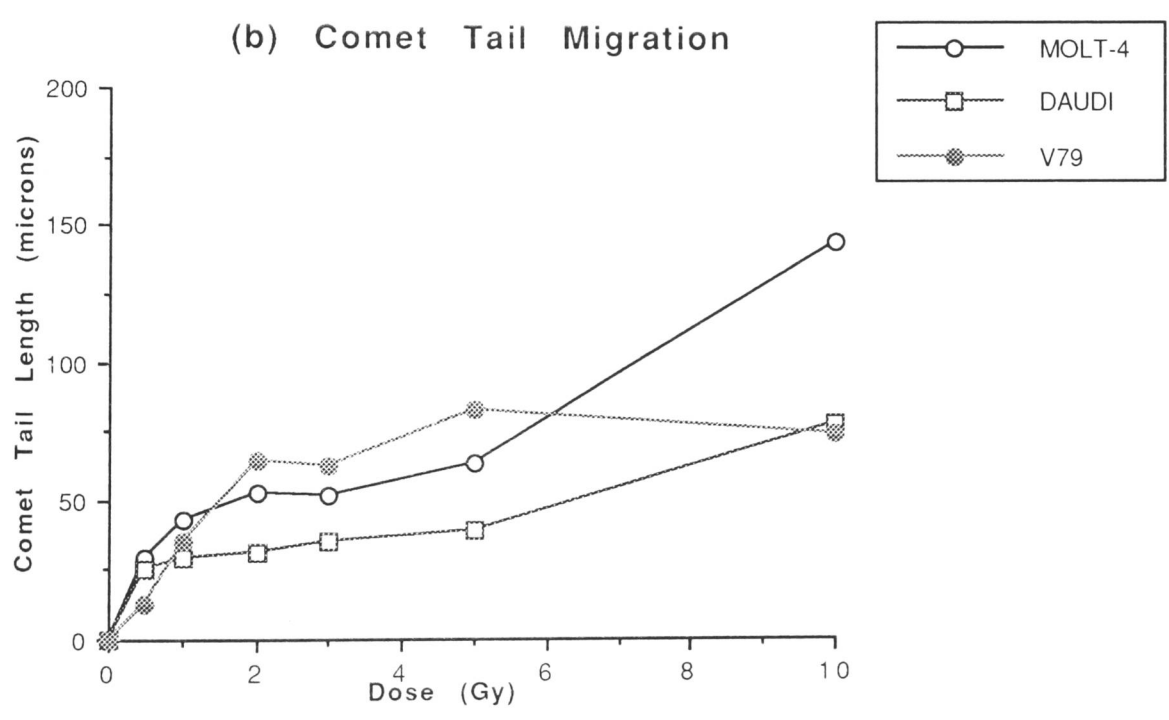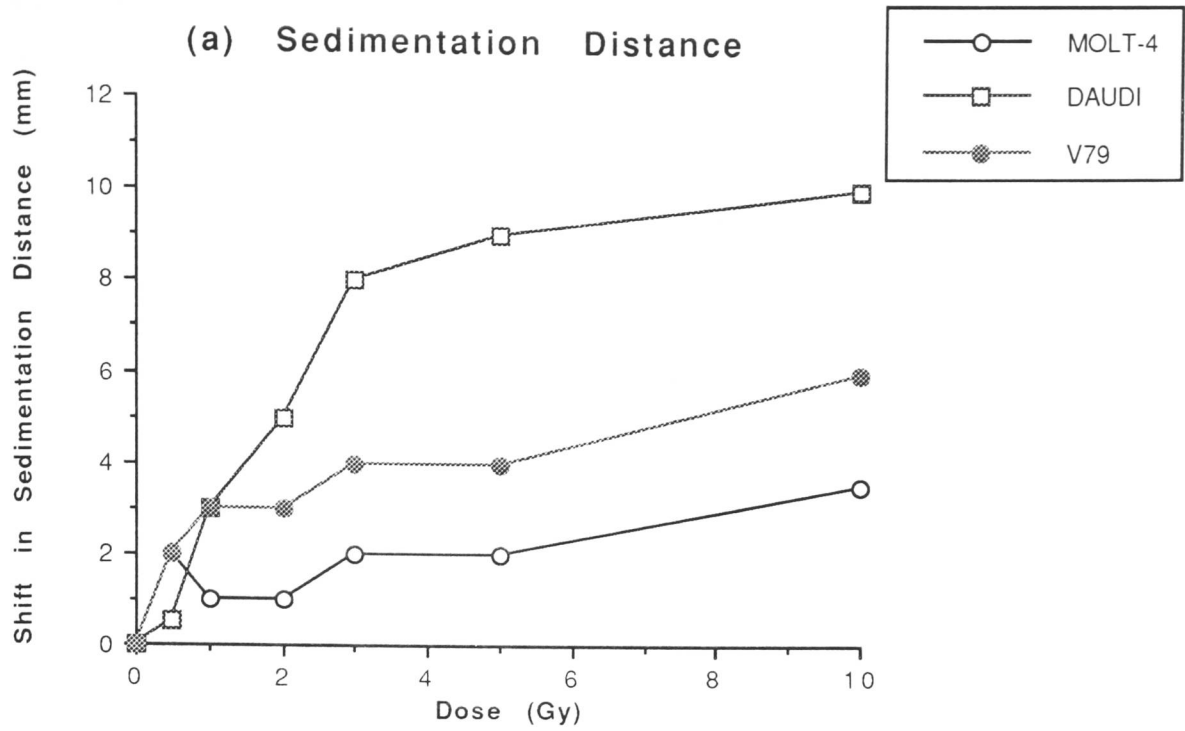
Figure 3.34. Dose response of MOLT-4, DAUDI and V79 to 0, 0.5, 1, 2, 3, 5 and10 Gy in cells during exponential growth (Day 3 cultures) using the NLS and MGE techniques. Figure 3.34.(a) refers to the shift in sedimentation distance of HF-DNA from the nuclei of MOLT-4, DAUDI and V79, respectively. Each point on the graph represents a single sedimentation measurement. The experiments were not performed on the same day but were run concurrently on the same cell line with the MGE technique. Figure 3.34. (b) represents the dose response as a shift in comet tail length in the MOLT-4, DAUDI and V79 cell lines respectively. Each point was derived from the mean of approximately 50 measurements with the S.E.M.'s less than 20% of comet lengths measured at each dose.

104

was detected as a decrease in the sedimentation distance of HF-DNA. If initial DNA damage induction is related to radiation sensitivity, then the graph suggests that DAUDI was more radiosensitive than V79 and that MOLT-4 was the least radiosensitive of the three cell lines. However, over the 0.5-10 Gy dose response, the HF-DNA sedimentation distances of MOLT-4 were high up in the sucrose gradients (that is, sedimentation distances were lower than 10mm). This may indicate the high radiosensitivity of the MOLT-4 cell line due to the presence of a large amount of DNA damage that could not be detected due to the low sedimentation distances. Furthermore, HF-DNA bands with sedimentation distances less than 10mm may not lie within the linear part of the sucrose gradient (Figure 3.2.) which would restrict the efficiency of damage measurement. Each of the cell lines expressed a repair proficiency greater than 1.0 at each dose in the 0.5-10 Gy dose response after the cells were incubated for 1 hour at 37°C. This suggests that repair proficiency did not correlate to the differential radiosensitivities of the three cell lines. However, these results should be interpreted with caution as the observations are based upon single experiments as difficulty was experienced with using cell lines in the NLS technique.

In MGE, the effect of increasing radiation dose was an increase in comet migration (Figure 3.34.(b)). If the shift in comet length after exposure to radiation is related to radiation sensitivity, then the dose response curves suggest a similar radiation sensitivity in the MOLT-4, DAUDI and V79 cell lines. Also, a repair proficiency greater than 1.0 was found following a 1 hour incubation at 37°C after each radiation dose. This suggested that each of the three cell lines expressed good DNA repair capacity.

3.3.2. Summary

The differential radiosensitivies of the MOLT-4, DAUDI and V79 cell lines have been reproduced using a cell count assay. However, when preliminary

investigations were performed using the NLS and MGE techniques to compare cell survival with initial DNA damage and repair status, the relative radiosensitivities of the cell lines were not reproduced. Further investigations are required to determine the role of direct DNA damage analysis in predicting radiosensitivity in tumour cell lines.

3.4. DONOR AND PATIENT STUDIES

The NLS and MGE techniques were used to investigate any differences that may exist in: (i) basal DNA damage, (ii) extent of '2 Gy shift' or (iii) DNA repair proficiency, in lymphocytes extracted from two groups (a) healthy donors and (b) patients with cancer of the cervix. The MGE technique was also used in a short study to illustrate a potential application in monitoring a patient's response to radiotherapy.

3.4.1. *Comparison of Donor and Patient HF-DNA Responses to Ionising Radiation.*

Similarities were found between the mean, standard deviation and range of sedimentation distances, comet tail migration and comet head fluorescence of HF-DNA from both donor and patient groups (Table 3.8.). Further, no significant differences were found between donor and patient groups (using a two-tailed unpaired *t* test) in: (i) basal sedimentation distance, basal comet length and basal comet head fluorescence, and (ii) in '2 Gy shift' in sedimentation distance, comet tail migration and comet head fluorescence. Also, no significant differences were present (using a two way analysis of variance) in the repair proficiencies derived from sedimentation distance, comet tail migration and comet head fluorescence between donor and patient groups. These results indicate that there were no differences in basal DNA conformation, the extent of radiation-induced DNA damage and DNA repair capacity between donor and patient groups.

The distribution of the shift in sedimentation distance, comet tail migration and comet head fluorescence after a 2 Gy irradiation in donor and patient groups is shown in Figure 3.35. Similar distributions were found in the shift in sedimentation distance, with most donors and patient samples expressing shifts in the 3-5mm range. Similar distributions were also found in the shift in comet length with most donor and patient samples expressing shifts less than 99μm.

107

Table 3.8. Comparison of donor and patient HF-DNA sedimentation distance, comet tail migration and comet head intensity as indicators of DNA damage status and repair proficiency

Method of Detection	Donors		Patients	
	Mean ($\pm$ 1 SD)	Range	Mean ($\pm$ 1SD)	Range
Sedimentation Distance (mm)				
Basal	18.95 $\pm$ 4.11	(11 - 30)	18.83 $\pm$ 5.47	(9.25 - 34.25)
'2Gy Shift'	5.24 $\pm$ 2.27	(2 - 11)	4.53 $\pm$ 2.60	(0.5 - 12.25)
Repair Proficiency	0.82 $\pm$ 0.34	(0 - 1.62)	0.91 $\pm$ 0.49	(0 - 1.93)
Comet Tail Migration (μm)				
Basal	96.90 $\pm$ 49.5	(28.6 - 256.9)	98.80 $\pm$ 29.10	(68.5 - 156.6)
'2Gy Shift'	134.00 $\pm$ 95.7	(7.2 - 364.7)	79.00 $\pm$ 76.80	(17.6 - 331.3)
Repair Proficiency	0.74 $\pm$ 0.37	(0 - 1.64)	0.72 $\pm$ 0.46	(0 - 1.41)
Comet Head Fluorescence (AB)				
Basal	7.43 $\pm$ 2.98	(3.66 - 13.62)	7.81 $\pm$ 3.44	(1.98 - 15.03)
'2Gy Shift'	3.53 $\pm$ 1.95	(1.23 - 6.97)	3.02 $\pm$ 1.88	(0.45 - 6.98)
Repair Proficiency	0.63 $\pm$ 0.45	(0 - 1.32)	0.74 $\pm$ 0.40	(0 - 1.27)

Sedimentation Distance (SD), donors, n=59; patients, n=38; Comet Tail Migration (CTM), donors, n=51; patients, n=27, and Comet Head Fluorescence (CHF), donors, n=15; patients, n=15. (AB) = arbitrary units.

Shift in Sedimentation Distance

Shift in Comet Length

Shift in Comet Head Fluorescence
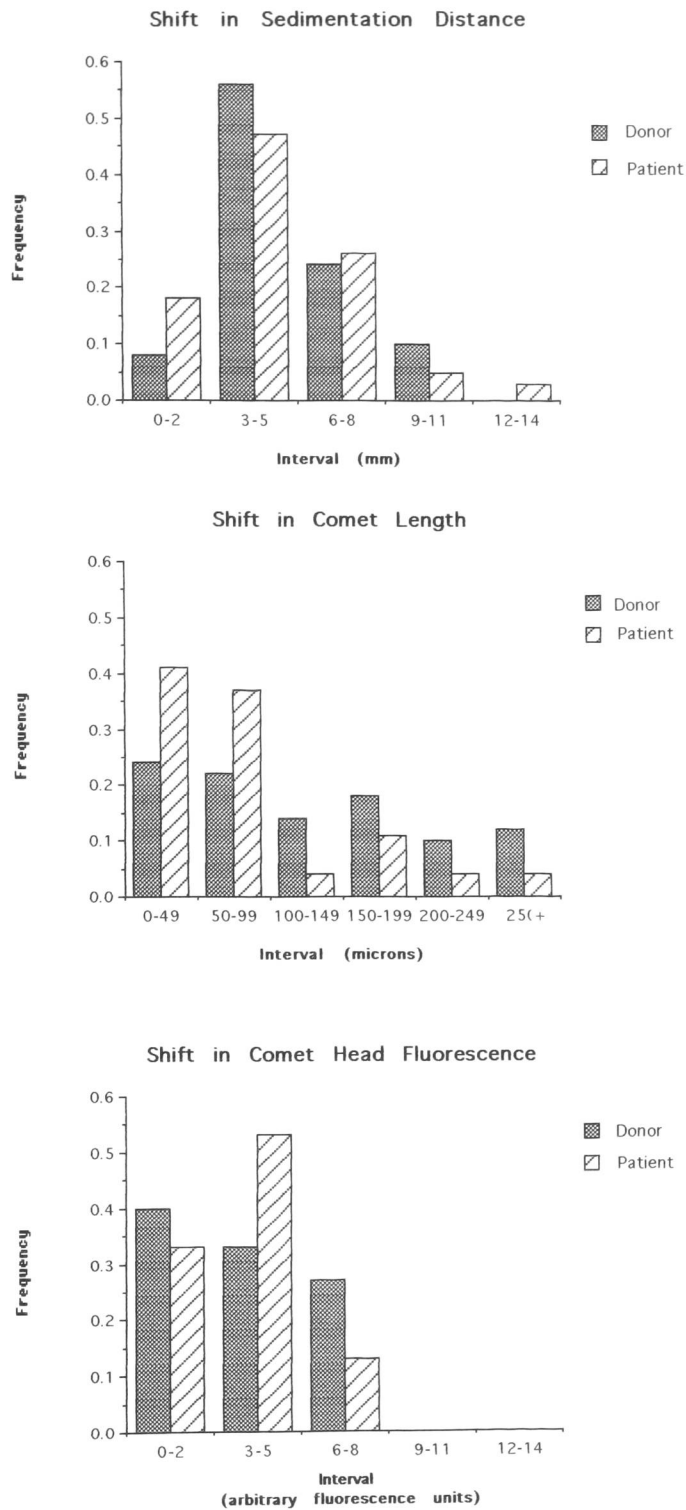
Figure 3.35. Comparison of '2Gy shift' distribution in sedimentation distance, comet tail migration and comet head fluorescence estimations of HF-DNA damage in donor and patient groups respectively. The histograms represent 59 donor and 38 patient samples for sedimentation distance; 51 donor and 27 patient samples for comet tail migration and 15 donor and 15 patient samples for comet head fluorescence.

However, approximately 15% more patients than donors expressed shifts in both the 0-49μm and 50-99μm range with at least 5% more donors than patients expressing shifts greater than 100μm. The distribution of shift in comet head fluorescence differed between donor and patient groups, with most donors expressing shifts in the 0-2 range and most patients expressing shifts in the 3-5 range. The shifts in fluorescence in both donor and patient groups were less than 8 arbitrary fluorescence units.

The distribution of repair proficiency following a 1 hour incubation at 37°C in donor and patient groups is shown in Figure 3.36. Generally, the distribution of repair proficiency derived from HF-DNA sedimentation distances differed between the donor and patient groups. Repair proficiency was between 0.40-1.09 in most of the donor samples and greater than 0.8 in most of the patient samples. Also more patient samples produced repair proficiencies less than 0.39 or greater than 1.10 than did the donor samples. Similar distributions were observed for repair proficiencies derived from changes in comet length in both donor and patient groups with the exception of about 20% more of the donors having repair proficiencies ranging from 0.40-0.79. Similar distributions of repair proficiencies derived from changes in comet head fluorescence were observed in both donor and patient groups but with a greater proportion of donors having a repair proficiency less than 0.39 than the patients and with more patients having a repair proficiency less than 0.39 than the donors. Interestingly, as with repair proficiency derived from HF-DNA sedimentation distances, twice as many patients as donors expressed a repair profiency greater than 1.00 (or 'over-repair').

3.4.2. Comet Tail Migration as an Indicator of DNA Damage in the Lymphocytes of a Patient receiving Radiotherapy

A patient with cancer of the cervix was studied throughout her radiotherapy course which involved six weeks of external beam therapy, a week
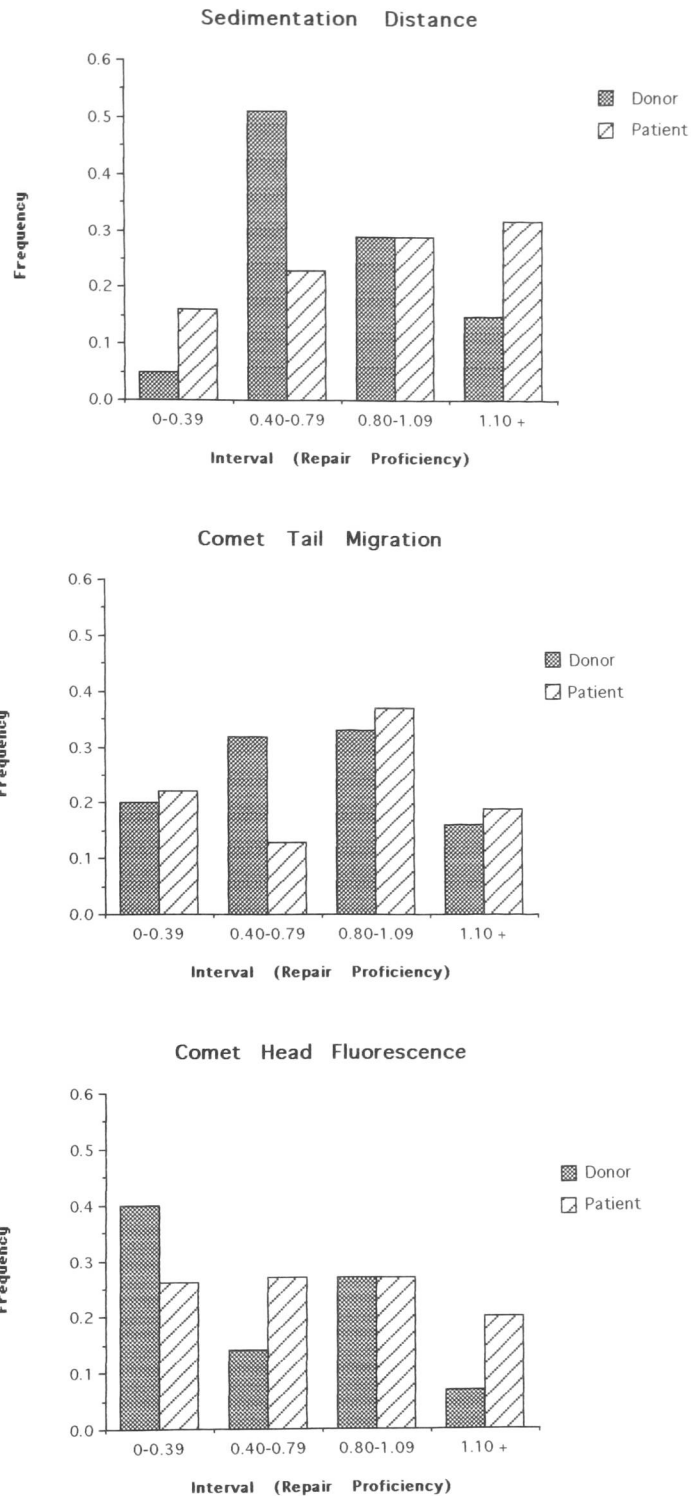
Figure 3.36. Comparison of donor and patient repair proficiency distributions derived from an increase in sedimentation distance, a reduction in comet tail migration and increase in comet head fluorescence of incubated samples after a 2 Gy irradiation. The histograms represent the same number of samples from both donor and patient groups as in Figure 3.35.

111

without radiotherapy and three weeks of internal cavity insertions. The patient had not previously received any radiation treatment and the first blood sample was received prior to her first appointment for radiotherapy. Whilst the patient was receiving external beam therapy, venous blood samples were obtained on a weekly basis as she proceeded to receive radiotherapy treatment as a hospital out-patient each day. Between week 1 and week 6 she received one external beam radiotherapy treatment (approximately 2 Gy) each day and a dose of approximately 5 x 2 Gy each week. The patient did not receive any radiation treatment on week 7 (this is usual according to the standard treatment for cancer of the cervix). The patient then received three weekly internal cavity insertions (approximately 3 x 1.5 Gy) as a hospital in-patient for the following three weeks. However, only the two blood samples were received from the patient after her first and second internal treatments. A final blood sample was received from the patient 4 weeks after the completion of her treatment when she had attended a post-radiotherapy out-patient clinic.

Figure 3.37. shows the comet tail migration of HF-DNA in unirradiated, irradiated, and irradiated and incubated lymphocyte samples that were obtained from the patient's blood samples during her radiotherapy treatment. During the external beam therapy, the mean comet tail length of unirradiated lymphocytes was higher in the pre-treatment sample (week 1) than in the following weeks (week 2-6) - $p < 0.0001$ using a two-tailed unpaired Student's t test. Similarly, mean comet length was higher on week 8 (immediately before intra-cavity treatment) than on week 9 and 13 following treatment - $p < 0.0001$ using a two-tailed unpaired t test. The '2 Gy shift' in comet tail length after the patient's isolated lymphocytes were exposed to 2 Gy gamma irradiation was fairly constant (CV < 29%) with the exception of week 4 and week 9. Even though repair proficiency ranged from 0.22 - 1.93 over the 13 weeks of the study, a repair proficiency greater than 0.62 was found in six out of nine of the samples. This compared favourably with repair proficiencies of 0.90 and 0.69 calculated from
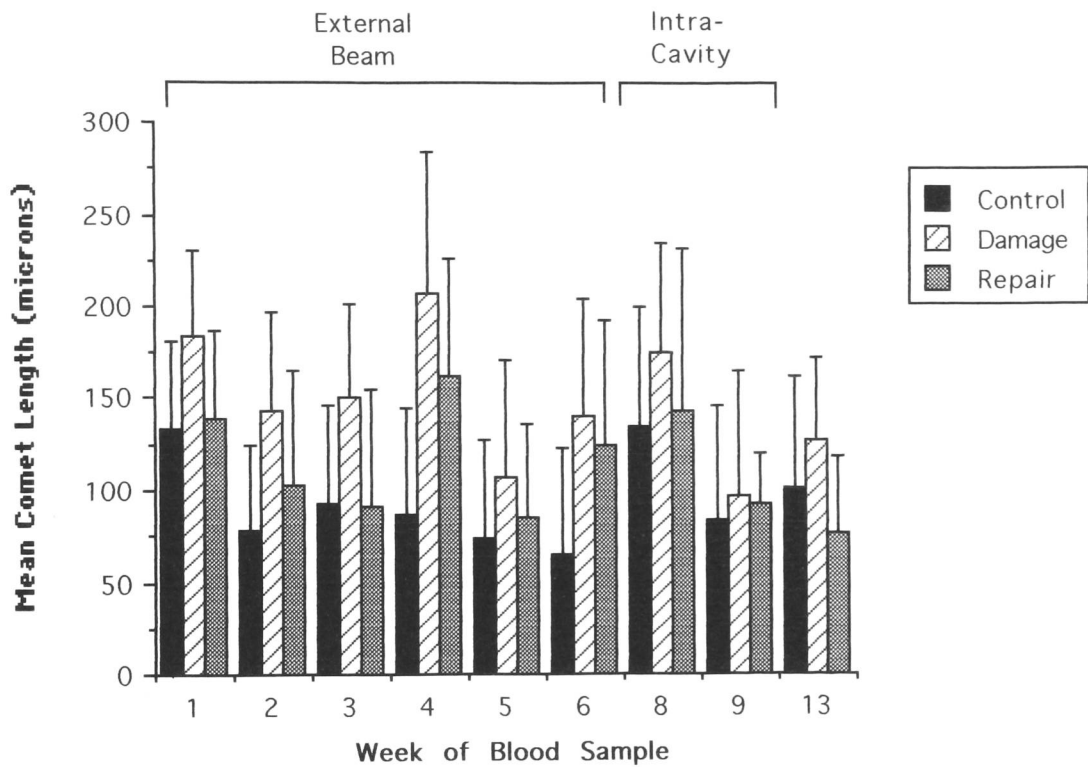
Figure 3.37. Mean comet tail length of unirradiated ('Control'), irradiated ('Damage') and irradiated with incubation ('Repair') lymphocyte HF-DNA obtained from a patient with cancer of the cervix during her radiotherapy course. Approximately 50 comets were analysed in respective 'Control', 'Damage' and 'Repair' slides in each of the blood samples received. Vertical bars refer to the standard deviation.

113

sedimentation distances and comet head fluorescence respectively, of lymphocyte HF-DNA received on week 1. Generally, no overall trend was observed in the irradiated and irradiated and incubated mean comet lengths and the amount of radiation received during radiotherapy.

Figure 3.38.(a) shows the frequency distribution of comet length of unirradiated, irradiated, and irradiated and incubated lymphocytes received from the patient over the six weeks of external beam radiotherapy. With the exception of the pre-treatment sample where most comet lengths were between 100 and 199µm, generally over 40% of the unirradiated lymphocytes exhibited small amounts of DNA damage (0-49µm) with less than 10% of the samples expressing comets longer than 199µm. In each analysis, 20-55% of irradiated lymphocytes produced comets in the 150-199µm range with a sub population of comets in the 200-249µm range. Of the irradiated and incubated lymphocytes, generally a broad range of comet lengths were found. Good repair was seen on weeks 1, 2, 3 and 5 and poor repair on weeks 4 and 6.

Figure 3.38. (b) shows the frequency distribution of comet lengths from unirradiated, irradiated, and irradiated and incubated lymphocytes immediately before intra-cavity treatment (week 8), after 1 intra-cavity treatment (week 9) and four weeks after the completion of the radiotherapy course (week 13). The comets of most unirradiated lymphocytes were between 150-199µm on week 8. On week 9 more comets were present in the 0-49µm interval indicating that less basal DNA damage was detected on week 9 than week 8. By week 13, two distinct populations of comet lengths were present with 40% of comet lengths between 0-49µm and 40% of comet lengths between 150-199µm. In irradiated lymphocytes, however, a broad spread of comet lengths were observed in each of the three histograms. The distribution of comet lengths in irradiated and incubated lymphocytes indicated that DNA repair had occurred on week 8, 9 and 13.

The difference in the distribution and mean comet lengths of unirradiated cells from: (i) the pre-treatment sample as compared to the other samples

114

External Beam Radiotherapy
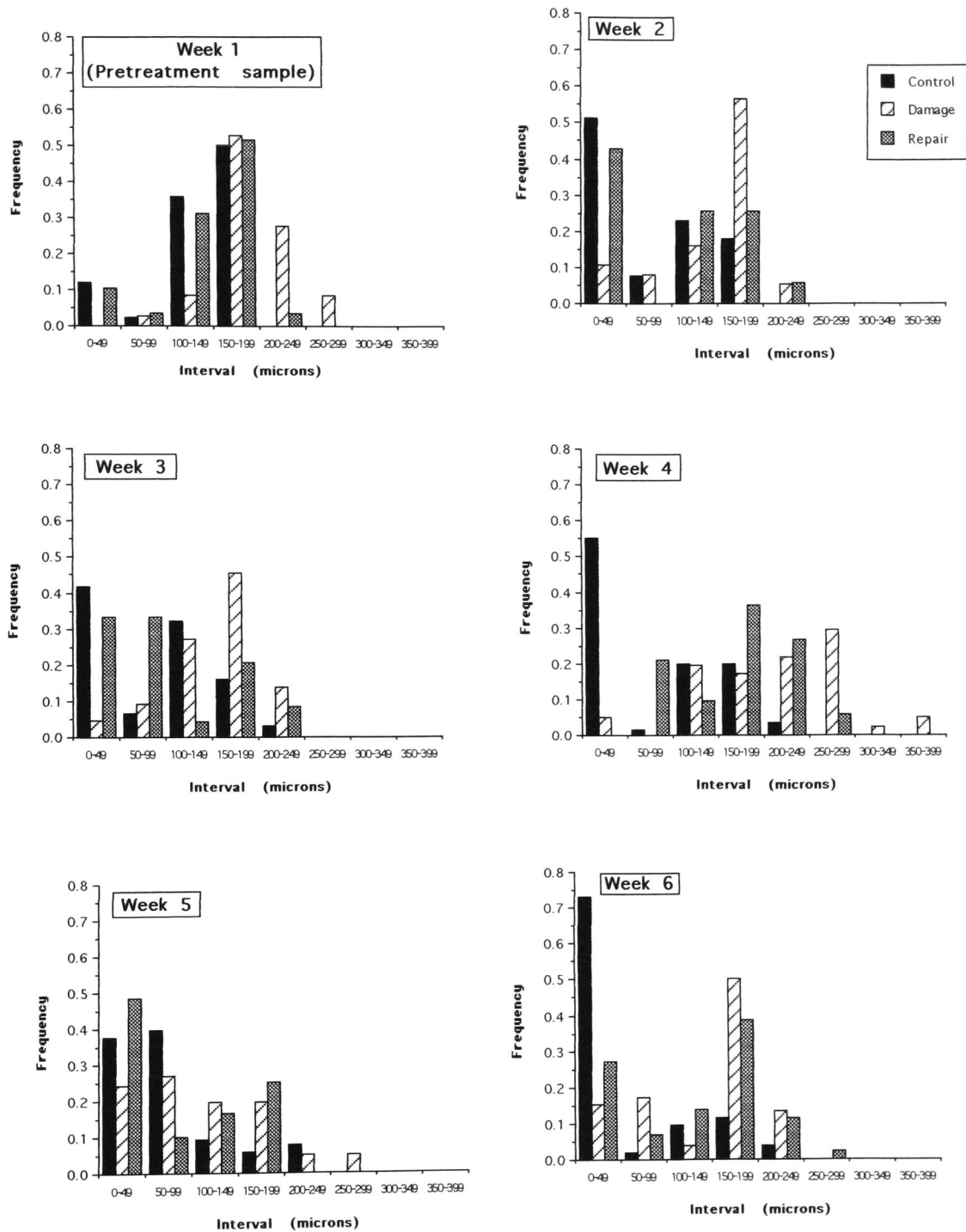
Figure 3.38.(a). Frequency histograms of the distribution of comet tail length observed in lymphocyte samples received weekly from the same patient during six weeks of external beam radiotherapy. Each histogram represents unirradiated ('Control'), irradiated for 2 Gy ('Damage') and irradiated plus incubated ('Repair') populations of the same sample. Comet tail length measurements were taken of approximately 50 comets for each of these populations.

115

Intra-Cavity Brachytherapy
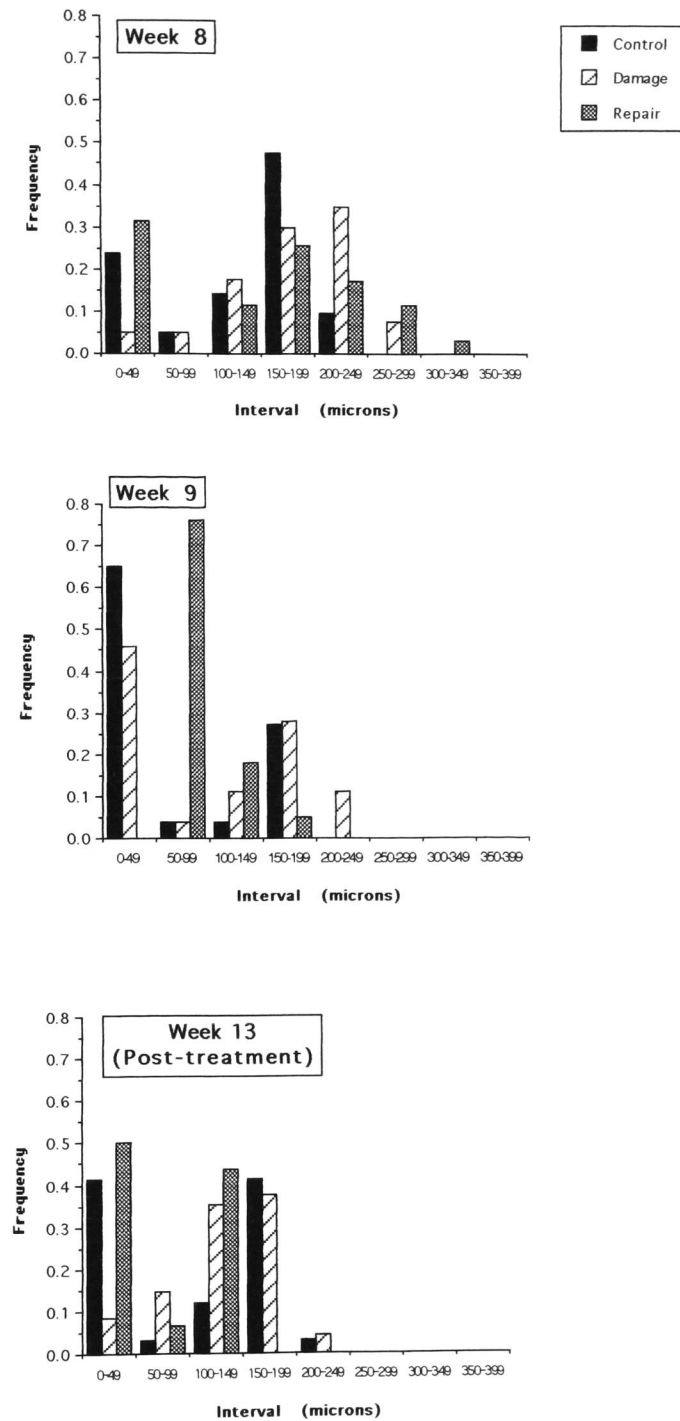
Figure 3.38. (b). Frequency histograms of the distribution of comet tail length observed in lymphocyte samples received immediately before,during and following intra-cavity brachytherapy. Each histogram represents unirradiated ('Control'), irradiated ('Damage') and irradiated and incubated ('Repair') populations of the same sample.

116

collected between week 2 and 6 and (ii) the sample on week 8 compared to the samples on week 9 and 13, suggests that the introduction or re-introduction of radiation treatment had reduced the amount of basal DNA damage or caused basal DNA conformation to alter. This suggests that radiation treatment may have contributed to: i) an alteration in the cell cycle ratio of peripheral blood lymphocytes, ii) the action of an "inducible" DNA repair system, or iii) the removal of lymphocytes possessing basal DNA damage and repopulation of circulating lymphocytes.

This study has highlighted the clinical potential of MGE as a simple technique capable of detecting changes in the distribution of DNA damage and repair in a population of single cells during radiotherapy.

3.4.3. Summary

The studies in this section have shown that:

(i) Overall no differences were found in NLS and MGE in basal DNA damage, the extent of '2 Gy shift' or the DNA repair proficiency between donor and patient groups.

(ii) MGE has clinical potential as a simple technique capable of detecting changes in the distribution of DNA damage and repair in a population of single cells during radiotherapy.

Chapter Four:

Discussion

4.1. Validation of NLS and MGE as DNA Damage and Repair Assays

The Nuclear Lysate Sedimentation and Microgel Electrophoresis techniques have been examined and compared as *in vitro* assays of radiosensitivity on the basis that direct measurements of DNA damage and repair proficiency can be achieved rapidly by simple and inexpensive means. Preliminary studies (Section 3.1.) have shown that under the experimental conditions employed, both NLS and MGE were:

(i) Capable of detecting radiation-induced DNA damage over a range of 0.5-10 Gy.

(ii) Sensitive at the clinically relevant 2 Gy dose.

(iii) Suitable for estimating repair proficiency of DNA after a 2 Gy dose.

(iv) Reproducible on an intra- and inter-sample basis (even though some variation was observed in both assays).

Once NLS and MGE had been demonstrated to be quick, reliable and sensitive methods of direct radiation-induced DNA damage and repair detection, studies were performed to examine:

(i) The extent to which NLS and MGE agree in estimating radiation-induced DNA damage and repair proficiency as a cell population response and as a response in single cells (Section 3.2.).

ii) The relationship of direct DNA damage and repair assessment and *in vitro* radiosensitivity expressed as cell survival (Section 3.3.).

118

(iii) The potential of both techniques to predict radiation sensitivity within donor and patient groups (Section 3.4.).

4.2. DNA Damage and Repair Assessment in NLS and MGE

Eukaryotic DNA is organised into supercoiled loops or 'domains' which are bound to the nuclear matrix (van Rensburg, 1989). When cells are lysed in the presence of non-ionic detergents and a high NaCl concentration, structures resembling nuclei ("nucleoids") are released (Cook & Brazell, 1976). The DNA in nucleoids is histone-depleted (HF-DNA) but remains folded into loops forming a compact supercoiled structure which is anchored to the nuclear matrix (Mattern, *et al.*, 1987).

Nuclear Lysate Sedimentation and Microgel Electrophoresis are assays that use HF-DNA to assess damage to DNA higher-order structure. A loss of DNA supercoiling can be attributed to radiation-induced strand breaks, for example, which cause the DNA to unfold in the affected domain. In NLS, the sedimentation behaviour of nucleoids is modified by the degree of supercoiling. Consequently, relaxed or uwound DNA will sediment more slowly than compact unirradiated counterparts.

Microgel Electrophoresis detects a loss of DNA supercoiling as radiation-induced strand breaks cause the DNA to relax which make it more disposed to migrate towards the anode during electrophoresis. Östling & Johanson (1987) have suggested that DNA which is organised into compact superstructure units (and attached to the nuclear matrix or membrane) is stretched towards the anode whereas smaller DNA fragments migrate more rapidly towards the anode during electrophoresis. The smaller fragments also diffuse laterally giving the shape of a cone to the comet.

On the basis that nucleoid sedimentation and single cell electrophoresis techniques both detect changes in DNA supercoiling, Östling & Johanson (1984) commented on their similarities whilst Green *et al.* (1992) considered the MGE

assay as a development of nucleoid sedimentation and the halo assay of Roti Roti (1987). Further, in a preliminary comparative study of NLS and MGE, Deeley *et al.*, (1990) found that the techniques agreed in the assessment of radiation-induced DNA damage ($r = 0.73$, $p < 0.05$) and in repair proficiency (ranked as 'good', 'moderate' or 'poor') in eight out of ten donors ($r = 0.559$, $p < 0.1$).

Dose Response to Ionising Radiation

The relative sensitivities of both NLS and MGE to detect the amount of DNA damage present following increasing doses of radiation were assessed in terms of the shift in sedimentation distance, comet tail migration and comet head fluorescence between unirradiated and irradiated DNA. The dose response curve obtained from a decrease in sedimentation distance of lymphocyte HF-DNA over a range of 0.5-10 Gy (Figure 3.5.) was similar to that of (i) van Rensburg *et al.* (1985) who studied the radiation response of B and T_1 lymphocytes in neutral (pH 8.0) 15-30% sucrose gradients over the range 0.25-6 Gy and (ii) Louw *et al.* (1991) who studied the response of human lymphocytes in neutral 15-30% sucrose gradients over a 0.25-5 Gy range. Also, the shift in comet tail length and in the shift in comet head fluorescence with increasing radiation dose (Figure 3.12.) was comparable to the extent of migration of lymphocte comet tail length observed by Singh *et al.* (1988) in human lymphocytes after exposure to 0.25-2 Gy X rays. At 2 Gy where the sensitivities were closest, the 20-fold increase in comet tail migration reported by Singh *et al.* was matched in the present study by a 15-fold increase in comet tail length and a 10-fold decrease in comet head fluorescence. Further similarities were observed in the increase in DNA migration of human lymphocytes exposed to 0.25-20 Gy of X rays as described by Tice *et al.* (1990). After 10 Gy, Tice *et al.* observed a 10-fold increase in comet length which compared to a 10-fold increase in comet tail migration and a 15-fold decrease in comet head fluorescence as described in Figure 3.12.

The linear relationships shown in Figure 3.19. indicated that both techniques were able to detect increasing amounts of DNA damage with increasing radiation dose. The sensitivities of the techniques are shown in Figure 3.20. where the relative shift per Gy indicates that NLS and MGE were both sensitive in the 0.5-2 Gy range. At doses higher than 2 Gy, comet tail length was the more sensitive measure of DNA damage. A plateau in the effect of radiation damage was apparent after 3 Gy in both techniques. It has been suggested that such a plateau is due to maximal DNA relaxation after a 3 Gy dose. (Östling & Johanson, 1984). Overall, the dose response curves generated from the shift in sedimentation distance, comet tail migration and comet head fluorescence indicate that both NLS and MGE techniques are sensitive in the 0.5-10 Gy range.

Relationship of Basal DNA Damage and Extent of '2 Gy Shift' and Repair Proficiency

Olive *et al.* (1991b) have proposed that intrinsic differences in DNA basal conformation affect the extent of radiation-induced damage and repair capacity. Thus, the relationship between basal DNA damage, the extent of '2 Gy shift' and repair proficiency was examined using the NLS and MGE techniques. Figure 3.24. showed that a linear relationship was observed between the extent of basal DNA sedimentation distance and basal comet head fluorescence and the extent of '2 Gy shift' after irradiation. Deeley & Moore (1989) have also shown that there was a linear relationship between the location of unirradiated HF-DNA sedimentation distance and the extent of shift following 4.5 Gy. These relationships indicate that a greater '2 Gy shift' is possible the when there is a large sedimentation distance or a bright comet head intensity of unirradiated DNA. Even though this relationship probably exists when measuring comet tail length as an indicator of DNA damage, the lack of correlation observed between basal comet tail length and '2 Gy shift' may have been influenced by: (i) Difficulty in determining the amount of DNA damage in unirradiated comets when sparse fragmentation of

the comet head had occurred - an effect of radiation which could be detected as a measuable shift in sedimentation distance and comet head fluorescence and, (ii) The presence of a point in sedimentation distance and comet head fluorescence where the shift after irradiation is maximal due to the constraints of the experiment whereas this is less defined when measuring comet tail length (Figure 3.20.).

Both NLS and MGE showed a lack of correlation between basal DNA conformation (indicated by unirradiated sedimentation distances, comet tail migration and comet head fluorescence) and repair proficiency as shown in Figure 3.25. It was concluded that NLS and MGE did not detect any relationships between basal DNA conformation and repair capacity in the lymphocyte samples studied.

DNA Repair Kinetics

Nuclear Lysate Sedimentation and Microgel Electrophoresis were compared as DNA repair assays using a radiation dose of 2 Gy and a post-irradiation incubation period of 1 hour. These conditions were chosen as 2 Gy is a clinically relevant dose of radiation and produced a measurable shift in sedimentation distance, comet tail migration and comet head fluorescence. Also, Deeley & Moore (1989) using NLS had shown that the majority of donors expressed a repair proficiency of 1.0 or greater after a 1 hour incubation period at 37°C.

The value of NLS and MGE to determine DNA repair kinetics following a 2 Gy irradiation was examined using incubation periods of 5, 30 and 60 minutes (Figure 3.22.). The profiles of the repair kinetics curves in NLS and MGE suggested that the majority of repair occurred within the first 30 minutes, followed by a second, slower component occurring between 30 and 60 minutes of incubation. Similarly, Louw et al. (1991), using nucleoid sedimentation, observed that most DNA repair occurred within the first 60 minutes of incubation with the

amount of repair continuing to increase with increasing incubation time. Also, Tice *et al.* (1990), using MGE, reported that the majority of repair occurred within the first 15 minutes, with a slower second phase completing repair by the end of a 2 hour incubation period.

The apparent biphasic character of DNA repair curves observed in the sedimentation technique have been attributed to the rapid repair of single-strand breaks and/or easily accessible lesions, followed by slow DNA conformational changes and nuclear protein rearrangements which may be associated with DNA double-strand break repair (Louw *et al.*, 1991). In Figure 3.22., the repair profiles of NLS and MGE, indicate that diverse processes encompassing rapid DNA strand join activity and higher-order topological changes occur during the repair of radiation-induced DNA damage.

Over-Repair Phenomenon

Stephens & Lipetz (1983) have noted that in approximately 20% of healthy lymphocyte donors, the sedimentation distances of repaired nucleoids (after a 2 hour incubation period) were greater than those of unirradiated nucleoids. Figure 3.37. showed that after a 1 hour incubation period, up to 15% of the healthy donors and up to 30% of the patients studied showed that HF-DNA sedimentation distance and comet head fluorescence was greater or HF-DNA comet tail migration was less, in irradiated and incubated lymphocytes than unirradiated lymphocytes. This suggests that the repair proficiency in these individuals was greater than 1.00, that is 'over-repair' had occurred. The possible explanations for over-repair include:

(i) An increased DNA supercoiling is a normal part of the repair processing of higher order DNA damage.

(ii) The repair of pre-existing DNA damage in unirradiated DNA. However, a lack of correlation was found between the extent of basal DNA damage and an over-repair proficiency in the same individuals (Figure 3.25.).

(iii) The presence of an alteration in DNA configuration due to mis-match repair, for example.

iv) A normal intermediate stage in repair as predicted by the nucleosome stacking model of Worcel *et al.* (1981). This model proposes that after the repair of DNA strand breaks, when nucleosomes have reassociated with the repaired region of DNA, prior to stacking there will be a period of abnormally high DNA supercoiling. This may be apparent in Figure 3.22. where a greater repair proficiency was observed in some individuals after 30 minutes rather than after 60 minutes of a post-irradiation incubation period.

Split-Dose Recovery

A variety of studies using clonogenic assays have indicated that cell survival is enhanced when cells are irradiated with doses of radiation which are split into two fractions, separated by a time interval, rather than when cells are irradiated with a single dose. The reappearance of a shouldered survival curve has been interpreted as the repair of double-strand breaks during the interval between the two doses (Frankenberg *et al.*, 1984). From such studies, the rationale of fractionated radiotherapy which would allow normal tissue recovery to occur was introduced. However, conflicting views exist as to whether the DNA damage is sublethal, potentially lethal or error-prone, (Seymour & Mothersill, 1989).

124

In the present study, split-dose recovery was examined in the NLS technique. The good linear relationships (shown in Figure 3.21.) between the shift in sedimentation distance in (i) a 2 Gy single-dose and a 4 Gy single-dose, (ii) a 2 Gy split-dose dose and a 4 Gy single-dose and (iii) a 2 Gy single-dose and a 2 Gy split-dose indicates that DNA repair (approaching a repair proficiency of 1.0) was occurring during the incubation period between the two doses of the 2 Gy split-dose sample. Thus, in the same individual, the extent of repair (indicated by the amount of DNA damage remaining after the 2nd dose of radiation in the split-dose sample), should be comparable to the actual repair proficiency as indicated by a sample irradiated with a 2 Gy single dose and incubated for 1 hour at 37°C. However, as shown in Figure 3.21., linear relationship was not observed when the actual repair proficiency after the 1st irradiation (derived from an irradiated and incubated lymphocyte sample) was compared to the estimated repair proficiency (derived from the remaining shift after the 2nd irradiation). From these results, the following interpretations were made of the DNA repair kinetics which may be involved in the cell's response to radiation-induced DNA damage:

(i) A single 2 Gy dose damages the DNA by causing single and double-strand breaks. During the repair process, (which occurs in the incubation period between the 1st and 2nd dose of the 2 Gy split-dose sample), the DNA unwinds, strand breaks are rejoined and the DNA assumes a similar but not identical supercoiled structure to that of the unirradiated sample. Thus, the DNA could yield a similar sedimentation coefficient but when a 2nd 2 Gy dose is administered, targets (that is, potential strand breaks) other than the ones originally activated following the 1st 2 Gy dose may be activated after the 2nd 2 Gy dose with a differing extent of assocxiated unwinding in the DNA. Thus, the shift in sedimentation may differ between a single 2 Gy dose and a split 2 Gy dose. The overall effect would be an actual repair proficiency of 1.0 and an estimated repair proficiency greater or less than 1.0.

(ii) Basal DNA damage (perhaps in the form of strand breaks) is present in the unirradiated sample. A single 2 Gy dose causes additional damage to the DNA. During the incubation period, DNA repair enzymes accomodate the original DNA damage as well as the radiation-induced DNA damage. Upon the 2nd irradiation of the split-dose sample, an equivocal amount of DNA damage occurs but the shift in sedimentation distance will differ between the 2 Gy single-dose and the 2 Gy split-dose samples as the original amounts of DNA differ prior to irradiation. Thus, the actual repair proficiency would be greater than 1.0 and the estimated repair proficiency, less than 1.0.

(iii) DNA repair processing during the incubation period between the two doses of the split-dose, causes the DNA to assume a more or less compact superstructure than the unirradiated DNA (due to the association of DNA repair enzymes or mis-match repair, for example). Thus, if a similar extent of DNA damage occurs after the single 2 Gy dose and after the split 2 Gy dose, the shift in sedimentation distance between the unirradiated DNA and the 2 Gy single-dose from the shift between the 2 Gy single-dose and the 2 Gy split-dose. Thus, actual repair proficiency could be greater than 1.0 when the estimated repair proficiency is less than 1.0 and the actual repair proficiency could be less than 1.0 when the estimated repair proficiency is greater than 1.0.

iv) In some individuals, the actual and estimated repair proficiencies may correlate in that:

(a) Cells which are repair deficient will exhibit a greater shift in sedimentation distance after a split 2 Gy dose than after a single 2 Gy dose (as DNA repair has not occurred during the incubation period between the 2 doses of the split-doese sample), thus the actual repair proficiency will be less than 1.0 when the estimated repair proficiency is also less than 1.0.

(b) Good repair may occur during the incubation period between the two doses of the split-dose sample. Thus, the actual repair proficiency and the estimated repair proficiency will both be about 1.0.

126

However, where there is agreement between the actual and estimated repair proficiencies within a sample, Figure 3.21.(d) showed that the correlation is masked by the variation of responses present within the group of donors studied.

It is suggested that studies similar to the NLS split-dose study outlined above are performed and compared to the differing effects of radiation when administered as single-doses and split-doses upon DNA damage, repair proficiency and cell survival. Further comparative experiments could be performed using direct DNA damage assays and clonogenic assays to examine the repair kinetics of split-dose recovery, optimisation of incubation time between doses and the relationship between fractionated dose and exhaustive DNA repair systems.

Repair Fidelity as an Age-Related Phenomenon

The premise of a major theory of the ageing process is based upon older members of a species exhibiting an increased level of DNA damage that is possibly accompanied by a decreased repair proficiency (Tice & Setlow, 1985). However, studies suggesting that an increase in basal DNA damage occurs with increasing age have been performed on pooled cell populations (Singh *et al.*, 1991a). For instance, Harris *et al.* (1986) concluded from nucleoid sedimentation profiles that lymphocyte DNA repair proficiency (after exposure to 2 Gy X-irradiation) was reduced in older donors (ages 66-99 years). They also identified that lymphocytes from older donors with good repair had lower background levels of chromosome damage than those who exhibited impaired DNA repair. Singh *et al.* (1990) used a microgel electrophoresis assay to identify the presence of subpopulations of lymphocytes with repair characteristics that differed with increasing donor age. They observed that: (i) following 2 Gy of X-rays, cells from older individuals (60-93 years) exhibited increased levels of DNA single strand breaks and/or alkali-labile sites and, (ii) that even though the DNA damage was

completely repaired within 2 hours in most lymphocytes, a small population of cells that did not repair were more likely to be present in samples from older individuals. Singh *et al.* (1991a) also used the microgel electrophoresis assay to study basal DNA damage in human lymphocytes received from older donors. They found that while average difference in the extent of DNA damage may be small between donors younger than 60 as compared to donors older than 60 (about 12%), the increase in a subpopulation of highly damaged lymphocytes in certain ageing individuals was 5-fold as compared to their younger counterparts.

In the present study, an age-related increase in basal DNA damage and/or decrease in repair proficiency was not apparent in lymphocyte populations from NLS and MGE studies in donors and patients aged between 21 and 76 years old (Figure 3.23.). Of the eight individuals who exhibited a repair proficiency less than 0.5 in either NLS or MGE, only one was aged over 60 years. However, the studies outlined above illustrate the potential of NLS and particularly MGE (as subpopulations of grossly damaged cells can be identified) for future testing of DNA damage and repair capacity in ageing individuals.

Cell Population Growth and DNA Damage and Repair

Ionising radiation has a variety of effects upon the growth of cell populations. These include: (i) Reproductive death, whereby cells function but no longer divide, (ii) Mitotic dealay, whereby cell division is delayed but is resumed after a period of time, (iii) Limited mitosis, whereby cells can still divide but not for an indefinite period of time, (iv) Inter-phase death, whereby cells are destroyed shortly after irradiation and (v) Resistance to radiation by the effective repair of radiation-induced DNA damage, thereby allowing the cells to function normally.

Generally, *in vitro* differential radiosensitivities of tumour cell lines have been based upon assays which assess cell survival and/or clonogenic capability following exposure to ionising radiation (Arlett, 1980; Elkind, 1985; Siemann,

1989; McNally, 1990). Cell kill is largely attributed to the occurrence of DNA lesions that irreversibly inhibit the ability of cells to proliferate ("lethal damage") and to lesions that are unstable and whose ultimate fate is determined by DNA repair fidelity ("potentially lethal damage") (Bertrand, 1980). Iliakis (1988), proposed that potentially lethal damage comprises of: single, pairs or groups of DNA double strand breaks and that fixation of this damage is transmitted to the double helix through alterations in chromatin conformation. In the present study, the differential radiosensitivity of MOLT-4, DAUDI and V79 cell lines were examined using the NLS and MGE techniques concomitantly with cell survival assays to investigate the relationship between DNA damage and repair and cell survival after exposure to ionising radiation.

Radiation responses of the highly sensitive MOLT-4 (Szekely & Lobreau, 1985), moderately sensitive DAUDI (Hanson, J.A., personal communication) and more resistant V79 (Okayasu & Iliakis, 1992), were reproduced in the population growth studies shown in Figure 3.31. as:

(i) Reduced cell numbers were observed after 1 Gy in MOLT-4, after 2 Gy in DAUDI and after 5 Gy in V79.

(ii) Population recovery was observed on Day 4 after 0.55 Gy in MOLT-4, 1 Gy in DAUDI and after 3 Gy in V79.

ii) the comparative dose responses observed during exponential growth in Figure 3.32. showed that over 0-10 Gy (in terms of a reduction of total cell number), MOLT-4 was the most radiosensitive, DAUDI was not as radiosensitive as MOLT-4 and V79 was the least radiosensitive.

iii) D_{37} values of 0.79, 2.19 and 4.66 Gy (as derived from Figure 3.32.) for MOLT-4, DAUDI and V79 cell lines, respectively.

Peacock *et al*. (1989) compared the extent of DNA damage using a Neutral Elution technique with colony forming ability of tumour cell lines after exposure to 0-16 Gy gamma irradiation. They proposed that initial DNA double strand break induction is correlated to cell survival. Kelland *et al*. (1988) studied the induction and rejoining of dsb in human cervix carcinoma cell lines following irradiation doses of 10 and 40 Gy using neutral filter elution. They found the more radiosensitive cell lines incurred more breaks and commented that the induction and rejoining of dsb appears to be a factor in determining radiosensitivity. Further, Olive *et al*. (1991a) used a gel electrophoresis technique to study rejoining of dsb in a repair-deficient mutant murine cell line. They found that the fraction of dsb remaining in the radiosensitive cells was invariably higher than in the less radiosensitive cells. If initial DNA damage induction is related to radiation sensitivity, the results obtained in the present study from the shift in sedimentation distance of HF-DNA extracted from MOLT-4, DAUDI and V79 (Figure 3.34.) support this view in that:

(i) MOLT-4 cells exhibited abnormally small sedimentation distances over 0-10 Gy. This may indicate the presence of a large number of dsb reducing the extent of DNA supercoiling.

ii) DAUDI cells generally exhibited a greater shift in sedimentation distance after each radiation dose than did the V79 cells. Also, over 2-10 Gy, the shift in DAUDI was consistently over 2mm greater than the shift in V79.

(iii) V79 cells only showed a 2mm increase in shift between 1 and 10 Gy whereas over the same range DAUDI showed a 7mm increase in shift.

The radiation response of MOLT-4, DAUDI and V79 cell lines was also examined using MGE. Figure 3.34 showed that the relative shift in comet tail migration over a range of 0.5-10 Gy for the three cell lines did not correspond to their relative radiosensitivities. Over 0.5-10 Gy, the smallest shift in comet tail migration was observed was in DAUDI cells whilst MOLT-4 and V79 exhibited similar shifts over 0.5-5 Gy.

However, the radiosensitivity of tumour cell lines is not only based upon the extent of DNA damage induction, but also upon repair fidelity (Olive et al., 1991a). Yet in NLS and MGE for each of the MOLT-4, DAUDI and V79 cell lines, a repair proficiency greater than 1.0 was observed after each radiation dose over a 0.5-10 Gy range following a post-irradiation incubation for 1 hour at 37°C. Muller et al. (1994) however, have used MGE to compare the amount of radiation-induced DNA damage and repair in a human melanoma and two human squmous cell carcinoma cell lines of differing radiosensitivity. Using the ratio of comet head to comet tail fluorescence as a measure of DNA damage, they found a similar extent of DNA damage in the three cell lines but markedly different repair chacteristics in two of them. The repair characteristics correlated wellto the radiosensitivity ranking of the cells from a clonogenic assay.

Even though, in the present study, the cell survival assays and NLS (in terms of initial DNA damage induction) agreed in their radiosensitivity ranking of MOLT-4, DAUDI and V79. These results should be interpreted with caution as: (i) difficulty was experienced in obtaining reproducible sedimentation distances of HF-DNA extracted from the three cell lines. This may have been so because the conditions employed in the NLS assay are suitable for the study of human peripheral lymphocytes but not mammalian tumour cell lines during exponential

131

growth, (ii) the lysis, centrifugation and electrophoresis conditions of the techniques need to be examined in order to maximise the efficiency of DNA damage detection in different cell types and (iii) the basis of differential radiosensitivity in tumour cell lines remains unclear. Therefore, differences due to changes in DNA content, its conformation or association with nuclear protein during the cell cycle may contribute to the intrinsic radiosensitivity of tumour cells but may also influence the reproducibility of the techniques.

It is proposed that the predictive value of NLS and MGE towards cell survival could be assessed by comparing cell survival assays with other *in vitro* assays detecting: (i) alterations in cell metabolism, (for example, dye exclusion techniques (Hanson, *et al*. 1989), (ii) alterations in DNA conformation (Olive, 1992a) and (iii) assays estimating the clonogenic potential of cell population. From these studies which combine the radiation effects upon cell growth characteristics (that is, the extent of radiation-induced immediate cell death, reproductive death and mitotic delay) with the direct assessment of DNA damage and repair activity, information could be gained concerning the basis of differential radiosensitivity of tumour cell lines.

DNA Damage and Repair in Donor and Patient Groups

Deeley & Moore (1989) used the NLS technique to compare the DNA repair proficiency of patients with post-radiotherapy complications (after treatment for cancer of the cervix) to the repair proficiency of healthy donors, pre-radiotherapy patients and 'well' post-radiotherapy patients. They found that: (i) 7 out of 16 of the patients with complications attributed to radiotherapy had a repair proficiency less than 0.44 (ii) 2 out of 29 of the healthy donors had a repair proficiency less than 0.40 (iii) 2 out of 25 of the pre-radiotherapy patients had a repair proficiency less than 0.40 and, (iv) all of the 'well' patients (11 out of 11) exhibited a repair proficiency greater than 0.88.

As the concurrent use of NLS and MGE assays could reveal additional information of DNA damage and repair status, a study aimed at investigating DNA repair proficiency with the lack of/or occurrence of post-radiotherapy complications in patients with cancer of the cervix was considered. The planned study group comprised of apparently healthy donors, new patients (pre-radiotherapy), 'well' patients (post-radiotherapy) and patients with post-ratiotherapy bowel and/or bladder complications. However, as can be seen in Table 2.1., the actual study group comprised of apparently healthy donors and new patients attending their first clinic appointment. Table 3.8. showed that no differences were found between donor and patient groups when HF-DNA sedimentation distance, comet tail migration and comet head fluorescence was used to assess basal DNA damage, the extent of radiation-induced DNA damage and repair proficiency. Interestingly, both NLS and MGE did detect a proportion of donors and patients who expressed a DNA repair proficiency less than 0.39 (as shown in Figure 3.36.). A repair proficiency less than 0.39 was found in 3 out of 59 of the donors and 6 out of 38 of the new patients in NLS, in 10 out of 51 of the donors and in 5 out of 27 of the patients from comet length measurements and in 6 out of 15 of the donors and 4 out of 15 of the patients from fluorescence readings. Generally, more of the patients than the healthy donors expressed a DNA repair proficiency less than 0.39 in NLS but not in MGE. However, no comparisons of DNA damage or repair proficiency were performed on 'well' patients who had received radiotherapy or on patients with post-radiotherapy complications. Thus, in the present study the relationship between poor repair proficiency (in NLS as compared to MGE) and the occurrence of post-radiotherapy complications was unknown.

133

4.3. Comparative Nature of NLS and MGE

From the studies previously described, NLS and MGE have been used to gain information regarding cellular DNA responses to ionising radiation. However, the techniques have been shown to differ in their sensitivity of DNA damage detection (Figure 3.20.) and in the assessment of changes that occur to the DNA superstructure during a post-irradiation incubation period (Figure 3.22.). Further, poor linear correlations were found to exist when the basal level of DNA damage, '2 Gy shift' and repair proficiency determined by HF-DNA sedimentation behaviour were compared to the basal level of DNA damage, '2 Gy shift' and repair proficiency determined by comet tail migration and comet head fluorescence, (Figures 3.27, 3.28, 3.29, respectively). Possible explanations for such poor correlations are as follows:

(i) In NLS, the sedimentation behaviour of HF-DNA is dependent both upon the degree of supercoiling and on the mass of the total particle (consisting of DNA supercoiled loops plus the residual nuclear matrix (Roti Roti, 1987)). Likewise, the extent of DNA migration in MGE is subject to DNA supercoiling plus the presence of associated protein. However, whilst the HF-DNA complex moves as a single mass through the sucrose gradients, the electrophoretic migration of DNA is complicated by tangling within the agarose matrix.

(ii) Olive *et al.* (1992a) have shown that alterations in lysis conditions (that is, different NaCl concentration, pH and detergent) prior to electrophoresis affects the ability of DNA to migrate. Figure 3.17. also demonstrated that lysis time and exposure to alkali influenced the sensitivity of MGE. As different lysis buffers and non-ionic detergents were used to extract HF-DNA in NLS and MGE, then the extent of DNA supercoiling and the amount of associated protein present in the HF-DNA complexes may differ between the techniques.

(iii) The techniques may differ in sensitivity as a neutral lysis buffer (pH 8.0) was used in NLS and an alkali lysis buffer (pH 10.0) and electrophoresis

buffer (pH > 13) were used in MGE. Thus, ssb and alkali-labile sites are probably more readily detected in MGE (Green *et al.*, 1992), than NLS, where due to neutral conditions, ssb are probably less readily detected.

(iv) Technical errors may be present in both techniques in that: (a) a higher level of basal DNA damage may exist in NLS than MGE. Even though naked DNA is gently harvested and layered onto the top of sucrose gradients, the centrifugation and pipetting steps of the technique may cause slight shearing to the DNA. (b) In MGE, errors may be introduced by the manual measurement of comet tail length. Difficulty was experienced in accurately estimating the extent of DNA damage in the sparse fragmentation of comet heads at low doses and discerning the end of highly fragmented comet tails at high doses.

(v) Discrepancies in results obtained may be based in the nature of the techniques themselves. Nucleoid sedimentation, is designed to directly detect DNA damage as a mean radiation response in a large population of cells. However, MGE is designed to directly detect DNA damage in the single cells of a cell population. In the present study, only about 50 comet tail lengths were measured or about 50 comet head fluorescence readings were taken. Thus, such small samples, which included wide heterogeneity in comet type and comet length, may not have been representative of the cell population considered in NLS. Further, the average radiation response in NLS may not detect extremes of radiation resistance or radiation sensitivity within cell subpopulations as detected by MGE.

4.4. Limitations of the Study

The principal limitations of this study are:

i) The use of comet tail length alone as an indicator of the extent of DNA damage expression in individual comets.

ii) The choice of patients with cancer of the cervix to comprise the patient study group.

135

Comet Tail Length

The manual measurement of comet tail length from photographic negatives is inexpensive, simple to perform and fairly acceptable in a rapid assay detecting either the increasing DNA damage with increasing radiation dose or the occurrence or absence of repair after a 2 Gy irradiation. Singh *et al.* (1989) and Green *et al.* (1992) have reported good correlations between an increase in comet length and increasing exposure to DNA damaging agents. Figure 3.12. showed that there was an increase in the shift in comet tail migration (measured manually in millimetres as comet length) after human lymphocytes were exposed to 0.5-10 Gy of gamma radiation. Further, significant linear relationships were found between the dose response produced from comet length measurements to those produced from a decrease in sedimentation distance and comet head fluorescence with increasing doses of radiation (Figure 3.19.). Thus, differences in the extent of DNA damage can be detected by measuring the associated increase in comet length. Further, the dose response to gamma irradiation produced from comet length measurements was comparable to those produced from decreases in sedimentation distance and comet head fluorescence.

However, when comet length and comet head fluorescence were compared in unirradiated, irradiated (2 Gy) and irradiated and incubated lymphocytes, no linear relationships were observed (Figures 3.27, 3.28. and 3.29., respectively). This suggests that comet tail migration and comet head fluorescence detect basal DNA damage, radiation-induced DNA damage and DNA repair proficiency to differing extents within the same lymphocyte sample. Also, Figure 3.20. showed that for doses greater than 3 Gy, more DNA damage was detected per Gy by the shift in comet length than the shift in comet head fluorescence. Even though the shift in comet tail length and the shift in comet head fluorescence were not directly comparable, it is suggested that at low doses of radiation, large

differences in comet head fluorescence were detected but only small differences in comet tail migration were detected. These results seem confusing in that one would expect to observe a concurrent decrease in comet head fluorescence with increasing DNA migration from the comet nucleus.

The apparent lack of correlation between comet tail length and comet head fluorescence can be explained in terms of the nature of comet formation during electrophoresis. The DNA of cells lysed in high salt concentrations and non-ionic detergents resembles intact nuclear DNA in that it maintains a compact supercoiled structure which is attached to the nuclear membrane. Thus the comet heads of unirradiated cells can be considered to consist of supercoiled loops of DNA attached to a nuclear matrix. Gedik *et al.* (1992) commented that strand breaks cause a release of supercoiling in the structural loops of DNA which enables strands of DNA to be pulled out from the comet head under an electrophoretic field. An increase in the frequency of strand breaks may not be represented by an increase in comet tail length but by an increase in the number of relaxed supercoiled loops that are displaced from the comet head. Consequently, comets of identical tail length may contain differing amounts of DNA within the comet tail. This model of comet formation suggests that comet tail length limits the estimation of the extent of DNA damage in that: (i) comet length measurements would not have detected any lateral diffusion of DNA strands (perpendicular to the electric field) from the comet heads, (ii) comet length is not a measure of the total amount of DNA which has migrated but is a measure of the distance migrated by the smallest detectable molecular weight fragment (Tice *et al.*, 1992) and (iii) in the present study, difficulty was experienced in determining (a) the amount of DNA damage in terms of comet length when sparse fragments were emitted from a bright compact comet head at low doses and (b) the end of a comet tail at high doses.

Olive *et al.* (1990) recognised that comet length may not be the most appropriate way of determining absolute measurements of DNA damage. They

correlated the frequency of DNA strand breaks to the size of the comet tail and the distribution of fluorescence within it. Also, using video image analysis, they defined appropriate "features" of the comet including: (i) its area, (ii) the DNA content, (iii) percentage DNA in the head and tail distributions, (iv) mean position of head distribution, (v) mean position of the tail distribution, (vi) head diameter, and (vii) tail length. These authors have described the "tail moment", which was computed by multiplying tail length by tail intensity, as "the most informative feature of the comet image". Deeley & Moore, (1992) examined the process of comet formation and are currently developing methods to quantify DNA damage and repair in individual comets using image analysis (OPTILAB). Figure 4.1. showed (a) a laser print image of a video signal of a typical comet formed after a 2 Gy irradiation, (b) a "3 D" profile of fluorescence intensity showing the spatial distribution of DNA in the comet tail, and (c) variation in fluorescence intensity along the longitudinal axis of the comet.

It is proposed that limitations may have been introduced into the comparative study of NLS and MGE by the manual measurement of comet tail length. For future studies involving MGE, it is suggested that comets are captured and analysed randomly using a video image analysis technique such as OPTILAB and that the available informative "features" of the comets are used to quantify DNA damage in single cells.

Patient Group

The basic aim of this study was to investigate the potential of NLS and MGE as quick, reliable cellular radiosensitivity assays to identify particularly radiosensitive individuals and so prevent unnecessary post-radiotherapy complications in clinical practice. Even though patients with cancer of the cervix comprised a suitable study group (Section 1.7.), the choice of these patients posed a number of limitations upon the study:
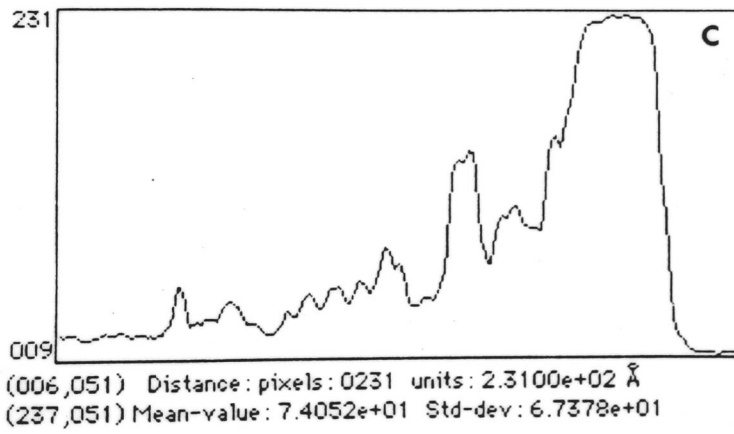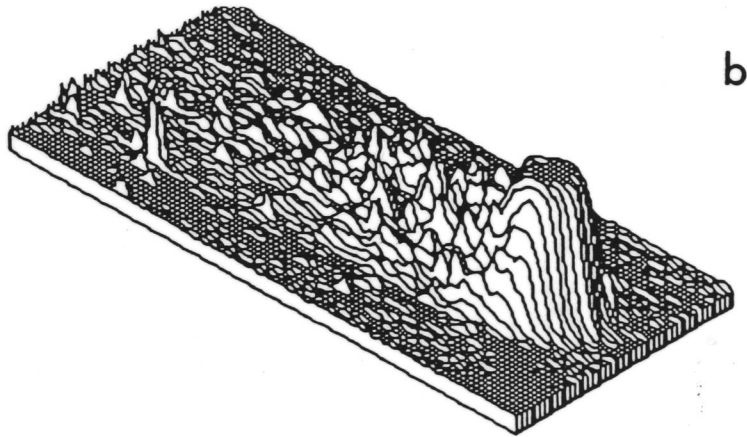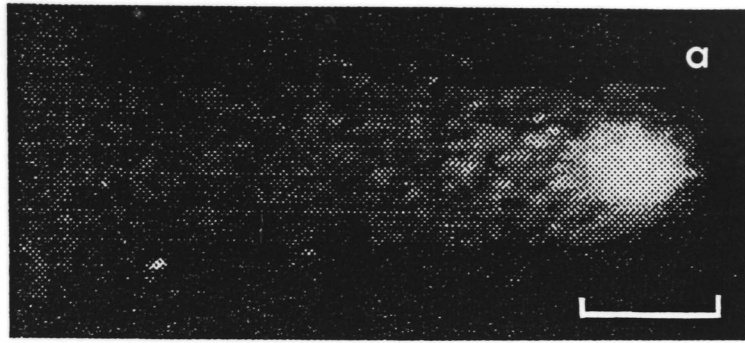
Figure 4.1. Image analysis of a typical comet formed by a 2 Gy irradiated cell after lysis and electrophoresis.

(i) Only a small number of patients presented post-radiotherapy complications during the course of this study from which it was not possible to obtain blood samples.

(ii) Patients in the "complications" group probably comprised of either (a) individuals who were unusually sensitive to radiation or (b) individuals whose bowel and /or bladder was in a close proximity to the treatment field. Consequently normal tissue would have received a similar dose to that of the intended field.

(iii) Inaccuracies of applicator insertion in intra-cavity treatment and differing abdominal anatomy may result in the organs of some patients receiving significantly higher radiation doses than the organs of other patients (Davies, 1985).

(iv) The practice of using combinations of external fractionated irradiation and intra-cavity continuous irradiation may be responsible for the difficulty in establishing a correlation between treatment dose and the incidence of complications (Visser *et al.*, 1985).

It is proposed that patients with cancer of the head and neck could be considered as a more appropriate patient group when comparing DNA repair proficiencies and the occurrence of post-radiotherapy complications:

(i) Early sensitivity in skin expressed as erthyma and late sensitivity expressed as telangiectasia are easily observable and ranked according to degree of severity.

(ii) Well-defined treatment regime and standardised dose with less variation in radiation field as the patient is completely immobilised during treatment;

(iii) Most radiobiological studies *in vivo* have been performed on early effects of radiation in skin and mucosa (Coggle, 1983) and numerous radiobiological studies in vitro have been performed on mammalian fibroblasts (Burnet *et al.*, 1992).

(iv) There are no apparent morphological manifestations of latent damage to late responding tissues after treatment for head and neck cancer so late damage can be difficult to assess clinically. Therefore, the use of simple DNA damage assys to measure tissue radiosensitivity would be appropriate in detecting unusual sensitivity to radiation within this patient group.

Further, patients with breast cancer could be also considered as another suitable choice of patient group with which to study variations in normal tissue radiosensitivity as there are well-defined early and late complications associated with type of treatment. Also, the group comprises long term survivors for whom it has been possible to cure primary cancer with radiotherapy.

4.5. Suitability of NLS and MGE for Clinical Development

The NLS and MGE techniques share a number of common advantages over other *in vitro* assays of radiosensitivity:

a) Direct measurements of DNA damage can be produced rapidly - within a few hours of receiving a sample.

b) The assays are easy to perform involving few critical steps.

c) Both NLS and MGE estimate the basal level of DNA damage in untreated cells.

d) Not dependent on a proliferating cell population with most eukayotic cell populations amenable to analysis.

e) Both assays are relatively inexpensive apart from the initial expenditure of an ultracentrifuge for NLS and an image analysis system for MGE.

NLS: Advantages and Disadvantages

The two main advantages of NLS are:

a) Sensitivity and range of detection - DNA damage can be detected at doses as low as 0.5 Gy and up to 20 Gy.

b) Assesses higher-order DNA conformation as well as DNA damage (van Rensburg, 1985).

The major disadvantages of NLS are:

a) Uncertain nature of the lesion detected.

b) Only provides information of the average population response.

c) Large cell population required for each test.

d) Only 4 or 5 blood samples can be analysed each day.

MGE: Advantages and Disadvantages

The major advantages of MGE include:

a) Relatively non-traumatic to cells.

b) Sensitivity and broad range of DNA damage detection from 0.5 to 20 Gy.

c) Large numbers of samples can be processed on the same day.

d) Only a small number of cells are required for each test making MGE useful for needle and/or aspirate tumour biopsies.

e) The method allows visualisation and assessment of DNA damage in individual cells:

i) Detection of heterogeneity in amount and type of DNA damage produced within a cell population.

ii) Identification of highly radioresistant or unusually radiosensitive subpopulations.

iii) Useful for studying the effect of cell cycle on radiosensitivity

iv) Potential incorporation of recombinant DNA technology into the technique.

The major disadvantages of MGE are:

a) The necessity for single cell suspensions

b) The assumption that the visible comets analysed represent the population response to radiation.

c) Gaining a representative sample size when measuring comet length or head intensity manually.

d) Discerning the most appropriate parameters to use in order to accurately quantify the extent of DNA damage in each comet.

The Clinical Potential of MGE

The advantages of NLS and MGE illustrate their potential for quick, simple routine radiosensitivity testing in a clinical situation. The potential of NLS is based on its ability to assess the basal level of DNA supercoiling (van Rensburg *et al*, 1985) and radiation-induced conformational changes in DNA superstructure (van Rensburg *et al.*, 1987), providing a vital link in the relationship of chromatin structure to radiosensitivity (Olive, 1992a). However, MGE, may have a broader clinical potential than NLS since it can provide information about the distribution of DNA damage and repair within a population of individual cells. Even though the studies presented in this thesis did not link clinical outcome with DNA repair ability using MGE, the following studies highlight the clinical potential of the technique as a radiosensitivity assay:

Östling, *et al.* (1986) analysed the induction and rejoining of radiation-induced DNA strand breaks in tumour biopsies obtained by fine needle aspiration before and after irradiation *in vivo*. An increase in DNA strand breaks were present in the tumour cells after irradiation with most cells repairing the DNA damage within 1 to 2 minutes. The authors commented that the MGE method could be used to investigate the relationship between the induction of DNA damage and DNA repair capacity in extracted tumour cells and the *in vivo* tumour response to radiation during treatment. Further, Olive *et al.* (1990) have studied heterogeneity in radiation-induced DNA damage and repair in tumour and normal cells within murine tumours. Once the tumour cells and infiltrating macrophage were separated (using differential antibody binding), the MGE technique provided a simple means of estimating relative heterogeneity in radiation response of both malignant and normal cells. This could be important not only in the identification of radioresistant and radiosensitive subpopulations of tumour cells but also in the correlation of radiation-induced DNA damage and repair capacity of tumour-infiltrating macrophages. Olive *et al.* (1992b) have also measured growth fraction of human colon carcinoma cells using MGE. They suggested that the specificity of this assay in detecting proliferating cells could be used to estimate the kinetics of tumour growth. Clearly, MGE has considerable clinical potential in the study of human tumour response during radiotherapy and in predicting the response of tumours prior to radiotherapy.

Singh *et al.* (1991b) studied DNA damage and repair in individual fibroblasts that were cultured on the same microscope slides that were used for comet analysis. They demonstrated that two main techniques (trypsinisation and scraping) used to collect normal mammalian cells cultured in monolayer induced additional DNA damage to that iinduced by radiation. The work showed the utility of MGE in the *in situ* evaluation of radiation-induced DNA damage and repair without the occurrence of additional DNA damage caused during cell collection. As MGE is not dependent on degradative procedures to quantify DNA

damage and repair in normal tissue, the ability of the assay to predict normal tissue response to radiation prior to and during a course of radiotherapy could be assessed.

These initial studies have shown that MGE can detect a heterogeneity of radiation response in normal and tumour cell populations. The technique could therefore provide valuable information regarding the basis of human tumour cell resistance and the nature of normal tissue response during and after radiotherapy.

Whilst the clinical potential of MGE as a radiosensitivity assay is clearly apparent, the future clinical applications of this technique are not confined to the radiosensitivity testing of normal and tumour tissue. Östling & Johanson (1987) studied the action of the anit-cancer agent, bleomycin in producing a variation of strand breaks in murine tumour cells and suggested the potential of MGE to detect the distribution and level of DNA damaging actions of chemo-therapeutic agents. Further, Tice *et al.* (1992) used MGE to study high-dose combination alkylating agents and DNA damage in peripheral blood lymphocytes of breast cancer patients. They proposed that MGE could be used to evaluate the levels of DNA damage during a course of chemotherapy and that the dose schedule could be altered to achieve a desired effect level.

Green *et al.* (1992) used MGE to study the relationship between sensitivity to UV irradiation expressed by individuals with the autosomal recessive disorder xeroderma pigmentosum (XP) and the extent of DNA damage in their isolated lymphocytes. They found that the mean comet length of human lymphocytes derived from XP donors was significantly less than those from healthy donors after exposure to 0-10 Jm^{-2} of UV-C radiation. It was proposed that comet tail migration in XP lymphocytes was lower because the level of excision is reduced (Cleaver, 1968) along with the level of excision-associated strand breakage. It was suggested that the method may offer a rapid diagnostic assay for XP. Further, MGE could used to investigate DNA damage and repair in the cells of individuals

with other syndromes displaying radiosensitivity including Cockayne's syndrome and trichothiodystrophy.

Tice *et al.* (1990) suggested that the assay could be used in future studies to i) examine the basic mechanisms of DNA damage and repair, ii) evaluate organ-specific levels of DNA damage in animals exposed to potential carcinogens, and iii) detect DNA damage induction and repair capacity in reproductive and teratological studies. Singh *et al.* (1991a) found a 5-fold increase in a subpopulation of highly damaged lymphocytes in ageing male donors (over 60 years) as compared to younger counterparts. They suggested that this assay could contribute to studies involving age-related changes in immune function and carcinogenesis.

Thus, it is clear that MGE has potential as a simple and rapid screening test to identify sensitivity in any population of mammalian cells to radiation, chemotherapeutic drugs and a variety of industrial, cosmetic and environmental agents.

4.6. Suggestions for Future Development in Radiosensitivity Testing

Cook & Brazell (1976) first drew attention to the clinical potential of nucleoid sedimentation as a screening technique to identify radiosensitive individuals. In the present study, the NLS technique has been shown to be comparable to the MGE technique in detecting individuals with a poor DNA repair proficiency (as shown in Figure 3.29.). However, the similar sensitivity yet novel ability of MGE to detect DNA damage and repair in single cells has caused the focus of cellular radiosensitivity testing to move from observing the effect of irradiation as an average population response to observing the heterogeneity of response in individual cells. In the last few years, MGE and to a lesser extent NLS, have been used extensively to to explore the potential of DNA damage assays as predictive and/or diagnostic techniques in identifying abnormally radiosensitive

normal and tumour tissue and to elucidate the mechanisms of radiosensitivity. However, the implementation of these techniques or other direct DNA damage assays as routine clinical tests is still far from a reality.

It is proposed that Microgel Electrophoresis is used in a comparative study to: (i) investigate the molecular processes involved in radiosensitivity, (ii) predict *in vivo* tumour response to radiation and, (iii) validate the reliability of MGE as a clinical radiosensitivity test.

Understanding the Molecular Processes of Radiosensitivity

Part of the work presented in this thesis attempted to link the differential sensitivities of MOLT-4, DAUDI and V79 cell lines with the extent of clonogenic cell survival and the corresponding level of DNA damage and repair capacity detected by NLS and MGE over a range of 0.5-10 Gy (Section 3.3.). It is claimed that results obtained from MGE are comparable with conventional gel electrophoresis and elution techniques (Singh *et al.*, 1989), DNA precipitation, alkali unwinding and cell clonogenicity assays (Olive *et al.*, 1990). Therefore, it is suggested that the MOLT-4, DAUDI and V79 cell lines or other well-characterised cell lines of differing radiosensitivity or repair-deficient mutant cell lines (for example. *xrs* series of CHO-K1 cells (Jeggo, 1990)) are studied. A range of assays to detect: (i) biochemical changes associated with DNA repair, (ii) DNA repair enzyme activity, (iii) DNA strand breaks, (iv) DNA higher-order damage, (v) chromosome aberrations, and (vi) cell survival after gamma irradiation may provide information on the nature of radiation sensitivity and possibly describe the relationship between DNA repair processing, repair enzyme activity, strand-break rejoin capacity, the role of chromatin organisation and the occurrence of chromosome aberrations to cell survival. Further, if the extent of DNA damage and repair detection in MGE correlated to differential radiosensitivity, then the potential of MGE alone to predict *in vivo* tumour response could be examined.

Prediction of In Vivo Tumour Response using MGE

Providing MGE was validated in its representation of radiosensitive cell populations, it is feasible that the technique could be used to predict the response of tumours in a sample of patients with superficial head and neck cancers. Pre-radiotherapy tumour cell samples could be obtained by fine needle biopsy and the DNA damage and repair proficiency profiles compared to the extent of tumour sterilisation after the termination of treatment. Further, fine needle biopsy samples could be obtained at intervals for the duration of treatment to compare DNA damage and repair with the *in vivo* tumour response to radiation. Thus, the usefulness of MGE to predict *in vivo* tumour response during and after treatment should be clarified.

Reliability of MGE as a Clinical Radiosensitivity Test

It is proposed that the role of MGE in predicting the radiosensitivity of normal tissue in the vicinity of the radiation field should also be explored. If possible, fibroblasts could be obtained by fine needle biopsy from the same head and neck patients from which fine needle tumour biopsies are taken. The relationship of DNA damage and repair profiles of the fibroblast populations could be examined in patients with and without early normal tissue damage during radiotherapy and late normal tissue damage after radiotherapy. The reliability of MGE as a test of radiosensitivity could then be assessed as an indicator for adjusting radiotherapy regimes.

In summary, the studies outlined above, would provide information regarding:

i) The mechanism and nature of radiosensitivity.

ii) The reliability of MGE as a test of cellular radiosensitivity.

iii) The readiness of MGE to be implemented as a routine predictive test of radiosensitivity

4.7. Conclusion

The work presented in this thesis has:

(i) Validated the appropriateness of Nuclear Lysate Sedimentation and Microgel Electrophoresis to clinical radiosensitivity testing.

(ii) Investigated the nature of DNA damage and repair from direct DNA damage detection in a population of cells and in single cells.

(iii) Highlighted the clinical potential of Microgel Electrophoresis to radiosensitivity testing.

It is held that the implementation of Microgel Electrophoresis as a routine predictive test of cellular radiosensitivity may have considerable impact upon the planning and tailoring of radiotherapy, thereby maximising treatment success for the individual.

REFERENCES

Agarwal, S.S., Katz, E.J., Krishan, A. and Loeb, L.A., (1981). DNA replication in X-irradiated human lymphocytes. *Cancer Research*, 41, 3973-3978.

Allen, I.M., Vaughan, A.T.M., Milner, A.E., Lunec, J. and Bacon, P.A., (1988). Structural damage to lymphocyte nuclei by H_2O_2 or gamma irradiation is dependent on the mechanism of OH radical production. *British Journal of Cancer*, 58, 34-37.

Ahnström, G., (1988). Techniques to measure DNA single-strand breaks in cells: A review. *International Journal of Radiation Biology*, 54, 695-697.

Ahnström, G., Edvardsson, K.A., (1974). Radiation-induced single-strand breaks in DNA determined by rate of alkaline strand separation and hydroxyapatite chromatography: an alternative to velocity sedimentation. *International Journal of Radiation Biology*, 26, 493-497.

Arlett, C.F., Harcourt, S.A. (1980). Survey of Radiosensitivity in a variety of human cell strains. *Cancer Research*, 40, 926-932.

Bernstein, C. and Bernstein, H., (1991). Aging, Sex and DNA Repair. Academic Press Ltd, London.

Bertrand, M., (1980). Factors influencing the recovery from potentially lethal damage (PLD) in mammalian cells *in vitro* and *in vivo*. *Cancer Treatment Reviews*, 7, 1-15.

Blackburn, G.M. and Gait, M.J., (1990). Nucleic Acids in Chemistry and Biology. Oxford University Press, New York.

Bohr, V.A., Phillips, D.H. and Hanawalt, P.C., (1987). Heterogeneous DNA damage and repair in the mammalian genome. *Cancer Research*, 47, 6426-6436.

Blocher, D. (1982). DNA double strand breaks in Ehrlich ascites tumour cells at low doses of X-rays: Determination of induced breaks by centrifugation at reduced speed. *International Journal of Radiation Biology*, 42, 317-328.

Burnet, N.G., Nyman, J., Turesson, I., Wurm, R., Yarnold, J.R. and Peacock, J.H., (1992). Prediction of normal-tissue tolerance to radiotherapy from in vitro cellular radiation sensitivity testing. *Lancet*, **339**, 8809, 1570-1.

Center, M.S., Richardson, C.C., (1970). An endonuclease induced after infection of Escherichia Coli with bacteriophage T7. 1. Purification and properties of the enzyme. *Journal of Biological Chemistry*, **245**, 6285-6291.

Cleaver, J.E., (1968). Defective repair replication of DNA in xeroderma pigmentosum. *Nature*, **218**, 652-656.

Coggle, J.E., (1983). Biological Effects of Radiation. Second Edition, Taylor and Francis Ltd. London.

Cohen A. and Thompson, E. (1986). DNA Repair in nondividing human lymphocytes: Inhibition by deoxyadenosine. *Cancer Research* **46**, 1585-1588.

Cook, P.R. and Brazell, I.A., (1976). Detection and repair of single-strand breaks in nuclear DNA. *Nature*, **263**, 679 -682.

Crump, P.W., Fielden, M,E., Jenner, T.J. and O'Neill, P., (1990). A comparison of the techniques of alkaline filter elution and alkaline sucrose sedimentation used to assess DNA damage induced by 2-Nitroimidazoles. *Biochemical Pharmacology*, **40**, 621-627.

Davies, S.E., (1985). Morbidity following low-dose rate selectron therapy for cervical cancer. *Clinical Radiology*, **36**, 131-139.

Deeley, J. O. T. and Moore, J. L., (1989). Nuclear lysate sedimentation measurements of peripheral blood lymphocytes from radiotherapy patients. *International Journal of Radiation Biology*, **56**, 963-973.

Deeley, J. O. T., Moore, J. L. and Mitchell, S.J., (1990). Microgel electrophoresis and nuclear lysate sedimentation measurements of DNA repair. *International Journal of Radiation Biology*, **57**, 1268-1269.

151

Deeley, J.O.T. and Moore, J.L., (1992). Single-cell microgel electrophoresis: an in vitro assay of radiosensitivity. *British Journal of Radiology*, 24, 65-69.

Dizdaroglu, M., (1992). Measurement of radiation-induced damage to DNA at the molecular level. *International Journal of Radiation Biology*, 61, 175-183.

Duckworth-Rysiecki, G. and Taylor, A.M.R., (1985). Effects of ionising radiation on cells from Fanconi's anaemia patients. *Cancer Research*, 45, 416-420.

Elkind, M. M., (1985). DNA damage and cell killing - cause and effect? *Cancer*, 56: 235 -2363.

Erixon, K., Cedervall, B. and Lewensohn, R., (1990). Pulsed-field gel electrophoresis for measuring radiation-induced double-strand breaks. Comparison to the method of neutral filter elution. *Ionizing Radiation Damage to DNA*: Molecular Aspects (Wiley-Liss, Inc.), 69-80.

Fender, M., and Malz, W., (1980). A simple test for repair kinetic studies of mammalian DNA applied to normal and CLL lymphocytes. *Studia Biophysica*, 78, 79-85.

Frankenberg, D., Frankenberg-Schwager, M. and Harbich, R., (1984). Split-dose recovery is due to the repair of DNA double strand breaks. *International Journal of Radiation Biology*, 46, 541-553.

Frenster, J.H., (1972). Ultrastructural probe of chromatin within living human lymphocytes. *Nature, New Biology*, 236, 175-176.

Fulop, G.M. and Phillips, R.A., (1990). The scid mutation in mice causes a general defect in DNA repair. *Nature* 347, 479-482.

Gedik, C.M., Ewen, S.W.B., and Collins, A.R., (1992). Single-cell gel electrophoresis applied to the analysis of UV-C damage and its repair in human cells. *International Journal of Radiation Biology*, 62, 313-320.

George, A.M., Sabovijev, S.A., Hart, L.E., Cramp, W.A., Harris, G. and Hornsey, S., (1987). DNA quaternary structure in the radiation sensitivity of human lymphocytes-a proposed role of copper. *British Journal of Cancer*, 55,1 41-144.

Green, M.H.L, Lowe, J.E., Harcourt, S.A., Akinluyi, P., Rowe, T., Cole, J., Anstey, A.V. and Arlett, C.F. (1992). UV-C sensitivity of unstimulated and stimulated human lymphocytes from normal and xeroderma pigmentosum donors in the comet assay: A potential diagnostic technique. *Mutation Research, DNA Repair*, 273, 137-144.

Harris, G., Cramp, W.A., Edwards, J.C., George, A.M., Sabovljev, S.A., Hart, L., Hughes, G.R.V., Denman, A.M. and Yatvin, M.B. (1985). Radiosensitivity of peripheral blood lymphocytes in autoimmune disease. *International Journal of Radiation Biology.*, 47, 689-699.

Harris, G., Holmes, A., Sabovljev, S.A., Cramp, W.A., Hedges, M., Hornsey, S., Hornsey, J.M. and Bennett, G.C.J., (1986). Sensitivity to X-irradiation of peripheral blood lymphocytes from ageing donors. *International Journal of Radiation Biology*, 50. 685-694.

Hanson, J.A., Bean, E.A., Nute, S.R. and Moore, J.L., (1989). A novel dye exclusion assay for measurement of cell response following *in vitro* exposure to radiation or drugs. *Leukaemia Research*, 13, 943-947.

Hamberger, A.D., Unal, A., Gershenson,D.M., Fletcher, G.H., (1983). Analysis of the severe complications of irradiation of carcinoma of the cervix: Whole pelvis irradiation and intracavity radium. *International Journal of Radiation Oncology Biology Physics.*, 9, 367-371.

Howard-Flanders, P., (1981). Inducible Repair of DNA, *Cancer Biology: Readings from Scientific American.*, 4, 33-41. W.H. Freeman and Company, New York.

Iliakis, G., (1988). Radiation-induced potentially lethal damage: DNA lesions susceptible to fixation. *International Journal of Radiation Biology*, 53, 541-584.

liakis, G., Blocher, D., Metzger, L. and Pantelias, G. (1991). Comparison of DNA double-strand break rejoining as measured by pulsed field gel electrophoresis, neutral sucrose gradient centrifugation and non-unwinding filter elution in irradiated plateau-phase CHO cells. *International Journal of Radiation Biology*, 59, 927-939.

Jeggo, P.A., (1990). Studies on mammalian mutants defective in rejoining double-strand breaks in DNA. *Mutation Research*, 239, 1-16.

Joslin, C.A.F., Smith, C.W. and Mallik, M.B., (1972). The treatment of cervix cancer using high activity ^{60}Co sources. *British Journal of Radiology*, 45, 257-270.

Klein, E., Klein, G., Nadkarni, J.S., Nadkarni, J.J., Wigzell, H. and Clifford, P., (1968). Surface IgM-kappa specificity on a Burkitt Lymphoma cell *in vivo* and in derived culture lines. *Cancer Research*, 28, 1300-1310.

Kohn,K.W., (1991). Principles and Practice of DNA Filter Elution. *Pharmacology and Therapeutics*, 49, 55-77.

Kovacs, E. and Langemann, H., (1990). Investigation of the repair of single-strand breaks in human DNA using alkaline gel electrophoresis. *Radiation Research*, 124, 137-140.

Kwock, L., Lin, P.S., and Ciborowski, L., (1979). Differences in the effect of ionizing radiation on Na^{+}-dependent amino acid transport in human T (MOLT-4) and human B (RPMI 1788) lymphoid cells. *Radiation Research*, 80, 512-522.

Lafleur, M.V.M., Woldhuis, J. and Loman, H., (1981), Alkali-labile sites in biologically active DNA: comparison of radiation induced potential breaks and apurinic sites. *International Journal of Radiation Biology*, 39, 113-118.

Louw, A.K.A., Van Rensburg, E.J., Izatt. H. and Engelbrecht, R.I., (1991). Nucleoid sedimentation analysis of DNA superstructure, gamma irradiation-induced damage and repair in human and chacma baboon (*Papia ursinus*) peripheral lymphocytes. *International Journal of Radiation Biology*, 59, 951-962.

Mak, A.C.A., Van' t Riet, A., Ypma, A.F.G.V.M., Veen, R.E. and Van Slooten, F.H.S., (1987). Dose determination in bladder and rectum during intracavity irradiation of cervix carcinoma. *Radiotherapy and Oncology*, 10, 97-100.

Mattern, M.R., Kerrigan, D.J., and Pommier, Y., (1987). Nucleoid sedimentation analysis of DNA strand breaks induced in cells exposed to DNA intercalating agents. *Pharmacology Therapeutics*, 34, 303-319.

McGrath, R.A. and Williams, R.W., (1966). Reconstruction *in vivo* of irradiated *Escherichia coli* deoxyribonucleic acid; the rejoining of broken pieces. *Nature*, 212, 534-535.

McNally, N.J., Hinchliffe, M., and Soranson, J., (1990). The effect of post-irradiation anisotonic treatment on cell survival and repair of DNA damage. *International Journal of Radiation Biology*, 57, 503-512.

Minowada, J., Ohnuma, T. and Moore, G., (1972). Rosette-forming human lymphoid cell lines: Establishment and evidence for origin of thymus-derived lymphytes. *Journal of the National Cancer Institute*, 49, 891-895.

Müller, W.U., Bauch, t., Streffer, C., Niedereichholz, F. and Böcker, W. (1994). Comet assay studies of radiation-induced DNA damage and repair in various tumour cell lines. *International Journal of Radiation Biology*, 65, 315-319.

Oleinick, N.L., Chiu, S-M., Ramakrishnan, N. and Xue, L., (1987). The formation, identification, and significance of DNA-Protein cross-links in mammalian cells. *British Journal of Cancer*, 55, Supplement viii, 135-140.

Okayasu, R., and Iliakis, G., (1992). The shape of DNA elution dose-response curves under non-denaturing conditions: the contribution of the degree of chromatin condensation. *International Journal of Radiation Biology*, 61, 455-463.

Olive, P.L., Chan, A.P.S. and Cu, C.S. (1988). Comparison between the DNA Precipitation and Alkali Unwinding Assays for Detecting DNA Strand Breaks and Cross-Links. *Cancer Research*, 48, 6444-6449.

Olive, P.L., Banath, J.P. and Durand, R.E., (1990). Heterogeneity in radiation-induced DNA damage and repair in tumour and normal cells measured using the "comet assay". *Radiation Research,* **122,** 86-94.

Olive, P.L., Wlodek, D. and Banath, J.P. (1991a). DNA double-strand breaks measured in individual cells subjected to gel electrophoresis. *Cancer Research,* **51,** 4671-4676.

Olive, P.L., Durand, R. E., Banath, J. P. and Evans, H.H., (1991b). Etoposide sensitivity and topoisomerase II activity in Chinese hamster V79 monolayers and small spheroids. *International Journal of Radiation Biology,* **60,** 4453-4466.

Olive, P.L., Wlodek, D., Durand, R.E. and Banath, J.P. (1992a). Factors influencing DNA migration from individual cells subjected to gel electrophoresis. *Experimental Cell Research,* **198,** 259-267.

Olive, P.L., and Banath, J.P. (1992b). Growth fraction measured using the comet assay. *Cell Proliferation,* **25,** 447-457.

Olive, P.L., Banath, J.P., and Evans, H.H., (1993). Cell killing and DNA damage by etoposide in Chinese hamster V79 monolayers and spheroids: influence of growth kinetics, growth environment and DNA packaging. *British Journal of Cancer,* **67,** 522-530.

Östling, O., and Johanson, K.J., (1984). Microelectrophoretic study of radiation-induced DNA damages in individual mammalian cells. *Biochemical and Biophysical Research Communications,* **123,** 291-298.

Östling, O., and Johanson,K.J., (1987). Bleomycin, in contrast to gamma irradiation, induces extreme variation of DNA strand breakage from cell to cell. *International Journal of Radiation Biology,* **52,** 683-691.

Östling, O., Johanson, K.J., Blomquist, E. and Hagelqvist, E. (1987). DNA damage in clinical radiation therapy studied by microelectrophoresis in single tumour cells: A preliminary report. *Acta Oncologica,* **26,** 45-48.

Peacock, J.H., Eady, J.J., Edwards, S., Holmes, A., Mc Millan, T.J. and Steel, G.G., (1989). Initial damage or repair as the major determinant of cellular radiosensitivity? *International Journal Radiation Biology*, 56, 543-547.

Perez, C.A., Breaux, S., Camel, H.M., Purdy, J.A. and Walz, B.J., (1984). Radiation therapy alone in the treatment of carcinoma of the uterine cervix: analysis of complications. *Cancer*, 54, 235-246.

Powell, S. and McMillan., (1990). DNA damage and repair following treatment with ionising radiation. *Radiotherapy and Oncology*, 19, 95-108.

van Rensburgh, E.J., Louw, W.K.A., Izatt, H. and Van der Watt, J.J., (1985). DNA supercoiled domains and radiosensitivity of sub-populations of human peripheral blood lymphocytes. *International Journal of Radiation Biology*, 47, 673-679.

van Rensburg., (1987). Changes in DNA supercoiling during repair of gamma-radiation-induced damage. *International Journal of Radiation Biology*, 52, 693-703.

van Rensburg, E.J., Louw, W.K.A., Engelbrecht, R.I. and Izatt, H.L. (1989). Aphidicolin inhibition of gamma-radiation-induced DNA repair in human lymphocyte subpopulations. *General Pharmacology*, 20, 433-436.

Ross, G. and Brown, R., (1992). The Role of DNA Repair Processes in Determining Response to Cancer Therapy, *European Journal of Cancer*, 28, 281-285.

Roti Roti, J.L., and Wright, W.D., (1987). Visualisation of DNA loops in nucleoids from HeLa cells: assays for DNA damage and repair. *Cytometry*, 8, 461-467.

Rydberg, B., (1975). The rate of strand separation in alkali of DNA of irradiated mammalian cells. *Radiation Research*, 61, 274-287.

Sabovljev, S.A., Cramp, W.A., Lewis, P.D., Harris, G., Halnan, K.E. and Lambert, J., (1985). Use of rapid tests of cellular radiosensitivity in radiotherapeutic practice. *Lancet*, ii, 787.

157

Schulte-Frohlinde, D., and von Sonntag, C., (1990). Sugar lesions in cell radiobiology. Ionizing Radiation Damage to DNA: Molecular Aspects, 31-42, Wiley-Liss, Inc.

Schwartz, J.L. and Vaughan, A.T.M., (1989). Association among DNA/chromosome break rejoining rates, chromatin structure alterations, and radiation sensitivity in human tumour cell lines. Cancer Research, 49, 5054-5057.

Seymour, C.B., and Mothersill, C., (1989). Lethal mutations, the survival curve shoulder and split-dose recovery. International Journal of Radiation Biology, 56, 999-1010.

Siemann, D.W., (1989). Do in vitro studies of potential lethal damage repair predict for in situ results? International Journal of Radiation Biology, 56, 567-571.

Singh, N.P., Mc Coy, M.T., Tice, R.R, and Schneider, E.L., (1988). A simple technique for the quantitation of low levels of DNA damage in individual cells. Experimental Cell Research 175, 184-191.

Singh, N.P., Danner, D.B., Tice, R.R., McCoy, M.T., Collins, G.D. and Schneider, E.L., (1989). Abundant alkali-sensitive sites in DNA of human and mouse sperm. Experimental Cell Research, 184, 461-470.

Singh, N.P., Danner, D.B., Tice, R.R., Brant, L. and Schneider, E.L., (1990). DNA damage and repair with age in individual human lymphocytes. Mutation Research, 237, 123-130.

Singh, N.P., Danner, D.B., Tice, R.B., Pearson, J.D., Brant, L.J., Morrel, C.H., and Schneider, E.L., (1991a). Basal DNA damage in individual human lymphocytes with age. Mutation Research, 256, 1-6.

Singh, N.P., Tice, R.R., Stephens, R.E., and Schneider, E.L., (1991b). A microgel technique for the direct quantitation of DNA on damage and repair in individual fibroblasts cultured on microscope slides. Mutation Research, 252, 289-296.

Smith, K.C., (1962). Dose dependent decrease in extractability of DNA from bacteria following irradiation with ultraviolet light or with visible light plus dye. *Biochem. Biophys. Research Communications,* **114,** 99-106.

Soszynski, M. and Schuessler, H., (1991). Effect of X-irradiation on erythrocyte membrane proteins. Primary radicals. *International Journal of Radiation Biology,* **60,** 859-875.

Srinivasan, S., Glauert, H.P., (1990). Formation of 5-hydroxymethyl-2'-deoxy-uridine in hepatic DNA of rats treated with gamma-irradiation, diethylnitrosamine, 2-acetylaminofluorene or the peroxisome proliferatior ciprofibate. *Carcinogenesis,* **11,** 2021-2024.

Stephens, R.E. and Lipetz, P.D., (1982). High order DNA repair in human peripheral leukocytes: A factor in aging and cancer? *Modern Aging Research,* Vol. 3B, 155-173. Alan R. Liss, Inc.,(1983), New York.

Szekely, J.G., Raaphorst, G.P., Lobreau, A.U., and Copps, T.P., (1982). Effect of X-irradiation and radiation modifiers on cellular ultrastructure. *Scanning Electron Microscopy,* **1,** 335-347.

Szekely, G.J. and Lobreau, A.U., (1985). High radiosensitivity of the MOLT-4 leukaemic cell line. *International Journal of Radiation Biology,* **48,** 2277-2284.

Teoule, R., (1987). Radiation-induced DNA damage and its repair. *International Journal of Radiation Biology,* **51,** 573-589.

Tice, R.R., and Setlow, R.B., (1985). DNA repair and replication in aging organisms and cells. *Handbook of the Biology of Aging,* 173-224. Second edition (1985), Van Nostrand Reinhold, New York.

Tice, R.R., Andrews, P.W., and Singh, N.P., (1990). The single cell gel assay: a sensitive technique for evaluating intercellular differences in DNA damage and repair. *DNA Damage and Repair in Human Tissues,* 291-301, Plenum Press, New York.

Tice, R.R., Strauss, G.H.S., Peters, W.P., (1992). High-dose combination alkylating agents with autologous bone-marrow support in patients with breast cancer: preliminary assessment of DNA damage in individual peripheral blood lymphocytes using the single cell gel electrophoresis assay. *Mutation Research,* **271**, 101-113.

Turesson, I., (1989). The progression rate of late radiation effects in normal tissue and its impact on dose-response relationships. *Radiotherapy and Oncology,* **15**, 217-226.

Unal, A., Hamberger, A.D., Seski, J.C., Fletcher, G.H., (1981). *International Journal of Radiation Oncology Biology Physics.,* **7**, 999-1004.

Vaughan, A.T.M., Lynch, T.H., Anderson, P, Kondratowicz, G.M., Wallace, D.M., (1991). The extraction of biologically relevant data from bladder carcinoma cells eliminated in the urine. *New Developments in Fundamental and Applied Radiobiology,* 292-298, Taylor and Francis, London.

Vijayalaxmi., Tice, R.T., and Strauss, G.H.S., (1992). Assessment of radiation-induced DNA damage in human blood lymphocytes using the single-cell gel electrophoresis technique. *Mutation Research,* **271**, 243-252.

Visser, P.A., Moonen, L.M.F., Van der Kogel, A.J. and Keijser, A.H., (1985). Application of the linear-quadratic-concept for the prediction of late complications after combined irradiation of the uterine cervix. *Radiotherapy and Oncology,* **4**, 133-141.

Vogelstein, B., Pardoll, D.M., Coffey, D.S., (1980). Supercoiled loops and eukaryotic DNA replication. *Cell,* **22**, 79-85.

Wardman, P. and Clarke, E.D., (1987). Redox properties and rate constants in free-radical mediated damage. *British Journal of Cancer,* **55**, Suppl. viii, 172-177.

West, C.M.L., Davidson, S.E. and Hunter, R.D., (1989). Evaluation of surviving fraction at 2Gy as a potential prognostic factor for the radiotherapy of carcinoma of the cervix. *International Journal of Radiation Biology,* **56**, 761-765.

Whitaker, S.J., Powell, S.N. and McMillan, T.J., (1991). Molecular Assays of Radiation-induced DNA Damage. *European Journal of Cancer,* **27,** 922-928.

Whitaker, S.J., (1992). DNA Damage by Drugs and Radiation: What is Important and How is it Measured? *European Journal of Cancer,* **28,** 273-276.

Worcel, A. and Benyajati, C., (1977). Higher order coiling of DNA in chromatin. *Cell,* **12,** 83-100.

Wun, K.L.W., and Shafer, R.H., (1982). Structural changes in mammalian cell DNA induced by low-dose X-ray damage and subsequent post irradiation incubation in the presence and absence of caffeine. *Radiation Research,* **90,** 310-320.